Study of Dross in Ductile Cast Iron Main Shafts

Studie av Dross i Gjutna Axlar av Segjärn

Sofia Andersson

Faculty of Health, Science and Technology

Master thesis, CBAEM1

30 hp

Supervisor Christer Burman

Examiner Jens Bergström

2015-06-12

Study of Dross in Ductile Cast Iron Main Shafts

Master of Science Thesis

Sofia Andersson
2015-06-12

Author **Sofia Andersson**
aks.andersson@live.se

Supervisor **Christer Burman**
Research Engineer, Karlstad University
christer.burman@kau.se

Supervisor **Marja Lindberg**
Quality Supervisor, Global Castings Guldsmedshyttan AB
mlind@globalcastings.com

Examiner **Jens Bergström**
Professor, Materials Engineering, Karlstad University
Jens.Bergstrom@kau.se

Department of Health, Science and Technology
Division of Science and Technology
Karlstad University, Sweden

Abstract

Keywords: Dross, Mg treatment, Main shafts, Ductile cast iron

The study of dross in ductile cast iron main shafts was performed at Global Castings Guldsmedshyttan AB and presented in this master thesis. The purpose of the study was to obtain answers to why dross defects were present in some of the foundry's casted main shafts, with the main problem located at the flange of the shaft. The chemical composition of the dross formations and which steps in the casting process that increased the dross formation were of interest. The study only included dross in main shafts manufactured at Global Castings Guldsmedshyttan AB.

Dross particles form when elements such as Mg, Ca, Si and Mn react with O. These elements, which are highly reactive to O, are used in ductile cast irons to achieve the spheroidal graphite nodules that regulate the cast materials ductile properties. If a higher amount of dross particles has formed, the particles will start to cluster, resulting in a growing dross formation. Dross formations works as surface crack initiation points and reduces the castings fatigue strength and ductility.

During the study it was seen that the cause of dross formations is a combination of many parameters increasing the melts exposure to O resulting in dross defects. The dross formations could be connected to worn out ladles, low melt temperatures, incorrect additions of Mg treatment, lack of an extra slag removal station and finally turbulence as the melt were poured into the mould.

At Global Castings Guldsmedshyttan AB a greater part of the main shafts containing dross defects were a result of worn out ladles and low melt temperatures. The types of dross found in the main shaft material were mainly Mg, Ca, Si and Al which had reacted with O. S bonded with Mg and Ca was also detected in the dross formations. It was shown that the dross particles could be derived from charge material, Mg treatment and inoculation.

To avoid dross defects the first step would be to set up an extra slag station, shorten the interval of maintenance of the ladles and to better adjust the melt temperature to the condition of the specific ladle. To minimize dross due to excess Mg a better controlled process would be recommended with an increased number of monitored manufacturing parameters.

Sammanfattning

Nyckelord: Dross, Magnesiumbehandling, Axel, Segjärn

Studien av dross i axlar tillverkade av segjärn gjordes hos Global Castings Guldsmedshyttan AB och presenteras i denna examensrapport. Syftet med studien var att hitta anledningar till varför drossdefekter bildas i flänsen på vissa av gjuteriets tillverkade axlar. Drossens kemiska komposition likväl de steg i tillverkningsprocessen som inverkade på drossbildning var av intresse. Studien inkluderade endast drossdefekter i axlar tillverkade av Global Castings Guldsmedshyttan AB.

Drosspartiklas bildas när till exempel Mg, Ca, Si och Mg reagerar med O. Dessa ämnen, vilka är väldigt reaktiva med syre, används vid framställning av segjärn för att de sfäriska grafitnodulerna som starkt reglerar materialets duktila egenskaper ska bildas. Ett större antal drosspartiklar i en smälta leder till kluster av dross vilka växer i takt med att nya partiklar bildas. Dross fungerar som sprickinitieringspunkter i gjutgodsytor och reducerar godsets utmattningshållfasthet och duktilitet.

Under studien kunde det ses att dross bildas på grund av en kombination av parametrar som ökar smältans exponering av syre vilket resulterar i drossdefekter. Drossdefekter kunde kopplas till slitna skänkar, låga smälttemperaturer, felaktig mängd magnesiumbehandling, brist på en extra slaggstation och slutligen turbulens när smätan hälls i formen.

Hos Global Castings Guldsmedshyttan AB är en stor del av axlarna med drossdefekter ett resultat av framför allt slitna skänkar och låga smälttemperaturer. Vid analys sågs det att ett antal olika typer av drosspartiklar kan bildas i det duktila gjutjärn som används till axlarna; främst Mg, Ca, Si och Al som reagerat med O. Mg och Ca som bundit med S kunde också hittas i vissa av de studerade drossformationerna. Det kunde visas att den kemiska kompositionen i drosspartiklarna var härrörande från grundmaterialet, magnesiumbehandlingen och ympmedlet.

Ett första steg Global Castings Guldsmedshyttan AB skulle kunna ta för att undvika drossdefekter är att ha en extra slaggstation, införa tätare underhåll av skänkarna och bättre anpassa smälttemperaturen till skicket på den specifika skänken. För att minimera dross som bildats på grund av ett överskott av Mg skulle en mer kontrollerad process rekommenderas med ett ökat antal bevakade tillverkningsparametrar.

Preface

This master thesis is a study of dross in ferritic ductile cast iron main shafts for the wind power industry. The study was made possible due to a collaboration between Global Castings Guldsmedshyttan AB and Karlstad University. The study of the main shafts was mainly performed on site at Global Castings Guldsmedshyttan AB in between January and June of 2015.

Acknowledgement

I would like to send my gratitude to my supervisor at Global Castings, Marja Lindberg, for her support and guidance during the past months. Without her metallurgical knowledge and sincere interest in casting this thesis would not have been the same. I would also like to thank Erik Andersson, Lars Sjöbacka and Erik Bertelshofer at Global Castings for all their time spent introducing me to the casting process at the foundry and Christer Burman, my supervisor at Karlstad University, for his help and guidance with SEM and EDS analyzes. Lastly I would like to thank my loving fiancé Anton and my family for all the support during the years, without you none of this would have been possible!

Sofia Andersson

Karlstad, June 2015

Nomenclature

BCC	Body-centred cubic
BSE	Backscattered electrons
DCI	Ductile cast iron
EDS	Energy dispersive spectroscopy
FCC	Face-centred cubic
Fe_3C	Cementite
Fe_3P	Steadite
GCGAB	Global Castings Guldsmedshyttan AB
NDT	Non-destructive testing
QDA	Quality data analysis system
SEM	Scanning electron microscope

Contents

CHAPTER 1

Introduction

1.1 Project Background

Global Castings Guldsmedshyttan AB (GCGAB) produce castings of ductile cast iron for the wind power industry. The company mainly manufacture rotor hubs, main shafts and machine fundaments. GCGAB operates in a site with long going traditions within the foundry industry, going back to the 1860's. During the past six years GCGAB has done relatively comprehensive changes in their organisation by implementing six sigma and lean manufacturing principles. The company now focuses on high quality products, effectiveness and safety.

As a step in the quality work, prevention measures are taken to minimize defects in the castings and effort is placed in understanding what causes these defects. Dross is one defect that has been observed in both melt and solidified castings and for which the company desires to reduce the levels. Dross is a type of slag inclusions that forms in ductile cast iron as a result of, mainly, Mg reacting with O [1]. Global Castings has several theories as to why dross defects occur in their products; for example high O levels, a high melt temperature, turbulence and/or the chemical composition of the melt. No specific reason to why the dross forms has, however, been established due to that the problem does not appear regularly (even though there have not been any comprehensive changes in the material or manufacturing process).

The product of interest in this study is the main shaft, an axis connecting the rotor hub to the turbine generator. Main shafts containing dross at higher levels sometimes needs to be discarded due to the risk of crack formations, degraded tensile strength and impact resistance.

1.2 Objective of Study

The purpose of the study is to find reasons as to why dross sometimes forms in the produced main shafts. The objective of the study is to present a suggestion of how dross formation in main shafts can be minimized. Three main questions have been formulated to match the purpose and objective of the study:

- Which types of dross can be found in the main shafts and which steps in the manufacturing process seems to be most critical for the formation of dross?
- Can any deviations in the chemical composition of the main shaft melt be detected which explains the dross formation?
- What changes could be made regarding the metallurgy and manufacturing process to prevent high levels of dross formation?

1.3 Limitations of study

- No other defects than dross will be studied.
- The study will only include dross formation in main shafts.

CHAPTER 2

Theoretical Background

2.1 Ductile Cast Iron

2.1.1 Background

Ductile cast iron (DCI) was developed during the 1940's in USA by H. Morrogh and K. Mills when Mg and Ce was added to an iron melt resulting in a cast with ductile properties and high tensile strength. Grey and malleable cast iron had up to this point been produced in large quantities used for heavy machinery, vehicles and war materials. Malleable iron was used for products where there were requirements on some ductility. To gain the ductile properties of malleable cast iron with spheroid shaped graphite (instead of sharper grains) heat treatments were necessary [2].

What was seen in DCI was that the Mg and/or Ce additive enabled the formation of graphite spheres in the melt which grew into nodules during cooling and solidification. The microstructure in DCI is ferritic and/or pearlitic, by request, depending on material properties and manufacturing parameters such as cooling rate and chemical composition. With the DCI a ductile material was obtained with an even distribution of nodules as well as homogenous ductile material properties. Heat treatment can be used for ferritic DCI to reduce undesired pearlite but no heat treatment is required to form the graphite nodules. Morrogh and Mills presentation of the DCI opened up for the possibility of new products and applications, such as castings for the wind power industry [2].

The usage of DCI has increased drastically since the middle of the 1960's when the beneficial properties of DCI started to be widely known; high castability and surface hardenability, good machining potential, a relatively high strength to weight ratio together with good vibration damping. DCI material replaced grey and malleable casting iron in many products and manufacturing of new products increased. Between 1965 and 2010 the worldwide production of DCI has increased with 13 fold; from 1.5 million tonnes/year to 20 million tonnes/year [2].

DCI is favourable in wind turbines due to good wear resistance, ductility, vibration damping and high tensile strength. The production of wind turbines and wind energy is expected to double within the next 15 to 20 years and with over 40 tonnes of DCI in a single (larger) wind turbine, the need of DCI will also increase. Since the wind power industry constantly develops and turbines are supposed to be lighter, more effective, withstand strong forces at low temperatures and operate for many years the quality of DCI's has been in focus for these types of manufacturers during recent years [3].

2.1.3 Dross in Main Shafts

At GCGAB the manufacturing is mainly focused on DCI products for the wind power industry. The material used for the products (the main shaft in this case) is an EN 1563:2011 standard ductile cast iron number EN-GJS-400-18-LT (5.3103) [4].

Dross is a non-metallic inclusion found in DCI containing for example Mg, Si and O [1]. The Mg in ductile iron is added to the melt to start spheroidization of graphite nodules which makes the cast ductile. As the melt is exposed to O (sometimes enhanced by convection or turbulence) primarily Mg, Si, Ca, Mn and Al reacts with O which can result in long accumulated particle formations; dross [1]. In Figure 1, two typical dross formations are seen at different magnifications.

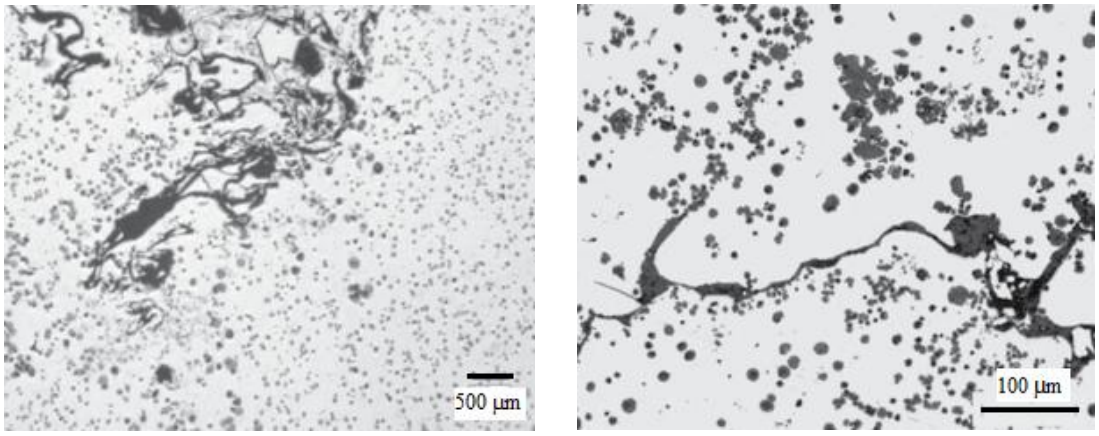

a) b)

Figure 1. Dross formations in DCI. Longer thread like accumulations of for example MgO, CaS, CaO, Al_2O_3. a) Overview of dross containing area b) Larger magnification on one single dross thread [1].

Dross has a lower density than the iron melt and can therefore be found in the near surface region of the solidified cast. Dross can, however, be caught in turbulent areas of the mould which can hinder the dross from surfacing before the melt temperature has passed the eutectic solidification point [5]. For the main shafts, Figure 2, at GCGAB the problem area for dross lies mainly in the flange which is a turbulent and rapidly solidifying area of the cast. The flange is placed downward in the mould, which is bottom fed, and the dross is commonly accumulated at the upper surface of the flange (red arrow in Figure 2). 380 of these main shafts were included in the study of dross.

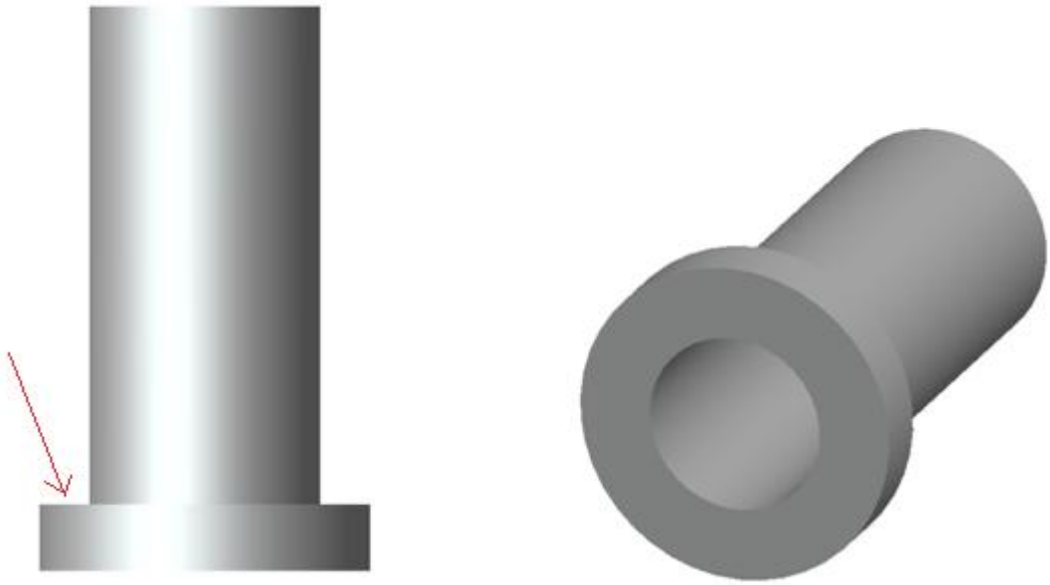

Figure 2. A schematic of a main shaft from different angles. The red arrow marks the upper surface of the flange which is the main problem area for dross formations.

2.2 Manufacturing Process

The casting process of main shafts at GCGAB is divided into a number of steps which all have an effect on the final quality of the casting. The manufacturing steps are general methods, but every foundry has its own custom solution when it comes to for example furnaces and gating system.

2.2.1 Flow Chart

In Figure 3 the flow chart of the main shaft manufacturing process is shown with focus on the larger milestones. Forming and casting takes place in Guldsmedshyttan, Sweden, as well as shake-out, shoot blasting and quality control (non-destructive testing). Machining (turning) of the main shafts takes place at Global Castings in Denmark before they are delivered to the customer. Each step in the flow chart is explained further in the coming text.

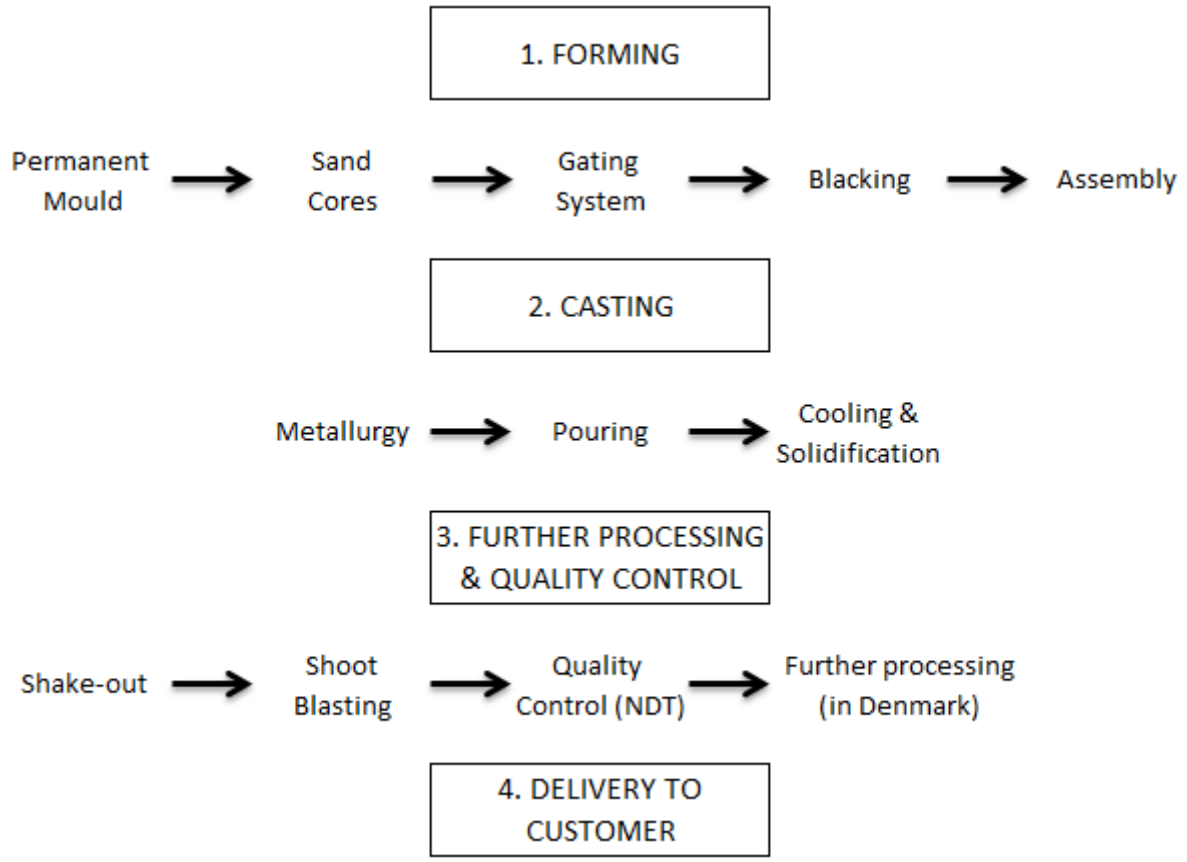

Figure 3. Main steps in the manufacturing process of the main shaft.

2.2.2 Forming

In Figure 4 a schematic of an assembled main shaft mould can be seen. When aiming for high quality products the condition of the moulds are of great importance. This is because the cooling rate, surface roughness and sand defects in the cast (to name a few parameters) can be directly related to the quality of the moulds and cores [2].

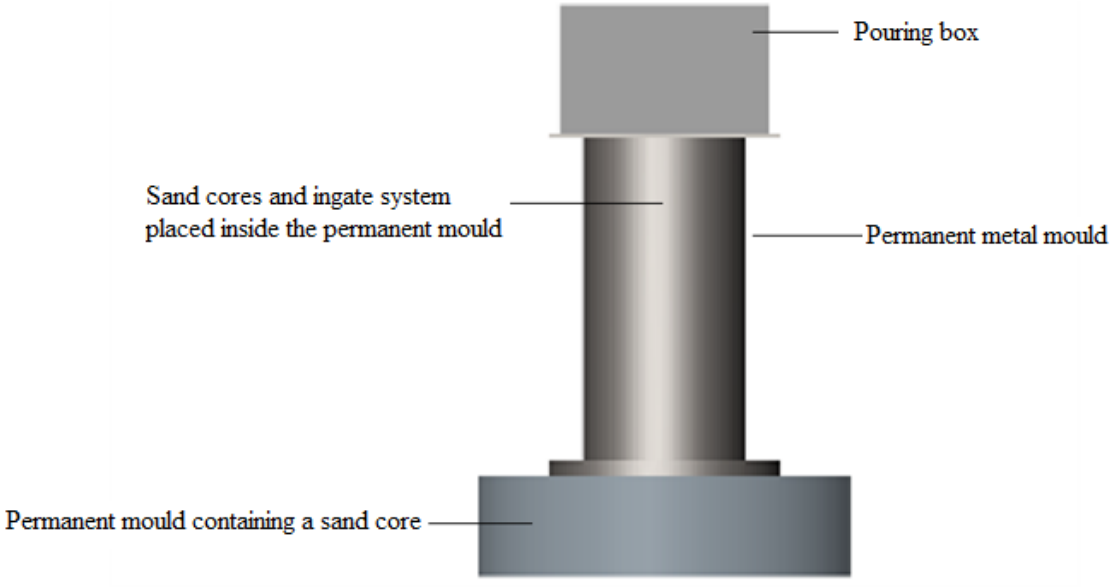

Figure 4. Schematic of an assembled main shaft mould.

2.2.2.1 Permanent Metal Mould

The main shaft is casted in a permanent iron mould instead of sand moulds as for GCGAB's other products. A metal mould increases the cooling rate and at the same time decreases the risk of volume changes due to graphite expansion during solidification. It is of importance that the mould material can withstand the high temperatures of the poured in melt without the inner surface of the mould being damaged or cracked. The moulds are controlled and maintained to a good condition between every casting so that there are no risk of leakage and/or a damaged product [2].

The inner surface of the metal mould is blackened to get an inert and durable surface finish closest to the cast, preventing surface damages and that the cast gets stuck in the mould. The black consists of fine grained particles, such as Zr, with a binder and additives. Blacking results in a dense coating that prevents for example S, N and O from penetrating the surface. For the permanent mould black is flowed over the inner surface resulting in a heat withstanding metal mould with an even and hard surface. If an external surface is treated (such as on the sand core), the black is normally sprayed onto the surface [2].

2.2.2.2 Sand Cores

The sand core is placed inside the metal mould during assembly to obtain a hollow main shaft. The sand cores consist of 20 % new sand and 80 % recycled sand, shaped in a permanent metal model. Additives (binders; acid and harts) are mixed into the sand before it is poured in the model. To get a compact sand core the model is placed on a vibrating table for maximum 1 minute at 30-70 Hz depending on geometry before it is set aside for 2 hours to dry. After the initial drying the sand cores are placed under infrared light to increase the rate of drying and to ensure that the binders set properly. When the cores have dried black is sprayed onto the surface. For sand cores or moulds it is of extra importance that the blacking layer is smooth and has the correct thickness so that sand cannot sinter to the cast surface [2]. It is of importance that the sand core is compact and hard to avoid larger volume changes or loss of sand into the melt during pouring. 70 % of all defects in the foundry industry is sand that has sintered to the cast surface due to low durability of sand moulds or cores (porosities and dross are the second and third most commonly found defects) [2].

Two extra sand moulds (used for material samples) are formed for each cast and placed in the bottom of the permanent mould at the ingate system. The side cast moulds are filled with melt at the same time as the rest of the main shaft mould and when the product has solidified the sample material is removed. Test specimens are then machined from the side casted material which then undergoes microstructure analysis, impact, tensile and hardness tests.

2.2.2.3 Gating System

The gating system is placed inside the permanent mould, through the sand core. A pouring box (a sand mould) containing a 30 kg inoculation stone is placed on top of the permanent mould. The melt is poured from a ladle into the box at the opposite side of where the gating system is placed, this to get a more stable flow and also so that the inoculation gets evenly distributed. A thin metal sheet (a cast lid) is placed inside the gating system and as the melt is poured in the cast lid slowly melts. To minimize turbulence and to ensure a steady melt flow the guideline at GCGAB is that at least 70 % of the pouring box should be filled before the metal sheet has completely melted. The sprude (the pipes creating the gating system) is made of ceramic and has few curves or sharp edges to minimize turbulence.

At GCGAB a new choke with a minimum diameter of 40 mm has been used for some main shafts resulting in less turbulence during mould filling and less defects in the manufactured main shafts. The gating system at the bottom of the mould consists of four gates placed at opposite sides of the mould. The mass of the melt and the gravity is enough to fill the mould from the bottom up. The bottom feed technique reduces turbulence and dross formation during mould filling [6].

In Figure 5 a schematic of the turbulent areas in the main shaft flange can be seen. The melt flows into the flange through four gates (blue oval areas in the schematic) which results in turbulent whirls in the areas between the gates (red rectangular areas in the schematic) where slag can be entrapped. GCGAB is working on a new ingate system to avoid turbulent areas, especially in the flange, as defects often have been observed there.

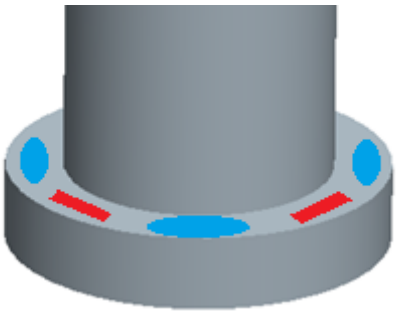

Figure 5. Schematic showing the turbulent areas (red) located between the melt that flows into the mould (blue).

2.2.3 Casting

The process time for casting a main shaft is 3-3.5 hours; from that the charge material is placed in the furnace until the melt has been poured into the mould. In Figure 6 melt in furnace and ladles can be seen.

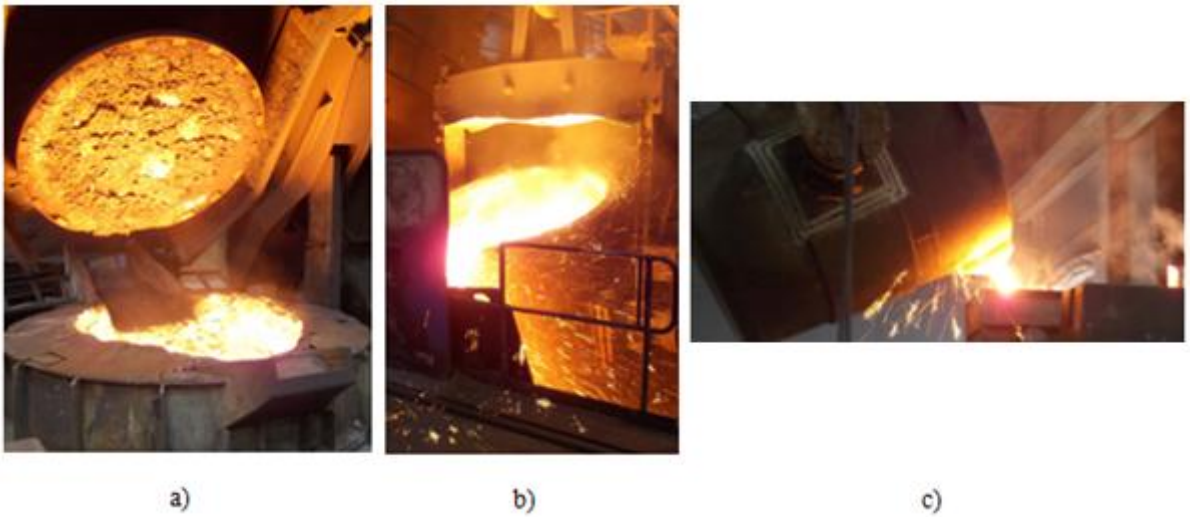

Figure 6. a) Melt is prepared in furnace b) Melt in ladle during Mg treatment c) Melt poured into mould.

2.2.3.1 Preparation of Melt

Charge material is placed in an induction furnace and alloys are added in steps to obtain the desired chemical composition. Coin sized specimens are taken from the melt at three different times for analysis in an arc spectrometer. When the correct temperature is reached in the furnace and the chemical composition is correct, the melt is poured into a ladle containing an Mg treatment. The melt temperature from furnace to ladle for the main shaft is 1,460-1,480 °C. Slag, such as oxides and sulphates, surfaces in the ladle where it is removed by the operator. The melt temperature is measured by an operator before transportation to the mould begins. The metallurgic part of the melt preparation is explained in detail in the section 2.3.2, page 20.

2.2.3.2 Pouring

The recommended pouring temperature of melt (from ladle to mould) for main shafts is 1,355-1,375 °C. A portable temperature equipment is used to measure the pouring temperature; the equipment has a tolerance of ±1 °C. The pouring temperature could be adjusted to compensate for, for example, chemical composition, pouring weight and the minimum wall thickness of the gating system. The melt temperature could be kept constant during pouring by maintaining an even melt flow. The recommended pouring time of an 18 tonne melt (as for the main shaft) is approximately 110 s. The flow also affects the turbulence of melt in the gating system and mould; turbulence should be kept to a minimum to avoid dross formation during pouring [7].

2.2.3.3 DCI Solidification

The cooling rate of DCI is primarily linked to: the pouring temperature of the melt, the metals thermal properties, the size and geometry of the cast and finally the moulds thermal properties. In order to ensure a ductile cast, pouring temperature and chemical composition is of importance if graphite nodules should form instead of cementite [2]. The cooling of the 18 tonne main shaft melt (from approximately 1,350 °C to 450 °C) is estimated to 24 h.

The crystallization (freezing/solidification) of the cast starts as the melt closest to the mould solidify into a shell of small equiaxed grains, Figure 7 [8]. When the melt inside the shell starts to crystallize it does so into columnar grains which grow in the opposite direction of the heat flow. For heavy castings (as for the main shaft) with a geometry that allows larger gathered volumes, the percentage of the casting containing large equiaxed grains will be greater than for a casting with smaller volumes. A fast cooling rate increases the area with columnar grains, leading to a harder and less ductile material [2]. For the main shaft a relatively slow cooling rate is desired (bearing in mind the permanent metal mould) and a higher percentage of large equiaxed grains.

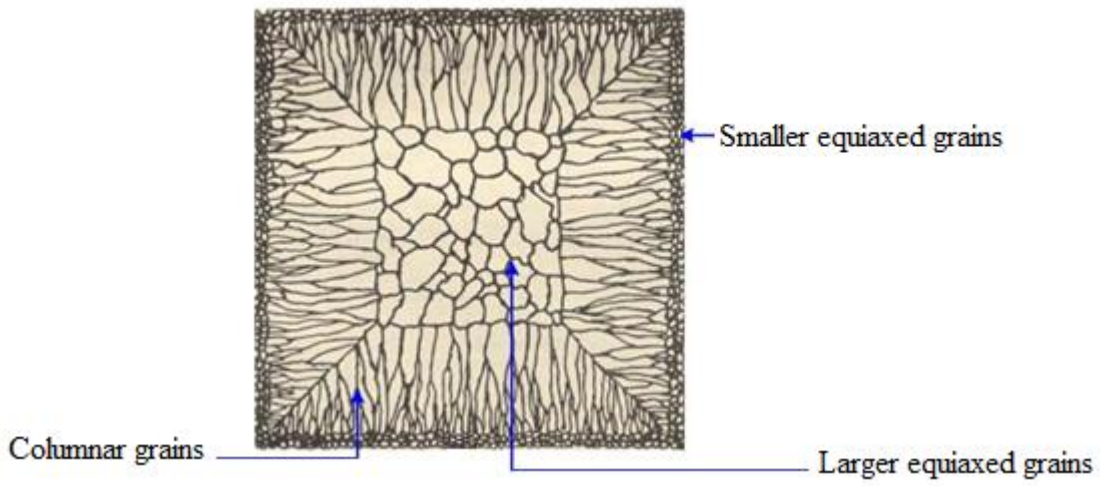

Figure 7. Solidification (crystallization) of DCI. Crystallization starts at the surface with small equiaxed grains, then columnar grains and finally large equiaxed grains forms in the centre. Adapted from [8]**.**

During the solidification volume changes takes place, nodule growth leads to an increase in volume but the metal solidification results in overall volume shrinkage. Longer cooling time and wider wall thickness are factors associated with a larger nodule volume change. When the melt initially expands the pressure in the mould may rise up to 50 times the atmospheric pressure. To avoid that parts of the mould divides, weights are placed on top of the permanent metal mould. The gating system (pouring box included) is of importance during solidification and volume changes. The excess material in the pouring box should pass the eutectic point later than the material in the mould so that volume changes in the mould could, to some extent, be compensated for by melt from the pouring box and gating system [2].

2.2.4 Further Processing and Quality

When the main shaft has cooled down to 450 °C it can be removed from the mould and sand remaining in the cast is shaken out as the cast is placed on a vibrating grate. Sand sintered to the surface of the cast is removed by shoot blasting and as a final step parts of the surface are grinded if necessary.

When sand and other surface imperfections have been removed, the main shaft is controlled by an operator using ultrasonic test. By using ultrasound, imperfections in the goods can be located and the volume of the defects (dross/porosities) are registered [9]. Material samples (from the side casted material) are machined into test rods for impact, tensile and hardness tests to insure that the mechanical properties of the main shaft are correct. A microstructure analysis is also performed where a material sample is studied in an optical microscope where the nodule count, size and distribution are of interest, as are the percentage ferrite and pearlite in the matrix. The main shafts approved during quality control in Guldsmedshyttan are transported to the company location in Denmark for further processing (turning of the main shaft surface and drilling in the flange), the main shafts are thereafter delivered to customer.

2.3 Microstructure

2.3.1 Fe-C Phase Diagram

DCI normally contain 3.5 – 4.5 wt.% C and 0.5-3 wt.% Si. In Figure 8, a Fe-C phase diagram is shown with eutectic phase transition points at 1,154 °C and 738 °C. Alloys, inoculants and Mg treatment are added to the melt during the cast process to start the spheroidization of graphite which during solidification grows into nodules. The alloying elements and amounts can vary but one key element for spheroidizing is Mg [10]. Due to the chemical composition the eutectic phase transition for the DCI melt used in main shafts is in the range of 1,140 °C [13]. The DCI starts to solidify as the melt reaches the eutectic temperature but the graphite spheres start forming in the first (liquid) phase. In the second phase austenite forms, spheroidization and nodule growth continues. In the final phase ferrite and nodules forms along with pearlite if there are residual austenite in the matrix [11].

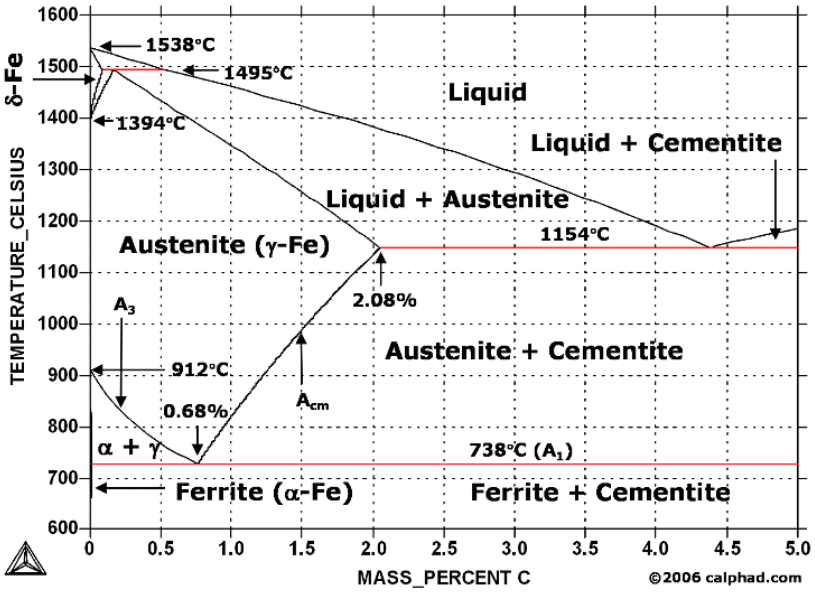

Figure 8. Fe-C eutectic phase diagram. DCI containing 3.5 – 4.5 wt.% C [11].

There are ferritic and pearlitic DCI's, Figure 9, both containing nodules for ductility. The amount and size of graphite nodules that forms (instead of cementite) depends on, for example, Mg treatment, inoculants and cooling rate [12].

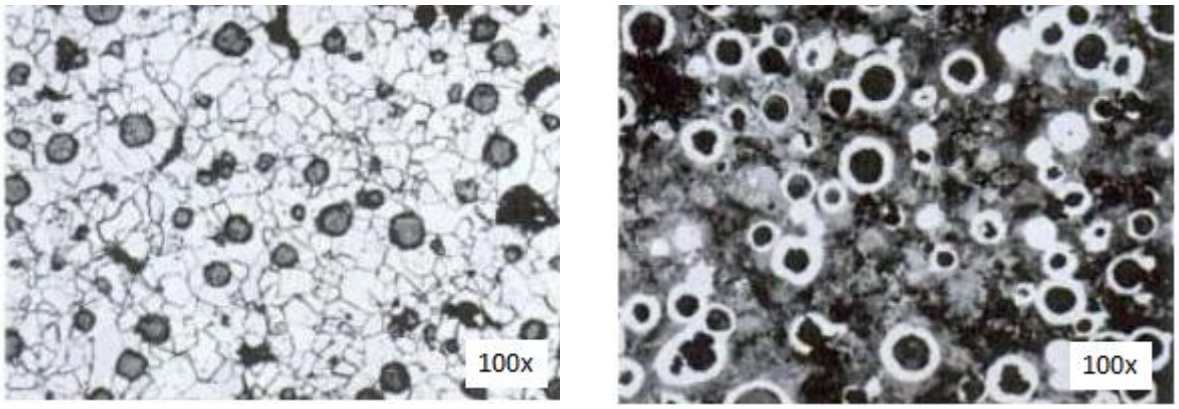

a) b)

Figure 9. Microstructures of DCI. a) 95% ferritic DCI b) 80% pearlitic DCI. Adapted from [7].

2.3.1.1 Ferrite

As ferrite forms in the cast it goes through two phases (δ and α). The δ ferrite has a BCC structure (body-centred cubic) and occurs immediately after the eutectic phase transition point (at 1,140 °C [13]) along with a small amount of graphite. The δ phase is not long lasting but transforms into austenite with FCC (face-centred cubic) structure with graphite spheres. When the cooling continues the austenite transforms into α ferrite with BCC structure along with the graphite, also pearlite can form from residual austenite [10].

FCC and BCC structures can dissolve different amounts of C atoms; FCC has due to its structure a higher solubility of C than the BCC structure. The size of the graphite nodules increases as the austenite FCC structure transform into α ferrite BCC structure when C diffuses from the matrix to the nodules. In Figure 10 a BCC and a FCC structure is shown; FCC with a total of 4 atoms and BCC with 2 atoms (but with access to 14 respectively 9 atoms) [10]. The microstructure of the ferritic DCI in main shafts contains a 95-100% α ferritic and 0-5% pearlitic matrix surrounding the graphite nodules.

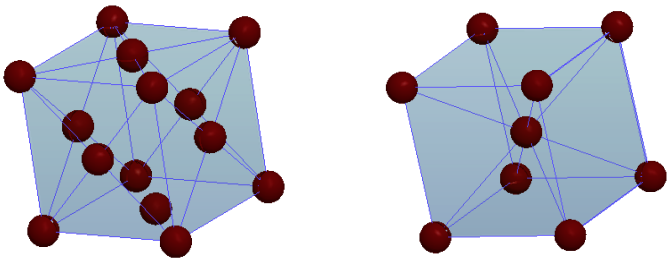

a) b)

Figure 10. a) Face-centred cubic crystal (FCC) b) Body-centred cubic crystal (BCC).

2.3.1.2 Pearlite

Pearlite has a lamellar structure containing α ferrite and cementite (Fe_3C). A variation of factors influences pearlite formation, for example: a rapid cooling rate and pearlite promoting elements such as Mn, Sn and Cu. A longer diffusion distance due to few or inhomogeneous distributed nodule nuclei can also result in a partly pearlitic matrix [10].

Pearlite has a higher solubility of C than ferrite and if there is residual austenite in the matrix when the temperature of the cast has reached the eutectic point (738 °C) areas of pearlite will start to form. Austenite (FCC) has during solidification a maximum solubility of 2.11 wt.% C. As the cast temperature approaches the eutectic point the austenite gets a BCC structure and a solubility of 0.77 wt.% C. At this point α ferrite (BCC) has started to form since C has diffused from the austenite to the nodules resulting in a ferritic area with a maximum solubility of 0.0218 wt.% C. In parts of the matrix containing more than 0.0218 wt.% C when diffusion ceases, pearlite will form which has a maximum solubility of 0.77 wt.% C. Pearlite contains a fixed amount of Fe_3C respective α ferrite; 11.3 % Fe_3C which solutes 6.67 wt.% C and 88.7 % α ferrite [10]. The proportion of pearlite, ferrite and graphite in a microstructure can be estimated by software when the microstructure is studied with microscope [10].

2.3.1.3 Graphite Nodules

There have been a number of theories to how graphite nodules form, for example: the gas bubble theory by Karsay, the graphite theory by Eash and Feest and also the sulphide/oxide theory by Jacobs [14]. The gas bubble theory states that graphite nodules can form inside a gas bubble. This theory is not applicable in a melt where deoxidation takes place by Ca and Mg, also it was shown that it is not likely that a compact graphite nodule would completely fill the gas bubble [14].

The graphite theory explains how a graphite nodule can grow from a graphite nucleus in an iron melt but it does not take the dissolution of graphite in a high temperature liquid melt into account. Both these theories have since the 1970's and 1980's been questioned and are not widely used today [14].

The theory for which the manufacturing of main shafts is based on is the sulphide/oxide theory developed by Jacobs in the 1970's and confirmed by a number of other scientists. Jacobs investigated the nature of the graphite nodule; the chemical composition and how alloying elements and inoculations effect the nodule growth [14].

In Figure 11 a schematic of a graphite nodule can be seen where the centre consists of a sulphide nuclei surrounded by an oxide shell from where the graphite grow. The sulphide nucleus (for example MgS, CaS) are derived from alloying elements added to the melt. Inoculation are later added (for example Ba, Ca, Si) which reacts with O, S and C and functions as a layer between the sulphide core and the surrounding graphite. MgO is also part of the middle layer and the most important factor when it comes to the spheroidal geometry of the nodule. Mg does however not react well with C and therefore the inoculation is necessary if the graphite should be able to form around the sulphide/oxide sphere [14].

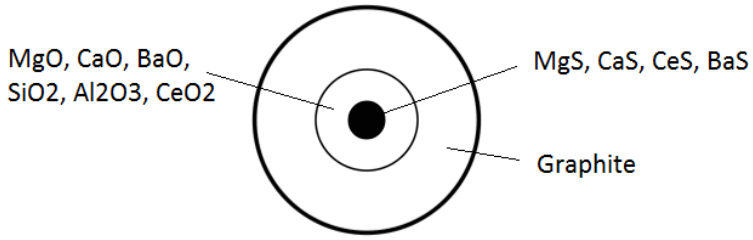

Figure 11. Graphite nodule; sulphide nuclei with an oxide shell surrounded by a growing graphite layer.

In Figure 12 the growth of a graphite nodule is seen. The graphite in the melt is derived from the charge material, alloys and an added carburizer. The spheroidizing starts in the melt as a graphite layer begins to form around a nucleus. The graphite nodules is below the eutectic (at 1,140 °C [13]) surrounded by a austenite matrix which grows approximately 1.4 times faster than the nodule during solidification [15]. A thicker austenite layer complicates diffusion and lowers the diffusion rate of C to the nodule. Nodule growth precedes as long as diffusion is on-going (usually until the diffusion distance has become too far). For the main shafts the austenite (in the best conditions) transform to 100 % α ferrite as the cooling precedes [16].

The temperature of the melt, both in the furnace and before pouring into the mould, affects the nuclei count and therefore also the nodule count. The nuclei of a nodule consists of relatively few atoms and a higher melt temperature weakens the bonds which can result in dissolved molecules and fewer nucleus [2].

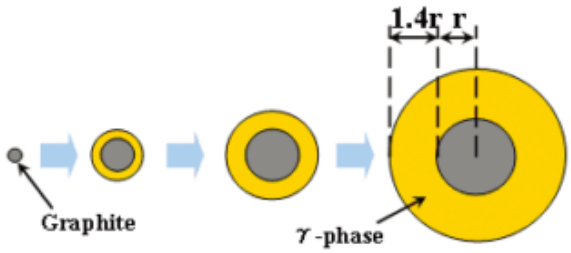

Figure 12. Schematic of a graphite nodule in DCI. From left to right: nuclei covered with oxides and graphite, austenite surrounding the nodule, diffusion distance increasing 1.4 times faster than r. Adapted from [17].

2.3.2 Preparation of Melt

2.3.2.1 Flow Chart

At GCGAB a material formula has been developed for each product from the EN 1563:2011 standard for DCI number EN-GJS-400-18-LT (5.3103) [4]. A standardized way of adding the different elements to the melt is followed by the operators, seen in Figure 13. The main steps for DCI melt preparation at GCGAB are; charge material, alloying elements and treatment methods. To ensure that the chemical composition of

the melt is as desired, spectroscopy analyzes are carried out before alloying elements or treatments are added to the melt. Information about each element and what effect the respective element has on the final cast result are presented in page 16-18.

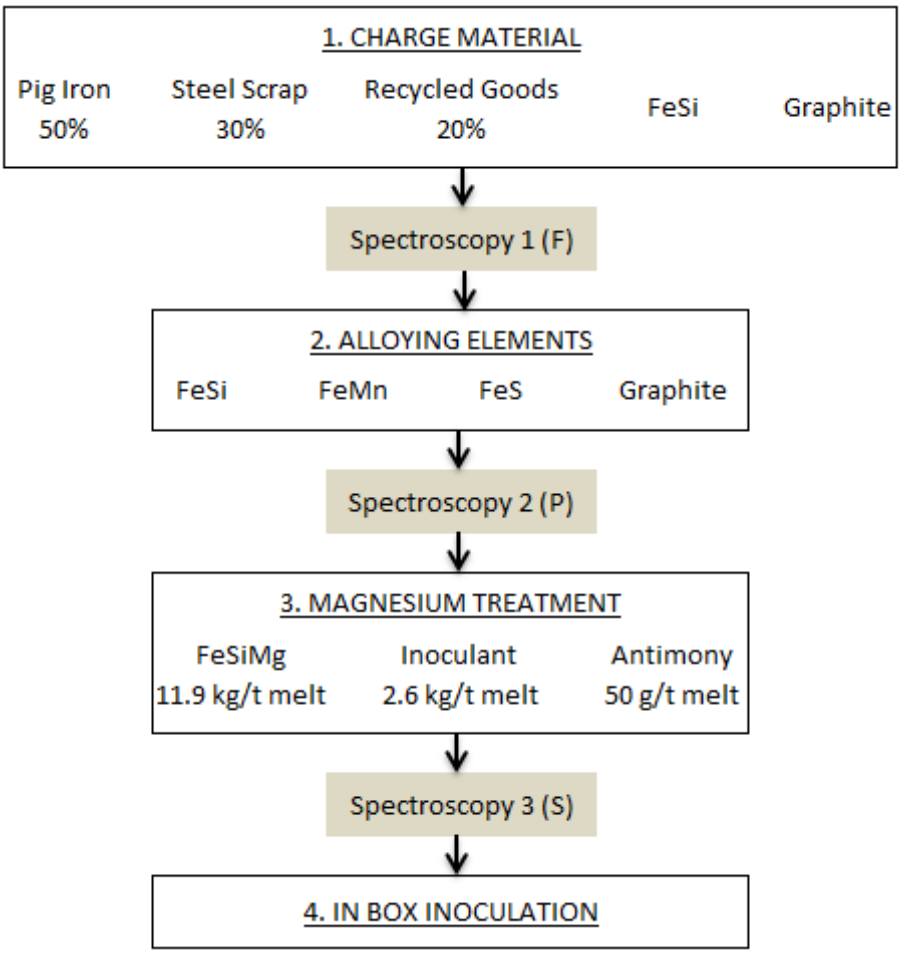

Figure 13. Flow chart showing the metallurgical steps in DCI melt preparation at GCGAB.

2.3.2.2 Charge Material

The charge material consists of pig iron, steel scrap and recycled goods from GCGAB's own production. The pig iron (Fe ingots) contains 3-4 wt.% C but the steel scrap does contain the same, high, amount of C. To maintain a high C content as the steel scrap is added to the charge and a carburizer (graphite) is mixed in from start. The pig iron and scrap material has a lower Si content than DCI, therefore a FeSi (25 wt.% Fe, 75 wt.% Si) alloy is added to the charge to increase the wt.% Si in the melt.

After the charge material has melted in the furnace the first spectroscopy analysis is conducted, spectroscopy 1 (F). The desired results and maximum and minimum values of spectroscopy analyzes 1 (F), 2 (P) and 3 (S) can be seen in Table 1. (F), (P) and (S) is the labels used at GCGAB for the different spectroscopy analyzes meaning: (F) = pre-analysis, (P) = pouring-analysis, (S) = final analysis.

C_{TL}, seen in Table 1, is a calculation of C where consideration has been made regarding the melts eutectic solidification temperature (C_{Temp}) and C_E (C equivalent). The C_{Temp} is a separate analysis but the result is entered in the spectroscope computer before the coin sample is analyzed since the C_{Temp} is used for calculations of C_{TL}. C_{Temp} is a measurement of at which temperature the melt solidifies (the eutectic temperature seen in the phase diagram in Figure 8), when the C_{Temp} is known the correct wt.% C of the melt can be established.

Table 1. Expected results and max, min limits for spectroscopy analyzes of main shaft melt at GCGAB

Element (wt.%)		C_{TL}	Si	Mn	P	S	Mg	Ni	Cr	Cu	Mo	Al
Spectr. 1 (F)	---	3.60	1.22	0.18	0.020	0.013	---	0.05	---	---	---	---
Spectr. 2 (P)	Max	3.82	---	0.26	0.030	0.016	---	---	0.06	0.10	0.02	0.03
	Min	3.78		0.14		0.012						
Spectr. 3 (S)	Max	3.85	2.05	0.26	0.030	0.013	0.045	---	0.06	0.10	0.02	0.03
	Min	3.75	1.85	0.14		0.007	0.033					

The equation used for C_{TL} is specific for the location at Guldsmedshyttan but has been derived from a standard Equation (1) for C_E in heavy section cast goods. The equivalent C is a compilation of elements that have a similar effect on, for example, material hardenability [7]. The % C in Equation (1) is derived from the melts $C_{Temp.}$

$$C_E = \%C + \frac{\%Si}{4} + \frac{\%P}{2} \qquad (1) \quad [7]$$

In Figure 14 a standard recommendation regarding the wt.% C and wt.% Si in a DCI for achieving the best range for castings is seen. The marked area show the C/Si compositions of the 380 main shafts included in the study. The melt formula was changed for the main shafts, from number 186 and forward, where the max wt.% Si at the final spectroscopy analysis was set to 2.05 instead of 2.15 due to mechanical factors. As can be seen, several main shafts are placed in the region for high chill tendency and C flotation, however, defects of this type has not been observed at GCGAB after the changing of the melt formula.

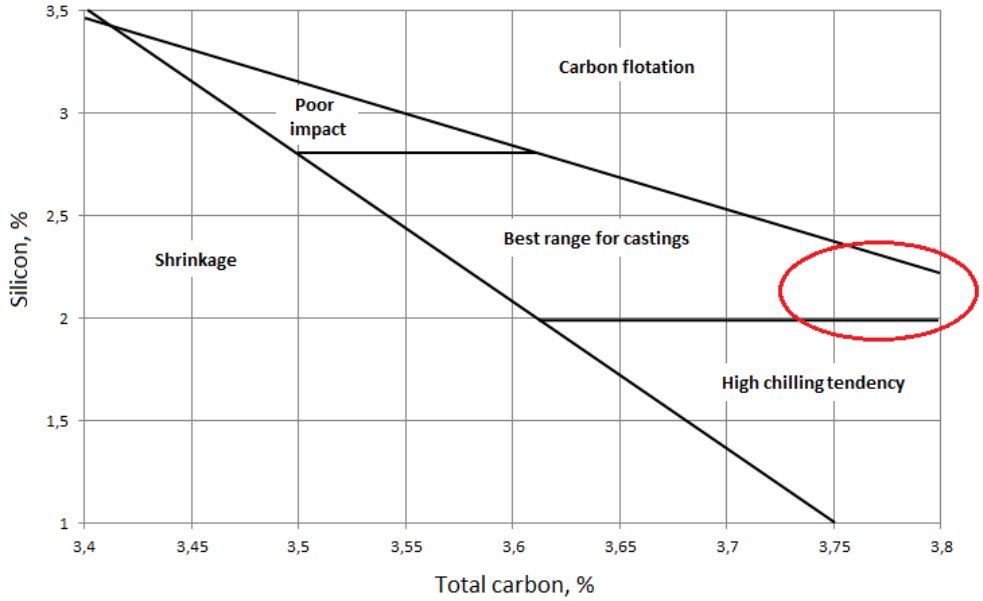

Figure 14. Diagram for best Si/C ratio. The red ellipse shows where main shafts are placed. Adapted from [7]**.**

2.3.2.3 Alloying Elements

Depending of the result from spectroscopy analysis 1 (F) different types and amounts of alloying elements are added to the melt in the furnace. Calculations of how much FeSi, FeMn, FeS and graphite that should be added are made by operators who should obtain a melt with a chemical composition within the limits seen in Table 1 for spectroscopy analysis 2 (P).

2.3.2.4 Mg Treatment

The Mg treatment is of high importance if graphite nodules are to form and the cast is to get the requested ductile properties. The Mg treatment (FeSiMg alloy) is an in ladle treatment that starts when the melt has reached the correct chemical composition and temperature and is poured from furnace to ladle. In Figure 15 it is shown how the FeSiMg is placed in the ladle and where the melt is poured in. Inoculation (alloy containing Ba, Ca, Si) and Sb are placed in the ladle along with FeSiMg and finally everything is covered with iron ingots to avoid a violent reaction of Mg. Another step taken to get a non-violent Mg reaction is that the melt always is poured into the ladle at the opposite side of the treatment, lowering the velocity of the melt when it reaches the treatment.

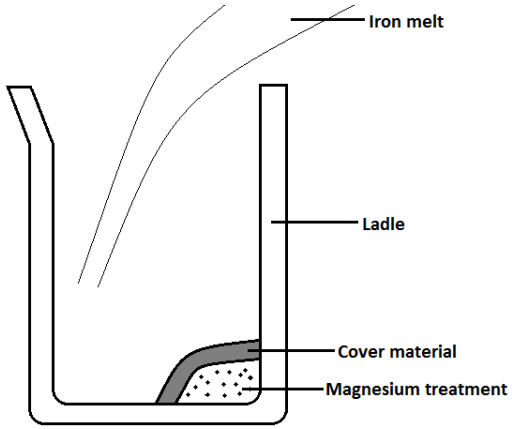

Figure 15. In ladle Mg treatment (FeSiMg). Melt poured at the opposite side of the alloy.

The FeSiMg used at GCGAB contains 4.5 to 4.75 wt.% Mg and up to 1 wt.% Ca (the inoculation contains additional Ca) which is equal to approximately 0.052 wt.% Mg and 0.012 wt.% in the melt. Both Mg and Ca are two elements highly reactive with S and O forming MgS, MgO, CaS and CaO. As the melt is poured into the ladle Mg and Ca starts to react with O contained in the melt and due to the low density of O the new formations surfaces as slag. After the melt has been deoxidized Mg and Ca reacts with S forming the MgS, CaS nodule nuclei. Normally 0.01 wt.% of S remains in the melt after excess S slag has been removed from the surface, enough to get a sufficient amount of nodules in the cast [7]. Slag removed from the ladle also contains Al and Si oxides along with slag remained from previous melt.

As the ladle is transported from the furnace to the location of the mould Mg continuously fades as it reacts with O at the melt surface. Mg also evaporates since it has a boiling point of 1,090 °C and the melt temperature is in the region of 1350 to 1480 °C. Due to thermal convection the melt constantly moves in the ladle when the melt temperature starts to decrease and colder metal gets a higher density and circulates downwards in the ladle, Figure 16 [6].

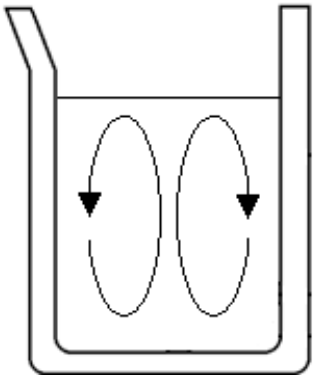

Figure 16. Thermal convection in the melt during Mg treatment in ladle.

Warmer metal has a lower density and therefore circulates upwards in the ladle resulting in a continuous fading of Mg. New MgS that reach the surface is dissolved when Mg reacts with O, leaving residual S in the iron melt. Melt poured into a ladle with good condition (low thermal conductivity) gets a slower convection rate than melt in a worn out ladle which has a higher conductivity [6].

Convection due to the starting temperature of the melt, from furnace to ladle, also has an effect on the rate of Mg fading. A higher melt temperature has a lower viscosity and circulates in a higher rate than a cooler melt. At a higher melt temperature convection increases the Mg fading [6]. From the point when melt is poured into the ladle and Mg treatment starts, it is estimated that the melt should be poured into mould within 20 minutes to ensure that enough Mg remains in the melt for a sufficient nodule count. About half way in to the treatment the wt.% Mg in the melt is at its maximum (around 0.05 wt.%) if the melt has been stirred sufficiently. At Mg levels above 0.04 wt.% carbides can, however, start to form, decreasing the casts material properties [7].

The recommended wt.% Mg when the melt is poured into mould is seen in Figure 17. A DCI with 90 to 100 % spheroidal graphite (as for the main shaft) should contain 0.030 to 0.04 wt.% Mg. A residual Mg of 0 to 0.01 wt.% results in grey iron with graphite flakes and between 0.01 and 0.025 wt.% mainly chunky graphite will form and a compacted graphite iron. If the Mg is not evenly distributed in the DCI melt local areas with flake graphite or chunky graphite can form [7]. At 3 to 4 minutes into the Mg treatment the spectroscopy 3 (S) analysis is conducted, desired results are seen in Table 1 (it should be noted that the 3 (S) result is before Mg fading, and is not representative to the graph in Figure 17.

.

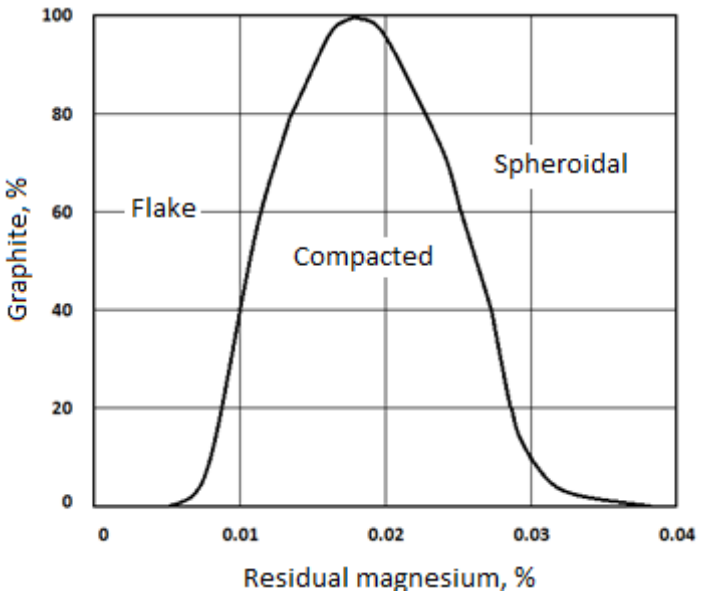

Figure 17. Residual Mg as a function of requested % graphite. A DCI should contain spheroidal graphite nodules. Adapted from [7]**.**

2.3.2.5 Inoculation in Pouring Box

Extra inoculation is added to the melt when it is poured into the pouring box. A 30 kg inoculation ingot containing Si, Al, Ca and Bi is used to ensure that there are enough inoculants in the melt to achieve fully spheroidal nodules. When the melt is poured into the box the inoculation ingot slowly melts, resulting in an even mixture of inoculants in the melt. The effect of the in box inoculants depends on for example the chemical composition of the melt, cooling rate and pouring temperature. The inoculant starts to fade immediately after it has melted, in which rate depends on reasons previously mentioned [2].

2.3.3 Common Elements in DCI

In Table 2 a typical result from a spectroscopy 3 (S) analysis at GCGAB is seen (Ca, O and N are not registered in Guldsmedshyttan). The measurement accuracy varies depending on the interest for a specific element (usually linked to the effect an element has on the melt and the final cast). In the following text, elements of extra interest when it comes to effect on the melt and on cast defects and are presented. The sum of elements in Table 2 exceeds 100 wt.% as Si and P are included in C_{TL}, see page 13.

Table 2. A typical result from a spectroscopy 3 (S) analysis at GCGAB

%Al	%As	%B	%Ca	%Ce	%Co	%Cr	%Ctl	%Cu	%Fe
0.005	0.001	0.0002	0.0018	0.003	0.016	0.03	3.86	0.01	93.93
%La	%Mg	%Mn	%Mo	%N	%Nb	%Ni	%O	%P	%Pb
0.001	0.042	0.19	0.00	0.009	0.006	0.03	0.0006	0.021	0.0008
%S	%Sb	%Si	%Sn	%Te	%Ti	%V	%Zn	%Zr	Ctemp
0.011	0.003	1.99	0.00	0.001	0.014	0.01	0.001	0.00	1135

2.3.3.1 Antimony (^{51}Sb)

Sb is added in the ladle with the Mg treatment as a spheroidization element. Excess Sb can form a lamellar structure, shell, in the area around the nodules which slows down the diffusion of C from the austenite phase. A thicker Sb shell reduces the diffusion of C in a higher grade than a thinner Sb coating. If there is excess Sb and the coating of the nodules gets to thick, the material can solidify before the austenite has turned into ferrite which results in a partly pearlitic matrix. An addition of Ce promotes the spheroidizing qualities of Sb in DCI and prevent Sb deterioration which start to occur over 0.004 wt.% Sb [18].

2.3.3.2 Boron (^{5}B)

B is an element with strong carbide forming properties which at levels around 0.003 wt.% can result in intercellular carbides. Carbides harden the material and thereby lower the ductility. Carbides derived from B are very stable which makes annealing an inefficient method for dissolving of these carbides. For DCI's, B is unwanted and can be traced back to scrap material and/or pig iron used in the charge material [2]. The chemical composition of the manufactured main shafts contains 0 to 0.0005 wt.% B.

2.3.3.3 Calcium (^{20}Ca)

Traces of Ca can be found in charge material but is mainly added to the melt at GCGAB through the FeSiMg and inoculation treatment. Ca is normally used for desulphurization (excess CaS that is removed from the melt as slag) and what Ca that remains is included in the graphite nodulization process. Residual Ca can lower the risk of graphite flakes as Ca reacts with any free surrounding S (usually in areas containing dross) which otherwise promote graphite flakes instead of nodules [7].

2.3.3.4 Carbon (^{6}C)

A standard value of C in DCI is 3.4–3.8 wt.%. At GCGAB C_{TL} (calculation which includes the equivalent C_E) is used instead of the wt.% C. If $C_E < 4.3$ wt.%, the Fe is hypoeutectic and primary forms dendrites, if $C_E > 4.3$ wt.% the DCI is hypereutectic and primarily graphite nodules will grow instead of dendrites (normally around 4.4 – 4.5 wt.%). As seen in Figure 14 a high C_{TL} can lead to C flotation and a low value can cause shrinkage and chill [7].

2.3.3.5 Cerium (^{58}Ce)

Ce is a rare earth metal included in the FeSiMg alloy used for the Mg treatment. Ce promotes the spheroidization qualities of Sb. Ce is reactive with N, P, As, Sb and Bi and to ensure that the Sb/Ce ratio

remains relatively constant the mentioned elements, except Sb, should be kept as low as possible [18]. Ce also bonds with S and O and can function as nuclei for graphite nodules [8].

2.3.3.6 Chromium (^{24}Cr)

Cr is normally used in stainless steels to increase corrosion resistance and is also a strong carbide promoting element. Cr and Mn forms carbides in approximately the same rate so at higher Mn percentages in DCI the Cr content should be kept to a minimum to avoid a reduced ductility. Carbides formed due to Cr can often be dissolved by annealing but if the Cr content becomes higher than 0.1 wt.% heat treatment is no longer effective. To avoid carbides at 0.03 wt.% Cr (as in the main shaft) a Si content at the higher recommended level can reduce carbide formation and instead the Cr will slightly increases the materials corrosion resistance [2].

2.3.3.7 Copper (^{29}Cu)

In a fully ferritic DCI Cu should be minimized (maximum 0.03 wt.% if it comes via scrap material). In charge material containing Cu other unwanted elements are often present such as As, Pb and Te. Cu is a high pearlite promoting element often used to reach a fully pearlitic matrix. Cu does not lead to formation of carbides and can in lower amounts contributes to graphite spheroidization [2].

2.3.3.8 Lead (^{82}Pb)

Pb in the range of 0.002 wt.% can cause graphite flake defects in DCI's, lowering the ductile material properties. At levels below 0.002 wt.% Pb an inefficient stirring of the melt can lead to a higher accumulated wt.% Pb in parts of the cast volume, resulting in local graphite flake defects [2]. Graphite flakes has been observed by GCGAB in the main shafts but not to a deleterious level.

2.3.3.9 Magnesium (^{12}Mg)

A recommended wt.% Mg after fading is 0.035 – 0.04 wt.% if the initial S content has been below 0.015 wt.% (otherwise the wt.% Mg should be 0.04 – 0.06 wt.%). If the Mg content is lower than the recommended, spheroidization might not take place to the desired extent and graphite accumulations can form. If the wt.% Mg is too high there will be excess Mg in the melt which then form dross or carbides [7]. Except fading of Mg, evaporation takes place due to the high melt temperature (approximately 1,470 °C) as the melt is poured into the ladle. Mg has a melt point at 1,090 °C and the relatively violent reaction when the melt reaches the FeSiMg alloy results in a decrease of wt.% Mg. The evaporation must be taken into account as the required FeSiMg for the Mg treatment is calculated [2].

2.3.3.10 Manganese (^{24}Mn)

Mn is usually derived from scrap material or added to the melt as a FeMn alloy. At wall thicknesses of up to 40 mm the wt.% Mn can vary depending on Si content and wall thickness, for example does a wall thickness of around 10 mm and 4 wt.% Si allow a Mn content of up to 0.5 wt.%. In heavy section castings, such as the main shaft, the maximum recommended Mn level is constant at 0.26 wt.% at a wall thickness increasing 60 mm [2]. Mn over the recommended limits promotes segregation, pearlite formation and lower ductility in heavy section castings as carbides forms in the grain boundaries and hinders the ductility [7].

2.3.3.11 Molybdenum (^{42}Mo)

Mo can be derived from the charge material. For ferritic heavy section castings Mo leads to carbides in a higher range than for thin walled castings (especially at levels over 0.3 wt.% or in combination with Cr, V and Mn). Mo increases hardenability and lowers the ductility for DCI. Mo is usually only added (1-2 wt.%) in materials where a martensitic microstructure is requested or to get a material with an increased tensile strength at elevated temperatures [2].

2.3.3.12 Nickel (^{28}Ni)

Ni is usually kept to a minimum in ferritic DCI as Ni lowers the solubility of C in Fe. Ni promotes nodule growth at lower levels but it also promotes a stabile austenitic matrix which can lead to residual austenite in

the ferritic matrix. Additions of Ni often results in a harder cast as Ni increases chunky graphite formation rather than spheroidal graphite. Ni is an unwanted element in the main shaft melts but is brought in with the scrap material and then often together with Cr since the combination often is used to get a hard material with carbides in a soft austenitic matrix [2].

2.3.3.13 Nitrogen (^{7}N)

N is an extreme pearlite and compact graphite promoting element. It increases chill and easily reacts with rare earth metals, lowering the recovery of these metals. Pinholes derived from collapsed N gas inclusions can often be seen in castings where N is higher than 0.00013 wt.%. The effect of N can be reduced with additions of for example rare earth metals and titanium but if possible N should be avoided completely by ensuring that the mould, furnace and scrap material are free from N [7].

2.3.3.14 Phosphorus (^{15}P)

P functions as nuclei points for nodule growth, a standard recommendation is a maximum level of 0.03 wt.%. As P increases the materials hardenability and brittleness also increases [7]. P and Fe form steadite (Fe_3P) that, during solidification, segregates to the grain boundaries resulting in a more brittle material. The effect of Fe_3P is normally noticed at P levels above 0.03 wt.% and for heavy section castings Fe_3P severely can reduce the materials ductility (at 0.06 wt.% P the ductility properties has been divided in half). An addition of 0.01 wt.% P can form 0.064 wt.% Fe_3P. A higher level of P also increases porosity, pearlite and reduces the materials toughness. Some defects derived due to P can be reduced by heat treatment but the guideline is to always minimize the wt.% of P in the charge material [2].

2.3.3.15 Silicon (^{14}Si)

Si is added to the melt via scrap material, alloying elements, Mg treatment and inoculation. The recommended amount of Si in DCI is 2.0 – 2.8 wt.%. The wt.% Si must be adapted to the C_{TL} as Si is part of the C equivalent. A wt.% Si at the higher recommended level prevents carbide formation but over the recommended amounts Si lowers the material ductility resulting in a more brittle and hard material. A wt.% Si below recommendation increases the ductility of the material but carbides can start to form [7].

2.3.3.16 Sulphur (^{16}S)

S is vital as nodalization agent and is derived through the charge material and FeS alloy. The wt.% S in the initial (charge material) melt should be kept at low levels to avoid slag, therefore the FeS is not added in the furnace until the melt is starting to reach the pouring temperature . The recommended wt.% S, applicable for main shaft melts, as the Mg treatment starts is set to a maximum of 0.015 wt.% [7].

2.3.3.17 Tin (^{50}Sn)

Sn is derived from charge material and is not desired in ferritic DCI's due to its pearlitic promoting properties. A melt containing 0.03 wt.% Sn can result in a fully pearlitic matrix with no carbides, so for a pearlitic DCI, Sn is a very effective element [2].

2.3 Dross

In this section dross will be explained further; factors leading to dross formation, dross in the form of bifilm, examples of defects that can be found in relation to dross, how dross effect the casts mechanical properties and in conclusion actions/methods which reduce dross formations. The material in this section is as far as possible selected on the basis of main shafts at GCGAB; manufacturing procedure, material and surrounding environment.

2.3.1 Factors Contributing to Dross Formation

O, melt temperatures and Mg are in research often presented as factors contributing to dross formation. The main reasons to why dross forms are relatively known within the foundry industry but since each foundry has its own melt formula and production method it is hard to establish where in the process dross forms and which factors that are causing the problem [6]. In the following text, some known dross promoting factors are presented as well as common types of dross.

O reactions; dross forms when O derived from the surrounding environment reacts with elements in the melt. Mg, Ca, Al, Si, Mn and Fe are elements included in a DCI melt and which are highly reactive with O. These elements are often found, to some extent, in each dross formation [1]. Turbulence increases the melts exposure to O, resulting in dross particles. A higher pouring height and thus pouring velocity (see page 20) when melt is poured into the pouring box results in a more turbulent melt inside the box. A varied flow also increases turbulence as do edges and bends along the gating system which increases the O level of the melt and the risk of larger dross formations [19].

Mg treatment; dross is a wider problem within DCI manufacturing than in production of grey or malleable iron, this due to the Mg treatment used for DCI's. Mg is highly reactive with O and the more Mg that is exposed to O, the higher the risk for severe dross formations. Excess Mg does automatically not lead to dross, however, if the temperature of the melt is higher and the circulation increases there will be more Mg in the melt that can react with O [19].

S; reactions; when there is a low O level in the melt MgS and CaS starts to form (the nodule nuclei). MgS and CaS can be found in dross formations if the particles has clustered in a turbulent area. Sulphides forming dross can also be a result of rapid solidification where the nuclei not have had the chance to get evenly distributed throughout the melt [1].

Temperature; melt temperature, both when poured into ladle and mould, affects dross formation. A high melt temperature leads to (as previously mentioned) an increased exposure of O and more dross particles. When the melt is in the ladle, dross particles forms a film on the melt surface which get thicker as new Mg, Mn, Al, Si and so forth reacts with O. When the surface film gets to thick the dross particles start to cluster (usually at a melt temperature reaching 1,350 °C). If the melt is poured into the mould at a temperature approaching 1,350 °C there is a risk that clustered, larger, dross formations ends up in the cast. If the temperature drops to 1,290 °C the dross formation has become severe and the whole surface is covered with dross. To avoid the risk that parts of the dross film follows the melt into the mould, it is of importance that the slag/dross film is removed from the melt surface before pouring [6].

Common dross particles: depending on melt temperature and chemical composition different types of dross forms, the most common type is $MgSiO_3$ and $MgSiO_4$. Plain MgO, FeO, Al_2O_3, SiO_2, MnO, CaO and other compositions can be found in or attached to dross formations. At O levels of 0.0003 to 0.0004 wt.% in the melt $MgSiO_3$ and $MgSiO_4$ start to form. Smaller dross particles such as MgO or SiO_2 can start to form in the melt at 0.0001 wt.% O. At higher Si contents (2-3 wt.%) the formation of SiO_2 is often favourable [1]. The level of O is linked to the amount of dross whilst other elements controls the shape of the dross formations [7].

2.3.2 Bifilm

Larger dross formations in a cast can be a result of high pouring velocity and pouring height, as studied by Campbell among others [6]. When melt is poured into the pouring box a thin oxide film starts forming on the melt surface. A film thickness of 20 nm forms within a few milliseconds and if the film is kept intact the layer thickens and the surface tension increases. When the melt is poured at a velocity exceeding the critical velocity ($V_{critical}$) of 0.45 m/s the melt surface will be turbulent and the surface film is pressed downward (at foundries the velocity often is at least 10 times greater than the critical velocity). In Figure 18 two pouring systems can be seen, a gravity system (used at GCGAB) and a counter gravity system. The effect of turbulence on the surface film depends on the melt flow direction [6].

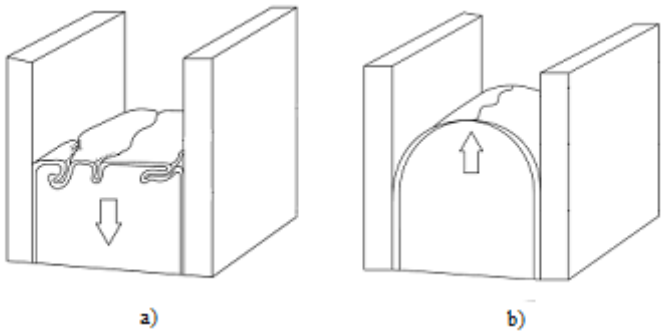

Figure 18. a) Bifilm (from turbulence) in gravity system b) Counter gravity system, no bifilm. Adapted from [6]**.**

If pressure is applied to a surface film in a gravity system the film will start folding (the folded parts are called bifilms). The (usually) thin bifilm often detaches from the thicker surface film and is dragged with the melt through the gating system and into the mould. Bifilms can enclose for example gas, dross particles and slag from the furnace or ladle which due to the films lower density places in the near surface area of the cast. In a counter gravity system the melt is pressed into the system and mould which hinders bifilm from forming. Surface film in a counter gravity system is pressed (instead of folded) along the sides of the ceramic ingate system, never entering the mould [6].

The equations Campbell used in the study of bifilms (critical pouring velocity and pouring height) are seen in Equation (2) and (3). An explanation of the parameters seen in Equation (2) to (4) can be seen in Table 3. The radius of the smallest disturbed surface area, r, could not be measured by Campbell but an approximate radius was estimated to $5.27 \cdot 10^{-6}$ m. Campbell did, however, assume that the critical height is 2 times the radius in Equation (4), forming Equation (5) from (2) & (3), where the radius could be excluded. Metal melts follow the rules of Newtonian fluid mechanics, thereby for calculations of pressures (dynamic, static, height) a standard Bernoulli equation can be used where the sum of all the pressures in a system is constant at zero friction. In the equations below used by Campbell, the melt friction for the specific melt and cast process has been included [6].

$$V_{critical} = 2\sqrt{\frac{\gamma}{r \cdot \rho}} \qquad (2) \quad [6]$$

$$h_{critical} = 2\sqrt{\frac{\gamma}{\rho \cdot g}} \qquad (3) \quad [6]$$

$$r \approx \frac{h_{critical}}{2} \qquad (4) \quad [6]$$

$$V_{critical} = 2\left(\frac{\gamma \cdot g}{\rho}\right)^{1/4} \qquad (5) \quad [6]$$

Table 3. Parameters and typical values used in Equation (2) to (5)

Parameter	Comment	Typical values for DCI
$V_{critical}$	Critical pouring velocity.	0.45 m/s
$h_{critical}$	Critical pouring height.	0.0104 m
γ	Melt surface tension.	1.872 N/m
r	Radius of disturbed surface.	$5.27 \cdot 10^{-6}$ m
ρ	Density of melt.	7000 kg/m^3
g	Gravitational acceleration.	9.81 m/s^2

Bifilm can practically not be avoided in a gravity gating systems but depending on type of melt feed system (bottom or side) the amount can vary. When bifilm ends up in the mould the thin bifilm, in the best cases, completely dissolves and the particles attaches to nodule nuclei. In a bottom fed, low turbulent system, a larger amount of bifilm dissolves than in a system with higher turbulence (such as side fed once). Bifilm can, despite gating system, get trapped in turbulent or fast cooling areas in the mould and thereby not be dissolved at all [6]. For the casting of main shafts a bottom fed system is used.

If the bifilm has entrained gas it can collapse as it starts to dissolve, resulting in shrinkage like porosities containing gas. According to Campbell there are seldom shrinkage in DCI products casted with a bottom fed gravity system, instead it is bifilm mistakenly taken for shrinkage. If dross particles or larger, clustered, dross formations gets trapped in a bifilm the dross formation might still be intact even though the bifilm dissolves. Bifilms containing dross is often located at the surface of the cast or in turbulent areas such as next to the ingate system. Bifilms of this type which remains intact can result in a cast with inhomogeneous and deteriorated material properties. In Figure 19 it can be seen how an intact, dross containing, bifilm has hindered inoculation from distributing evenly. A lack of inoculation has caused graphite flakes (grey iron) in the upper part of the figure whilst there are nodules (DCI) in the lower part of the figure [6].

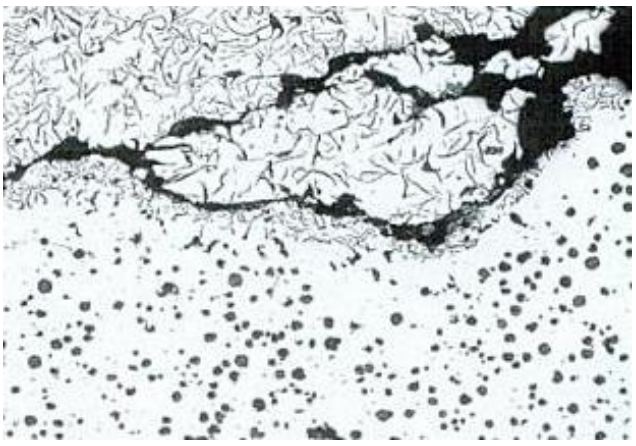

Figure 19. A bifilm (dross) isolating inoculants to the area under the film. x50 magnification, adapted from [7]**.**

2.3.3 Defects Found in Relation to Dross

2.3.3.1 Graphite Flakes

When the melt is exposed to O MgS, CaS and other S molecules can dissolve and instead MgO and CaO forms. The enrichment of S increases in the melt surrounding the MgO and CaO particles which promotes formation of graphite flakes instead of nodules. Graphite flakes is often found in dross containing areas as a result of excess S after a MgO reaction. Graphite flakes also form in melts containing a higher wt.% Si or C, as seen in Figure 14. Graphite flakes has a lower density than the iron melt (just as dross) and therefore often surfaces to the same areas as dross formations. By chemical analysis (for example spectroscopy or EDS) a better understanding can be obtained of from where the graphite flakes appear to have derived. A higher C content can, except from forming graphite flakes, also lead to that the thin C layer which normally covers dross formations increases with increasing wt.% C [1].

2.3.3.2 Chunky Graphite (CHG)

A common defect in especially heavy section DCI's is chunky graphite (CHG). The formation of CHG is a result of excess or insufficient inoculation and Mg treatment. Inoculants are used to insure that the graphite is formed into a sphere. If there is a lack of inoculants (or Mg from the Mg treatment) the graphite will get a more angular shape. A combination of different elements, such as Sb and Ce, have a positive effect on the graphite spherical shape if added in correct amounts (if not, the positive effect can be cancelled out or even promote CHG formation). A high wt.% Mg in the melt can lead to dross and carbides but a low amount can result in CHG (both lowering the cast ductility). Experiments has shown that alloying elements and inoculants such as Ce, P, Sb and La kept at the lowest recommended level generates the most consistent, spherical graphite nodules [18].

In Figure 20 the formation of graphite flakes, chunky graphite and graphite nodules is seen. The chemical composition of the melt controls the shape of the graphite, as mentioned above, and if graphite flakes or CHG has started to form it is not possible to get a correctly shaped nodule. If there are graphite flakes in the same area as the nodules and CHG then flakes will grow faster than both the CHG and nodules as the diffusion rate of C to the flakes are more rapid. Graphite in CHG and nodules are surrounded with austenite from where C diffuses, leaving a ferritic matrix. The growing part of graphite flakes are instead placed outside the austenite grain which increases the diffusion further. To get a high amount of nodules there should only be spheroidal graphite nuclei as solidification starts, this to ensure that C diffuses to the slower growing nodules and not to graphite flakes or CHG [17].

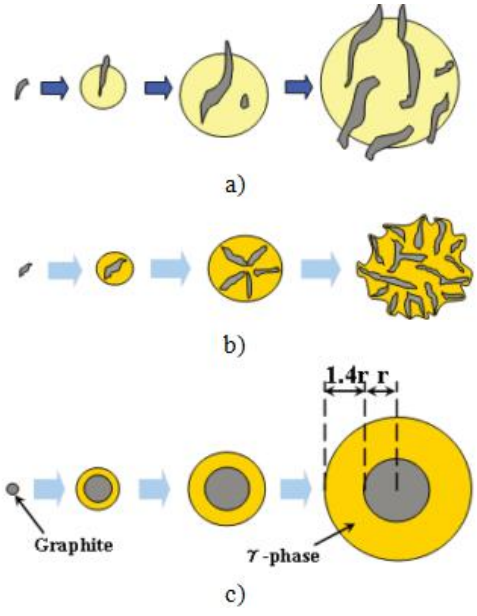

Figure 20. Growth of a) graphite flakes b) chunky graphite (CHG) c) graphite nodule [17]**.**

2.3.4 The Effect of Dross on Mechanical Properties

2.3.4.1 Properties of DCI

In Table 4 mechanical properties for standard grey and ductile iron are presented where variations in properties depending on microstructure are clearly noticeable. Pearlitic areas, graphite flakes or small volumes of grey iron can be found in ferritic DCI's, lowering the mechanical properties of the cast [20]. In Table 4 the experimental mechanical properties of manufactured main shafts at GCGAB can also be seen.

Table 4. Mechanical properties of grey and ductile iron. Adapted from [20]

Cast Iron	Type	Ultimate Tensile Strength (MPa)	Yield Strength (MPa)	Elongation at break (%)
Grey	Ferritic	170	140	0.4
	Pearlitic	275	240	0.4
Ductile	Ferritic	415	275	18
	Pearlitic	550	380	6
Main shaft	Ferritic	415	256	21

2.3.4.2 Fatigue Limit

Since dross mainly is located in the near surface area of castings, studies of how dross effect mechanical properties are often focused on the fatigue limit. Dross functions as surface crack initiation points and studies have shown that for casts containing dross the fatigue limit can be reduced with 20 to 50 % [1]. For the main shafts, the precision lies in the flange since during its use it experiences extensive stress cycles. To avoid a reduced fatigue limit (due to surface cracks) dense slag cannot be larger than 2 mm before machining. Dross formations are not allowed to appear more than 5 % into the flange before machining (this to ensure that all dross particles are removed from the main shaft surface) [13].

The fatigue limit of heavy section wind turbine casts has been studied by Shirani and Härkegård [3] using Weibull's weakest link theory and Weibull distribution. According to Weibull's weakest link theory a single surface crack results in complete failure of a structure. Weibull distribution states that the probability of failure increases with a larger volume or surface area as do the amount of defects. Weibull analysis can be used to estimate the probability of failure at a specific stress amplitude, volume and number of cycles. Shirani and Härkegård showed that Weibull analyzes can be used when estimating the fatigue life of a wind turbine cast. By comparing the Weibull fatigue life of a defect free cast to one containing for example dross, the effect of the amount of dross in these kinds of castings can be predicted before taken into use [3].

Based on the Weibull statements [3] and the requirements regarding dross in the flange [13], dross should be avoided as far as possible in areas exposed to stress since dross can lead to surface cracks and also due to the fact that the main shaft is a heavy section casting with a large surface area.

2.3.4.3 Ductility

Normally yield strength, tensile strength and ductility is controlled by the cast microstructure (amount of pearlite, ferrite and the nodule count and size). DCI's material properties, such as tensile strength and impact toughness, increase in line with nodule count. A homogenous distribution of smaller nodules increases fatigue strength and a high nodule count increases the materials impact toughness [15].

How and if dross contained inside a cast may have a severe effect on the mechanical properties of heavy section castings has rarely been studied. It is usually assumed that any contained dross is in such small amounts that it not will affect the properties of the cast. Dross has, however, been observed in studies of DCI; for example a study where test rods with larger deviations showed to have dross inclusions. The ductility in these samples were reduced by around 30 % compared to the rods without noticeable inclusions

[1]. Another study of DCI, specifically the effect of Mg-O films (bifilm/dross) on ductility, showed that dross reduced ductility in a higher grade than pearlite or nodule defects. By using statistical methods (similar to Weibull) it could be computed that test rods with dross inclusions larger than 2 mm had a 50 % higher probability of failure due to a lowered ductility than rods without any noticeable defects [21].

2.3.5 Methods on How to Reduce Dross Formations

Dross is a problem among DCI manufactures but also in for example aluminium foundries where material highly reactive to O are used. Methods/suggestions on how to reduce dross formations are presented in the literature and by a number of companies. Suggestions that were found on how to avoid dross were for example: lowering the air humidity, using a filtering system, adding small amounts of alloying elements, installing new furnaces and designing new gating systems or moulds [6]. In this section a selection of methods that could be used for the production of main shafts at GCGAB are presented.

2.3.5.1 Ceramic Filters

Until recently it has not been possible to filter melts exceeding 1 tonne because filters could not withstand the high pressure from large pouring weights. Because of higher quality requirements of castings, companies have now started to manufacture ceramic filters specialized on heavy section castings. Filters of this kind have mainly been developed in order to lower the amount of dross and other types of slag inclusions in castings. One example is a zirconium oxide foam filter by Foseco seen in Figure 21. The zirconium filters can withstand 4.7 kg melt per cm^2, to maintain a relatively short pouring time the number of filters has to be adapted to the melt volume. The filters can be used at pouring temperatures up to 1,680 °C. In addition to catching slag, the filters reduce turbulence and the risk of gas inclusions or further dross formation. In the long run filtering of melts lower the amount of disposed casts, reduces machining time and results in a more homogenous material [22].

Figure 21. Zirconium oxide foam filter by Foseco for heavy section castings [22]**.**

Even though manufacturers have a positive attitude towards the use of filters, studies have shown that modifications have to be made to the casting process before filtration becomes an effective method. For example, an adjustment of the gating system and pouring velocity could lower the amount of bifilm in the cast with up to 90 %. Filters in an unimproved system would only capture 10 % of the thin film passing. Filters can ensure a melt with few slag formations but first after improvements has been implemented in problem areas such as those mentioned above [6].

2.3.5.2 Furnace and Ladles

Between maintenance, slag and left over material from previous casts remains in furnace and ladles. If there has been a larger slag build-up after a number of uses this could have an effect of the quality of the upcoming melt. For the ladle, slag and left over material can melt as new material is poured in, changing

the chemical composition of the new melt. Slag/dross can also detach from the walls of the furnace or ladle after the operator has done the final removal of surface slag and it may thereby end up inside the mould. A ladle free from slag and left over material reduces the risk of dross formations. This due to a more chemically stable process and because a ladle in good condition keeps a more stable melt temperature and the convection rate is kept down, limiting the amount of melt that is exposed to O. By properly maintain ladles and furnaces between melts (or when slag starts to build up) defects such as dross or slag inclusions could, to some extent, be avoided [6]. In Figure 22 examples of two ladles in different conditions are shown.

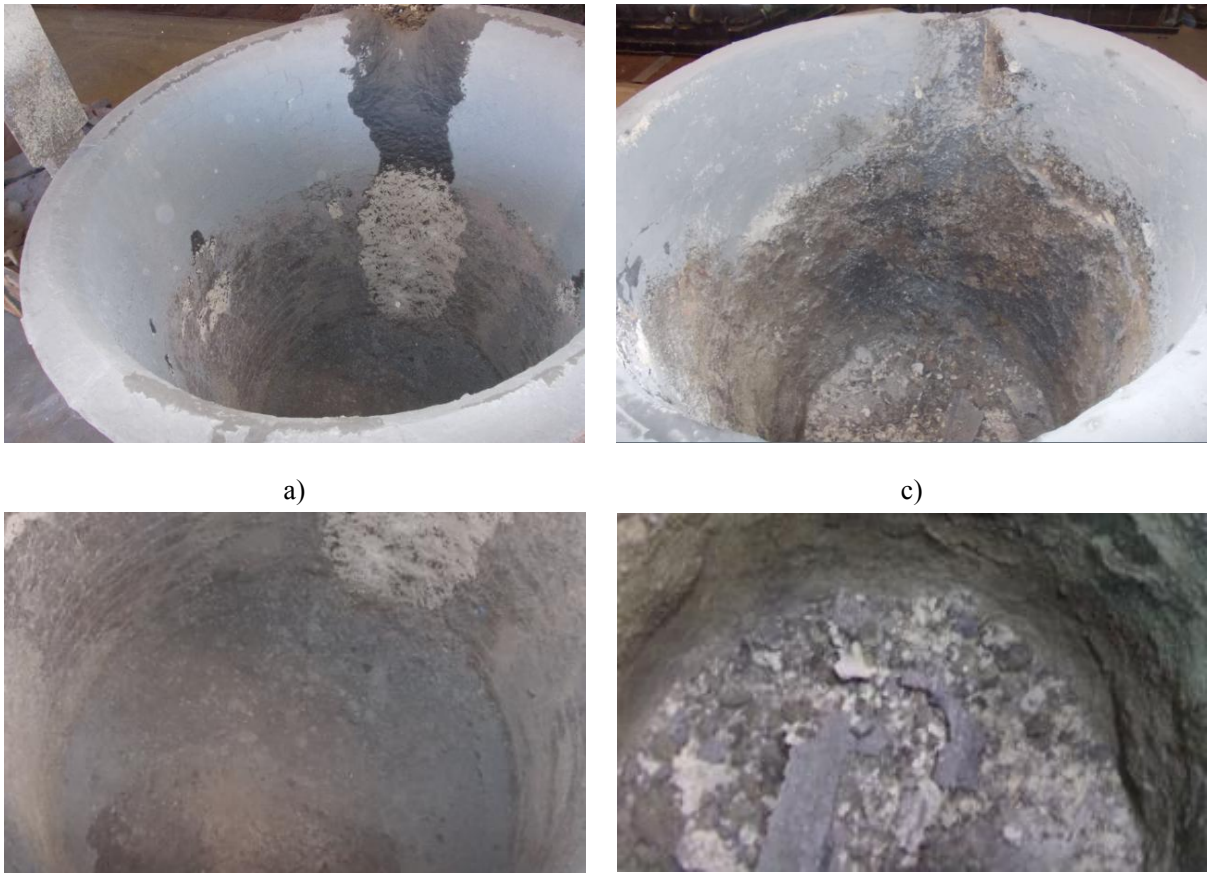

a) c)

b) d)

Figure 22. Melt ladles in production. *Ladle 1:* a) recently maintained, smooth surfaces b) bottom of ladle. *Ladle 2:* c) poor condition, slag at the surfaces d) bottom of ladle, detached slag and left over material.

2.3.5.3 Correct Amount of Mg Treatment

Dross formed as a result of the Mg treatment can be reduced by better adapting the amount of Mg treatment to each specific melt. A better controlled Mg treatment can also lead to material and energy savings as the melt temperature in a more precise way can be adjusted to the treatment, thereby the melt temperature could be lowered in many cases [23]. In Equation (6) a standard equation of recovered Mg (ηMg) in the melt (after desulphurization) is seen. For a MgS bond approximately 76 wt.% Mg and 24 wt.% S is required, hence $0.76(S_I - S_F)$ in the equation [7]. Parameters used in Equation (6) to (8) are explained in Table 5.

$$\eta Mg = \frac{0{,}76(S_I - S_F) + Mg_{final}}{Mg_{added}} \cdot 100 \qquad (6) \quad [7]$$

Equation (7) is developed by the foundry industry and is an extension of Equation (6). In Equation (7) the effect of melt temperature and time has been included and thereby the fading and evaporation of Mg. Instead of recovered Mg, yield of the Mg treatment (R), is used to show the percentage of the added Mg that remains in the melt [23]. The yield of Mg treatment for a DCI is usually around 60 % for a FeSiMg containing 5 wt.% Mg at a melt temperature of 1,450 °C. Fading of Mg is included in Equation (7), c, which usually is in the region of 0.001 wt.% per minute [7].

$$R = \frac{(Mg_{final} + 0{,}76(S_I - S_F)) \cdot 100 + c \cdot t}{Mg_{added}} \cdot \left(\frac{T}{1450}\right)^2 \qquad (7) \quad [23]$$

The wt.% Mg that needs to be added (Mg_{added}) to the melt through the Mg treatment can be calculated if the desired Mg_{final}, S_F and R is set and the initial S is known through spectroscopy. The time should be constant if the transport distance or procedure does not change between melts and the temperature should be kept as close to 1,450 °C as possible to avoid unnecessary Mg evaporation [23]. When Mg_{added} is known, Equation (8) can be used to calculate how much FeSiMg that the operator should place in the ladle for the specific melt.

$$W_{FeSiMg} = \frac{Mg_{added} \cdot W_{ladle}}{Mg_{FeSiMg}} \qquad (8) \quad [23]$$

Table 5. Parameters used in Equation (6), (7) & (8). Adapted from [23]

Parameter	Comment	Unit
ηMg	Recovered Mg from Mg added.	[wt.%]
Mg_{final}	Residual Mg in melt after desulphurization.	[wt.%]
Mg_{added}	Mg added in ladle in wt.% of the whole melt.	[wt.%]
S_I	The melts initial S content.	[wt.%]
S_F	The melts final S content after desulphurization.	[wt.%]
c	Fading of Mg, normally 0.001 wt.%/minute.	[wt.%/minute]
t	Time. From start of Mg treatment to pouring into mould.	[minute]
T	Melt temperature (when poured from furnace to ladle).	[°C]
R	Yield of Mg from Mg added. The same as ηMg but with consideration taken to time and temperature.	[wt.%]
Mg_{FeSiMg}	Amount of Mg in the FeSiMg treatment.	[wt.%]
W_{FeSiMg}	Weight of FeSiMg that should be placed in the ladle.	[kg]
W_{ladle}	Weight of the melt that is going to be Mg treated.	[kg]

2.4 Quality

The quality of each manufactured main shaft is closely monitored, from charge material to finished product. QDA (quality data analysis system), spectroscopy, mechanical and ultrasonic testing are carried out at GCGAB on each product whilst SEM and EDS analyzes mainly are used for main shafts containing defects such as dross or pearlite. The procedures and equipment included in the quality control of main shafts at GCGAB are further explained in this section.

2.5.1 Quality Data Analysis System

During manufacturing, data for each main shaft is gathered and stored in a quality data analysis system (QDA). Information regarding for example charge material, the melts chemical composition, melt temperature, operators and forming can be found in QDA along with results from tensile, impact and ultrasonic tests. The data is used in certificates for each main shaft (provided for the customer), for statistics of consistency and to locate deviations which can explain possible defects.

2.5.2 Arc Spectroscopy

An excitation arc spectrometer is used at site at GCGAB during the preparation of each melt. The spectrometer is used in analyzes of chemical compositions by measuring wavelengths excited from a material sample. For chemical analyzes of solid metal samples the most commonly used instrument is an arc spectrometer. A coin sized sample, Figure 23, is placed in the spectrometer where an electric discharge between the sample and a tungsten electrode generates vaporized atoms. Numerous spectrums are detected by the spectrometer as the excited atoms goes through a diffraction grating, each spectrum representing an element. A spectrum containing certain intensities and wavelengths corresponds to a wt.% of a specific element [24].

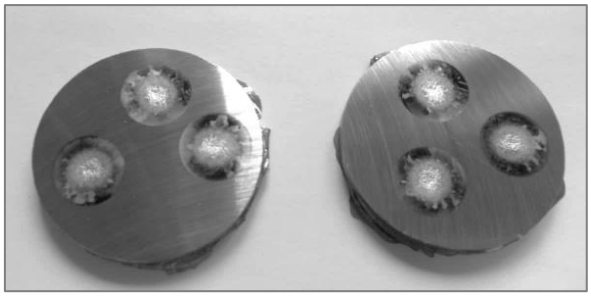

Figure 23. Coin sized (27 mm diameter) metal samples analyzed in an arc spectrometer.

2.5.3 Infrared Spectroscopy

Infrared spectroscopy is a non-destructive test method (NDT) that can be used for chemical analyzes of materials for which a, for example, arc spectrometer cannot register due to high frequencies and long wavelengths. In this type of analysis a infrared beam is run through a sample where a specific type of molecules in the sample can absorb a specific IR frequency. The molecules start to vibrate as a result of the increased energy in the molecules due to the absorbed frequency. By using a harmonic oscillator the resonant frequency of the molecules is measured which corresponds to a element.

A infrared spectrometer can (unlike the arc spectrometer) be used for both solids, liquids and gases and is used for metals when the wt.% of gases such as O and N in a melt is of interest [25].

2.5.3 Ultrasonic and Mechanical Testing

2.5.3.1 Ultrasonic Testing

Ultrasonic testing is a NDT method for detection of defects in near surface areas, used for every GCGAB manufactured cast to control any quality deviations. During ultrasonic testing an operator scans a probe over the cast surface from which high-frequency sound waves are emitted into the cast. When the sound waves reach a defect or the back wall of the cast they are reflected back to the probe. Energies from the reflective waves are shown on a monitor where the energy level varies depending on for example the material and thickness of the cast, the distance to the defect and type of defect [9].

Defects such as pores, cracks, delamination between nodules and matrix, shrinkage, dross and graphite flakes can be detected by ultrasound and are clearly shown on a monitor as these types of defects results in a clear reflection. Uneven inclusions and other types of inhomogeneity can also be registered during ultrasonic tests but the signal is not as clear as for previously mentioned defects due to a higher energy loss. It is hard to know exactly what types of defects the registered energies corresponds to; x-ray or material samples from the defect area could present more knowledge about the specific defect if it is of interest [9].

2.5.3.2 Mechanical Testing

Standard impact, tensile and hardness tests are performed on each main shaft at GCGAB. Test bars with a diameter of 14 mm are used for tensile and impact tests, a smaller material sample is used for Brinell hardness tests. The hardness for a main shaft is around 140 HB. Deviations in the mechanical properties of these material samples because of dross inclusions are rarely noticed.

2.5.4 Electron Microscope and Spectroscope Analysis Methods

Scanning electron microscope (SEM) and energy dispersive spectroscopy (EDS) are analyze methods that are used if more severe defects are detected in the flange of main shafts during ultrasonic testing. This type of analysis is not conducted at site at GCGAB instead material samples are sent to an external company. The results of these analyzes are used to reach a decision on how to proceed with the specific main shaft; if it has to be disposed or if for example machining or heat treatment could be used to reduce the defects.

2.5.4.1 Scanning Electron Microscope

A SEM is used to study for example microstructures, inclusions and fractured samples. In a SEM an image is created as a focused electron probe scans over a sample placed inside a vacuum chamber. In Figure 24 a schematic of a SEM is seen with focus on the main parts; electron gun, condenser lens, scanning coils, probe lens, specimen stage and detectors [26].

The electron beam generated by the field emission gun has normally an energy of 3-30 keV (depending on for example the sample material). The electron beam is remained focused by the coils and lenses. The electron probe remains focused on the sample by the probe lens. The sample is placed in a vacuum chamber with a pressure of maximum 10^{-6} Torr [26]. The size of samples studied in a SEM can vary from 2 to 100 mm. Samples where microstructure is to be studied are mounted in for example Bakelite and then grinded, polished and etched to obtain a smooth surface. When fractures are to be studied the main preparation is to clean and dry the sample to avoid C contamination in the vacuum chamber [26].

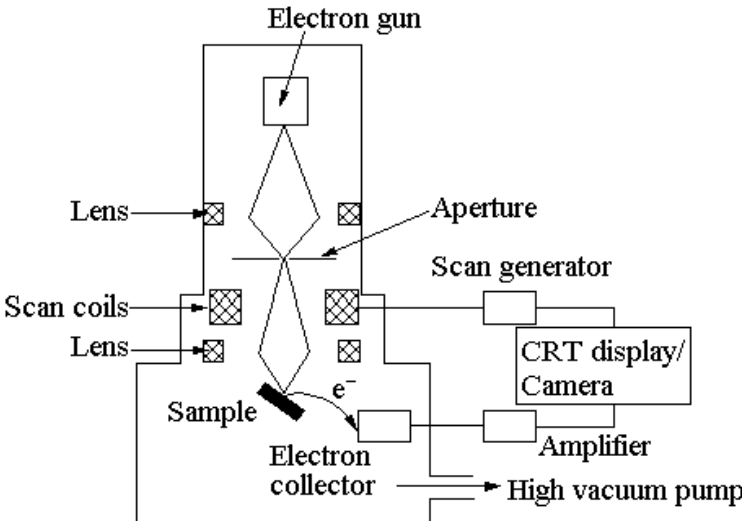

Figure 24. Schematic of a SEM [27]**.**

The image of the sample is build up by scattered electrons (from the scanning electron probe) registered by detectors. Incident electrons reach the sample where elastic and inelastic collisions start between the incident and sample electrons. In Figure 25 the different types of scattered electrons and x-rays resulting from collisions on/in the sample can be seen where secondary electrons are low energy electrons (up to 50 eV) that leave the surface after inelastic collisions with incident electrons. Backscatter electrons (BSE) are a result of elastic collisions where the high energy BSE can scatter from a couple of layers within the surface. The energy level of BSE is in the same energy range as the incident electrons (in keV). It can often be easier to get an image by detecting BSE since, as shown in Figure 25, the number of BSE and the area from where the BSE scatter is significantly larger than for secondary electrons [26].

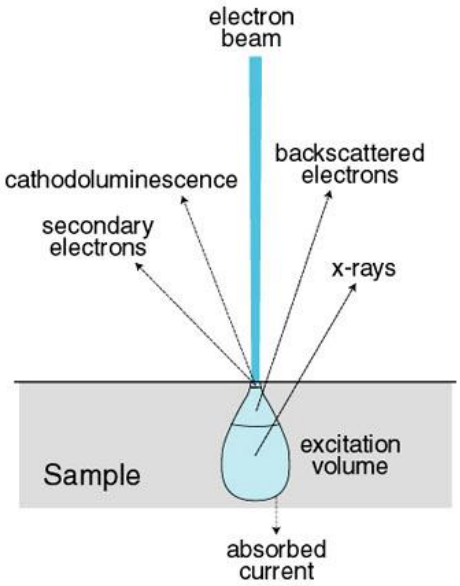

Figure 25. Schematic of scattered electrons and x-rays from a scanned surface in a SEM [28]**.**

When studying a SEM image, materials with low atomic number are shown as darker areas and materials with a high atomic number are shown as brighter areas. The best result when studying a microstructure is achieved if there is a large difference in the atomic numbers of the elements included in

the sample since it increases the contrast [26]. SEM analyzes of main shaft material samples can, in detail, show for example nodule distribution, inclusions, dross and ferritic and/or pearlitic matrixes.

2.5.4.2 Energy Dispersive Spectroscopy

EDS is used to characterize the chemical composition of a material sample. The EDS is a detector that can be mounted inside a SEM and which analyzes photon energies to get the chemical composition of a sample or a particularly interesting part of a sample.

The energy of the incident photon generates an electric charge in a solid-state X-ray detector consisting of semiconducting crystals. As a final step the electric charge results in a current pulse which is shown as a peak in a diagram. The peak created by the pulse is proportional to the incident photons energy and thereby the specific material composition can be analyzed. Numerous photons are registered from the scanned area and the material composition is shown as a peak for each element, presented in weight or atomic percentage [26].

In Figure 26 the steps in the emission of photons are shown. If the incident electron has a higher energy than the atoms ionization energy an inelastic scattering will take place [26].

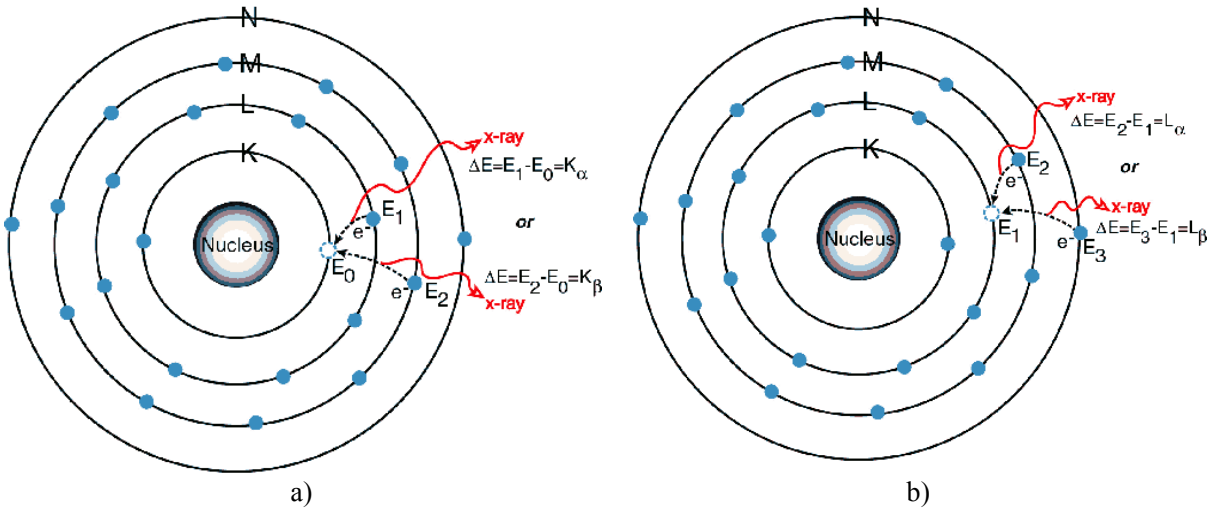

Figure 26. Photon emission, energies registered in EDS showing chemical composition. a) Emission from energy state K b) emission from energy state L [29]**.**

In Figure 26 a vacancy is seen in the K state after one electron has been scattered (a secondary electron) by an incident electron. When the incident electron collided with the electron, the atom gained ionization energy retrieved from the incident electron. The, now, excited atom can reduce its energy by a transition of an electron from a higher energy state to the vacancy in the lower energy state. When electrons transfers from a higher to a lower state, a photon is emitted with the same amount of energy that the atom was excited with. The atom then has no extra energy, but is still ionized as one electron has been scattered. A K_α photon is emitted when the atoms excessive energy is equivalent to an electron transition from the L to K state. If the atom is excited with a higher energy a K_β photon is emitted from the M to K state. A vacancy in the L shell can also be seen in Figure 26. Emissions of L_α (M to L) and L_β (N to L) photons are shown. The EDS registers the emitted photons and presents the possible elements corresponding to the registered energies [26].

CHAPTER 3

Methodology

The methodology during the study of dross at GCGAB included a literature study, analysis of manufacturing data collected by GCGAB and an experimental part. The experimental section was developed on the basis of common causes of dross formations in DCI (found during the literature study) and trends observed during analysis of manufacturing data for main shafts in QDA. The methodology was aimed to answer the following questions (a repetition from the introduction on page 1):

- Which types of dross can be found in the main shafts and which steps in the manufacturing process seems to be most critical for the formation of dross?
- Can any deviations in the chemical composition of the main shaft melt be detected which explains the dross formation?

3.1 Analysis of Data

The data stored in GCGAB's QDA system regarding for example spectrometer results, charge material, Mg treatment, melt temperatures and ladles were studied. The purpose was to find a connection between manufacturing parameters of main shafts containing dross. Data from 380 main shafts were included in the analysis.

3.1.1 Identifying Main Shafts Containing Dross

Before any connections of QDA data could be made the main shafts were divided into four groups; A, B, C and D. The main shafts were divided based on the severity of the dross formations observed by GCGAB in each cast, group A being the most severe and group D being free from any noticeable dross.

To categorize the main shafts, following material from GCGAB was studied: written reports regarding quality faults, results from microstructure and ultrasonic tests and photos of main shafts showing the area containing defects. The groups are presented below:

Group A: Main shafts where larger defect areas were located during ultrasonic test or where dross has been visible on the cast surface. For all main shafts in group A it had been established that the defects were dross formations as the microstructure of material samples (drill samples from the defect areas in the flange) had been analyzed.

Group B: Main shafts where larger defect areas in the flange had been detected during ultrasonic tests. No drill samples were taken from the main shafts in group B but the defects were noticed in the turbulent areas of the flange, as for group A, strongly indicating dross formations. For both group A and B some dross indications could be detected by ultrasonic tests after machining of the cast surface, however, nearly all casts could still be delivered to customer as the amount of dross were acceptable.

Group C: Main shafts for which ultrasonic tests only showed disruptions in smaller, near surface areas of the flange. For the main shafts in group C, all dross formations had been removed during machining and no dross indications could be seen during the following ultrasonic tests.

Group D: All main shafts in group D had been free from any dross indications during ultrasonic tests.

3.1.2 Chemical Composition and Process Parameters

All QDA material regarding chemical composition of melts and manufacturing process parameters were compiled. The content included in the chemical composition and process material were studied separately as well as together in order to find parallels which could explain the dross formed in the main shafts.

3.1.2.1 The Link Between Spectroscopy Results and Dross

During the analysis of the chemical composition of melts, elements highly reactive with O (and thereby likely to increase dross formation) were of extra interest. Elements such as Mg, Si, Mn and rare earth metals were during the literature study found to be connected to dross as well as ratios of for example Mg/Si and Mg/S [1]. The analysis included for example average and median values, linear relations and normal distributions within and between the main shaft groups. For information regarding the chemical composition of each main shaft melt, results from spectroscopy analyzes were used (mainly 3 (S) analyzes which were taken after the Mg treatment had been added to the melt).

The specific melt composition of each main shaft was also studied in order to find a connection between dross formations and the amount of charge material, Mg treatment and inoculation.

3.1.2.2 Variations of Process Parameters

Data regarding melt temperatures, ladles, furnaces and operators was gathered and video recordings of castings were studied (in order to observe slag and turbulence). Studies were made on connections found between manufacturing process parameters which could possibly have caused dross defects.

The information of interest regarding furnaces and ladles was: how many times or days in a row the furnace or ladle had been in use between maintenance and/or reparation. Parallels between the condition of the ladles and an increased dross formation were studied.

Data regarding operators was used to see how accurately the specified range for melt temperatures was followed and if deviations made by the operators could have resulted in dross defects.

Finally video recordings were studied, showing how main shaft melts are poured into pouring boxes. The time it took until the cast lid (placed in the ingate system) melted was of interest as well as how much of the pouring box that had been filled at this point. Turbulence and variations in pouring height and flow was also observed in order to see if this could be linked to that more slag/dross ends up in the mould leading to cast defects.

3.2 Experimental Procedures

The experimental procedures were conducted in order to gather new data to verify the results from QDA analyzes. The experimental part of the methodology included: analysis of dross in material samples, measurements of melt temperatures and analyzes of the chemical composition of main shaft melts (with focus on the Mg treatment). During the experimental procedures conducted at the foundry, notes were taken regarding observations of the manufacturing process and variations in routines between operators and shifts.

3.2.1 SEM and EDS Analyzes of Material Samples

Two types of material samples were prepared for SEM and EDS analyzes, Figure 27. The first type of samples was taken from side casted material of four different main shafts where dross had been located in the flange. The second type of samples was taken from excess material in a turbulent area of an ingate system.

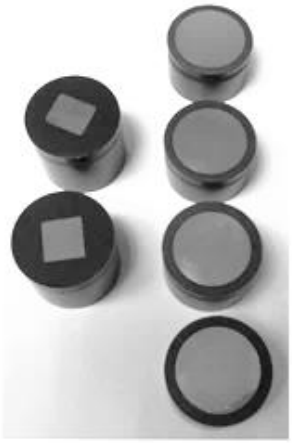

Figure 27. Material samples analyzed in SEM and EDS. To the right, samples from four main shafts. To the left, samples derived from excess material in an ingate system.

The samples in Figure 27 were prepared for the SEM/EDS analyzes by a standard SEM preparation consisting of the following steps:

- Mounting in Bakelite (PolyFast).
- Grinding with a 120 mesh paper with 25 N at 300 rpm, water cooling.

(All grinding and polishing was held at 25 N and 300 rpm.)

- Between each grinding/polishing step samples were placed in ethanol and cleaned by ultrasound.
- Grinding with a 320 mesh paper for 2 minutes, water cooling.
- Polishing with a 500 mesh paper for 3 minutes, water cooling.
- Polishing using a 6 µm spray during 3 minutes, cooling with lubricant.
- Polishing using a 3 µm diamond paste during 3-4 minutes, cooling with lubricant.

For the main shaft samples, the grinding and polishing steps of the preparation had to be done twice as graphite nodules detached from the samples during polishing which scratched the surfaces. The best result was achieved by grinding and polishing each sample separately and thereby lowering the total amount of detached particles which could scratch the sample surface.

The samples were studied with a Zeiss Gemini 1530 SEM and an Oxford INCA EDS. The backscatter detector in the SEM was primarily used to locate small scale dross defects. When defects were detected the EDS was used to acquire the chemical composition of the defect. The purpose with the EDS analysis was to detect elements included in dross formations and which element was the most dominant in a specific dross formation.

3.2.2 Measurement of Cooling Rates

The cooling rate of six main shaft melts were measured in order to detect variations due to the condition of the ladle, start temperature of the melt and the melt weight. The temperature was measured with a portable

test equipment 5 to 10 times for each melt during the transport from furnace to mould (a continuous measurement was not possible due to limitations in the equipment). The temperatures were measured in the centre of the ladle at a depth of approximately 0.1 meters.

Except the time between the measurements, the total and transport time were also of interest in order to see if (for example) a longer transport time could result in more dross defects. The transport time starts as the melt is poured into the ladle and ends just before the melt should be poured into the mould. The total time includes transport time plus the time it takes to fill the mould. The results from the temperature measurements were plotted in diagrams.

3.2.3 Identification of the Amount of O and Ca in a Melt

With the purpose of identifying the wt.% O and Ca in a main shaft melt, coin samples were analyzed by two different methods: arc and infrared spectroscopy. Neither the wt.% O or Ca are analyzed at GCGAB where a Thermo Scientific™ ARL™ 4460 spectrometer is used. Coin samples were taken before the Mg treatment (2 (P)) and during the Mg treatment (3 (S)) from main shaft melt 11D, 12D and 13D.

The wt.% O (and also wt.% N) were examined by infrared spectroscopy analysis in a Leco TCH600. Other common DCI elements were analyzed with a second Thermo Scientific™ ARL™ 4460 spectrometer where the wt.% Ca were included. Coin samples from the same main shaft melts were also analyzed in the spectrometer at GCGAB to detect any differences in the results derived from the two spectrometers included in the examination.

The results from the analysis of wt.% O and wt.% Ca where a Leco TCH600 and a Thermo Scientific™ ARL™ 4460 were used are marked DF (as the analyzes were conducted in Degerfors). The results from the spectroscopy at GCGAB are marked GSH (as the analysis was conducted in Guldsmedshyttan).

3.2.4 Determination of the Usefulness of wt.% Mg in QDA

To determine if the wt.% Mg reported in QDA could be used when studying the reasons for dross formations in certain main shafts, several coin samples were taken from three main shaft melts. Since the wt.% Mg in a melt changes with time it was of interest to examine if a significant change in wt.% Mg could be seen in coin samples taken only a few minutes apart. Two coin samples (3 (S)) were taken from each melt and analyzed with a Thermo Scientific™ ARL™ 4460 spectrometer.

3.2.5 Spectroscopy Analysis of the Final Mg Content in a Melt

In Figure 17 (page 15) it could be seen that the final wt.% Mg (the Mg that remains as the melt is poured into the mould) strongly influence the shape of the graphite nodules. Since Mg is one of the elements causing dross [6] it was of interest to identify if there was a lack of (or excess) Mg when the pouring of the melt into the mould approached.

Coin samples were taken from two main shaft melts towards the end of the transport time. The wt.% Mg in the coin samples was analyzed with a Thermo Scientific™ ARL™ 4460 spectrometer. In addition of the final wt.% Mg, the rate of Mg fading in between coin samples were calculated.

CHAPTER 4

Results

The results from analyzes of QDA material and experimental procedures follow the methodology seen in chapter 3. The reader will, if so found necessary, be referred to specific pages of chapter 3 to clarify the result.

4.1 Factors Resulting in Dross

When the QDA material (method, page 31) for the 380 main shafts was analyzed, three categories appeared for which main shafts containing dross could fit into. Category 1: main shafts with dross due to worn out ladles and/or low melt temperatures. Category 2: main shafts with dross mainly due to an incorrect amount of Mg treatment. Category 3: main shafts with dross as a result of turbulence and/or chemical composition.

No single cause or clear pattern could be found for each respective group (A, B, C, D) in the large number of variables in both the cast material and the manufacturing process. However some loose connections could be found in the data, resulting in the three dross forming categories. All main shafts containing dross were divided into the categories on the basis of what caused the dross formation instead of the severity of the dross defect. In Table 7 (page 38) main shafts representative for each category can be seen. Examples of main shafts that could be placed in respective category but where no indications of dross were found are also included in Table 7. For a complete list of main shafts containing dross, see *Appendix A*.

4.1.1 Category 1: Worn Out Ladles and Low Melt Temperatures

In the analysis of QDA material it was seen that a number of main shafts containing severe dross formations had been prepared in ladles which been used for several melts in a row without maintenance. The conditions of ladles vary and the material from QDA showed that ladles that started to become worn out could not keep the melt temperature. The worn ladles resulted in that the melt reached a temperature below 1,360 °C before it was poured into the mould.

It was seen in QDA that some ladles, without problems, could be used for up to 10-12 main shaft melts in a row (5-8 days) before the melt started to drop in temperature. Other ladles, newly maintained, showed clear signs of being worn out already after a few usages. For the main shafts placed in category 1, worn out ladles and low melt temperatures were seen as the main reasons to the dross defects. The influence of operators in this category is up for further discussion, however, it was noticed that a number of main shafts containing dross had been prepared in worn out ladled at a melt temperature as low as 1,425 °C (the melt temperature at GCGAB should be 1,460 to 1,480 °C).

The cause for dross formation is always a combination of many parameters and the categories show the ones that were deemed most prominent in each case.

4.1.2 Category 2: High Amount of Mg Treatment

In the QDA material regarding melt composition and FeSiMg (Mg treatment) it was seen that up to 12.6 kg FeSiMg per tonne melt had been added in the ladle for several main shafts that contained dross. The recommended addition of FeSiMg at GCGAB is 11.9 kg per tonne melt. The analysis of Mg treatment for

all main shafts showed that a FeSiMg addition in the range of 11.0 kg per tonne melt did not appear to result in dross, at least not due to the treatment (in contrast to excess FeSiMg).

No conclusions could be made regarding if the wt.% Mg from spectroscopy could be used when connecting Mg to dross formations. A Mg reaching 0.042 – 0.046 wt.% was however used as an indication that the Mg levels in the melt had been excessive (in the cases where a FeSiMg in the range of 11.9 kg per tonne melt or increasing had been added to the melt). For the main shafts included in this category the main reason for dross is likely a high amount of Mg treatment resulting in excessive Mg.

4.1.3 Category 3: Turbulence and Chemical Composition

For the main shafts containing dross and which are placed in category 3, one (or several) of following factors have been seen as the main reason to the dross formations:

- Turbulence because of rapid or slow filling of the pouring box and/or due to variations in pouring height and flow.
- A high level of Si and/or Mn.

4.1.3.1 Rapid/Slow Filling of the Pouring Box

During the study of video recordings available for main shafts it was seen that several main shafts where the melt had been poured in a rapid or slow pace contained dross. Dross was not as common for main shafts where the box had been filled in a normal pace. In Figure 28 it can be seen how three different main shaft melts are being poured into pouring boxes, the pictures are taken as the cast lid (the thin metal sheet placed in the ingate system) has melted completely and the box is filled.

The definition of a full pouring box is (in this case) that the box is assumed to be full before the cast lid has melted completely. When melt is poured in rapidly it takes approximately 15 seconds to fill the box all the way up but then the cast lid might not melt until a few seconds later. For a slow filling of the box, the cast lid melts after 20 to 25 seconds but the box is then not more than half full. An average filling time for all main shafts was 25 seconds with 5 cm remaining of the box as the cast lid melted.

A slow filling of the box appeared to be more severe than a rapid filling. More slag/dross from the ladle could be dragged down into the mould when the surface of the melt was closer to the gating system at the point when the cast lid melted. For a rapid filling dross/slag could end up in the mould as a result of turbulence in the box because of a high/varied melt flow.

It was noted that the inoculation stone mounted in the bottom of the pouring box almost exclusively cracked and surfaced when the box was filled rapidly. This did however not seem to effect the formation of dross nor the nodule count, size or shape.

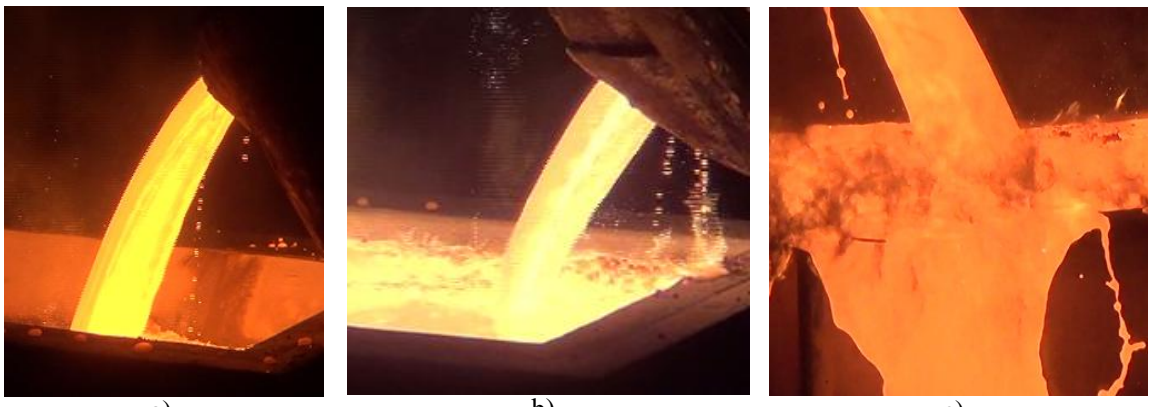

a) b) c)

Figure 28. Filling of the pouring box. a) Slow b) normal, 25 seconds to fill the box c) rapid [13]**.**

4.1.3.2 Variations in Pouring Height or Flow

When the video recordings of main shaft melts were studied it was noticed that there were larger variations during the pouring of the melt for some main shafts containing dross. The varied pouring height/flow could in these cases be found as explanations for the dross defects.

4.1.3.3 A High Level of Si and Mn

Main shafts containing a high wt.% Si (up to 2.15 wt.%) and Mn (up to 0.27 wt.%) showed ultrasonic indications more often than those containing Si and Mn at the minimum recommended level. For casts containing 2-3 wt.% Si the risk of dross formation normally increases [7], which could be seen in the QDA material where main shafts with more than 2 wt.% Si contained dross in a higher range.

High amounts of Mn (and Mg) can result in carbides which during ultrasonic testing indicates defects in the same way as dross [7]. If the main shafts in category 3 contains dross due to Mn or if it in fact is a combination of carbides and dross cannot be established as no drill samples had been taken from these main shafts.

4.1.4 Variations in Pouring Temperatures Among Operators

The result from studying the information of operators available in QDA is seen in Table 6. Average and median melt temperatures (from furnace to ladle) used by each operator are presented as well as the operators deviation from the specified pouring temperature (1460 – 1480 °C). As seen in Table 6 the largest difference in pouring temperature between operators is 13 °C and one operator has deviated from the specification 40 % of the times. Take notice; the number of castings per operator which contained dross cannot be seen as a direct result of how the operator works.

Table 6. Variations in pouring temperatures among operators working on main shafts

Operator	OP1	OP2	OP3	OP4	OP5	OP6	OP7	OP8	OP9
Castings by operator containing dross/noise	9/48	11/62	20/77	15/43	20/82	2/10	0/10	9/48	1/4
% of times the operator poured outside the specified temperature (1,460-1,480 °C)	40%	8%	5%	5%	15%	0%	0%	13%	0%
Average temperature (°C)	1461	1467	1469	1473	1470	1470	1470	1474	1472
Median temperature (°C)	1463	1468	1470	1473	1475	1470	1470	1475	1471

Table 7. Results from analysis of QDA material. Main shafts devided into 3 categories

MS number in Group		Ladle		Melt temp. (°C)			Chemical comp. (wt.%)				Pouring of melt into box/mould		
		Nr.	[2]Used in row	Into ladle	Into mould	[1]FeSiMg Kg/tonne	Si	Mn	S	Mg	[3]Cast lid melt (s)	[4]Height in box (cm)	[5]Turbu-lence
CATEGORY 1 (Ladles & Temperature)													
1	A	6	8	1462	1355	11.1	2.11	0.17	0.01	0.042	30	0	
2	A	2	10	1425	1365	11.0	2.11	0.21	0.01	0.039	24	3	
3	C	2	7	1440	1365	11.7	2.09	0.24	0.01	0.035	31	15	
4	A	2	8	1470	1365	12.0	2.14	0.17	0.011	0.04	23	10	X
5	A	2	9	1440	1365	12.1	2.07	0.18	0.011	0.038	N/A	N/A	N/A
4	C	2	10	1470	1365	10.3	2.16	0.21	0.01	0.036	25	10	
5	C	2	11	1465	1365	12.0	2.15	0.19	0.01	0.036	25	7	
6	C	2	12	1465	1365	12.0	2.14	0.18	0.01	0.037	N/A	N/A	N/A
1	D	6	6	1465	1358	11.3	1.99	0.16	0.01	0.044	N/A	N/A	N/A
2	D	6	10	1480	1358	11.7	1.99	0.18	0.012	0.043	N/A	N/A	N/A
3	D	1	14	1470	1355	12.1	2	0.2	0.011	0.042	17	10	X
CATEGORY 2 (Mg treatment)													
22	C	6	1	1470	1365	12.5	2.16	0.2	0.01	0.038	27	0	X
23	C	6	3	1470	1365	12.5	2.1	0.16	0.01	0.036	22	3	
10	B	6	8	1470	1365	12.5	2.11	0.17	0.011	0.038	25	5	
24	C	1	1	1475	1365	12.5	2.11	0.17	0.011	0.035	30	10	
12	A	1	3	1465	1365	12.6	2.17	0.17	0.012	0.042	18	25	X
13	A	1	4	1475	1365	12.6	2.15	0.21	0.01	0.037	20	7	
25	C	6	4	1465	1365	11.8	1.95	0.16	0.01	0.043	N/A	N/A	N/A
26	C	2	3	N/A	N/A	N/A	1.85	0.18	0.011	0.042	N/A	N/A	N/A
14	A	6	1	1470	1365	N/A	2.06	0.26	0.01	0.046	N/A	N/A	N/A
4	D	6	3	1450	1375	11.6	2.09	0.17	0.01	0.043	26	10	
5	D	1	3	1460	1365	12.1	2.02	0.16	0.01	0.045	N/A	N/A	N/A
CATEGORY 3 (Chemical composition & Turbulence)													
11	B	1	N/A	1463	1370	12.1	2.07	0.19	0.009	0.037	15	0	
12	B	1	1	1450	1375	10.6	2.07	0.23	0.01	0.037	17	P.O	X
11	A	7	N/A	1470	1368	11.2	2.13	0.16	0.011	0.043	27	25	
33	C	1	N/A	1475	1365	N/A	2.08	0.2	0.01	0.037	15	10	X
16	A	2	9	1465	1365	11.3	2.08	0.19	0.009	0.039	20	20	X
34	C	1	3	1470	1365	11.5	2.09	0.27	0.011	0.034	18	10	X
35	C	1	4	1460	1365	11.9	2.15	0.26	0.01	0.038	N/A	N/A	N/A
6	D	6	4	1470	1368	11.4	2.13	0.24	0.009	0.037	23	10	
7	D	2	8	1465	1365	11.3	2.11	0.22	0.01	0.039	25	25	
8	D	6	1	1465	1365	12.3	1.96	0.19	0.009	0.039	22	P.O	X

[1] Kg FeSiMg (Mg treatment) added per tonne melt.
[2] The number of times a ladle has been used for main shafts without maintenance.
[3] How long it takes for the cast lid to completely melt during filling of the pouring box.
[4] How much of the pouring box that remains unfilled as the cast lid completely has melted.
[5] Turbulence in the pouring box due to varied pouring height or flow.

4.2 Results from Experimental Procedures

The results from the experimental part of the study are in line with the analysis of QDA material. The experimental results (regarding for example cooling rates and dross due to Mg) will be used in the discussions to confirm/contradict the categories into which the dross containing main shafts have been divided.

4.2.1 Types of Dross in Material Samples

In the side casted main shaft samples (method, page 33) no dross could be found. The two samples, X1 and X2, from excess material from an ingate system did however contain a number of dross types. The EDS analyzes showed that elements derived from charge material, Mg treatment and inoculations could be part of dross formations. The results from material sample X1 and X2 are seen as representative for the types of dross which can be formed in the main shafts. In Figure 29 and Figure 30 dross formations in samples X1 and X2 can be seen along with the dominate composition of each spectrum. The complete EDS analysis of sample X1 and X2 can be seen in *Appendix B*.

a)

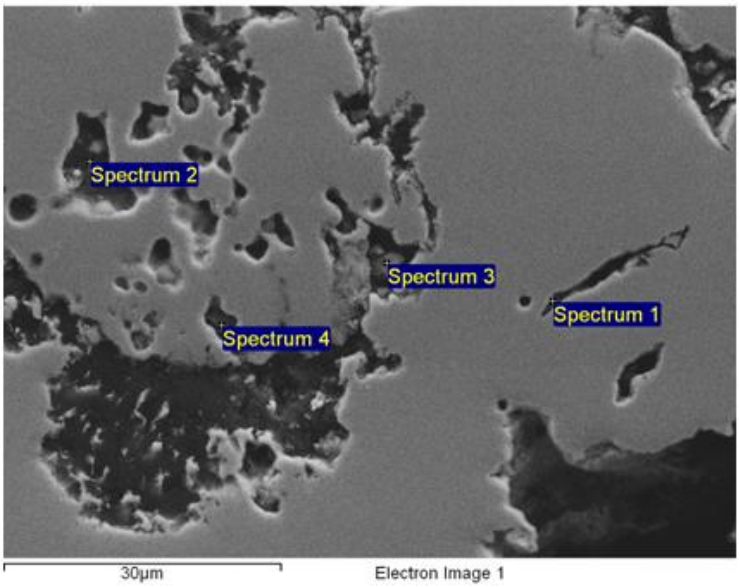

Spectrum	Dross
1	MgO
2	MgO, MgS
3	MgO
4	MgO

Sample X1-1

b)

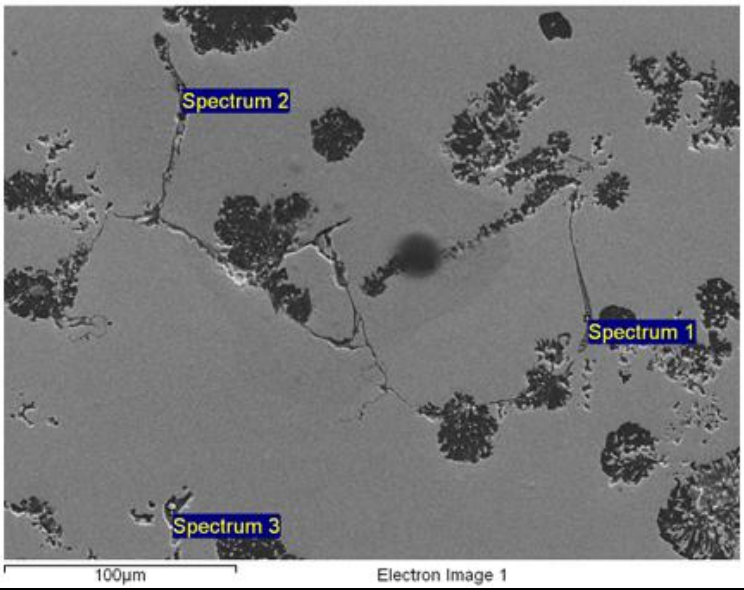

Spectrum	Dross
1	MgO
2	MgO
3	N/A, (hole)

Sample X1-2

Figure 29. Result from EDS analyzes of dross formations in sample X1. a) EDS area 1 b) EDS area 2.

a)

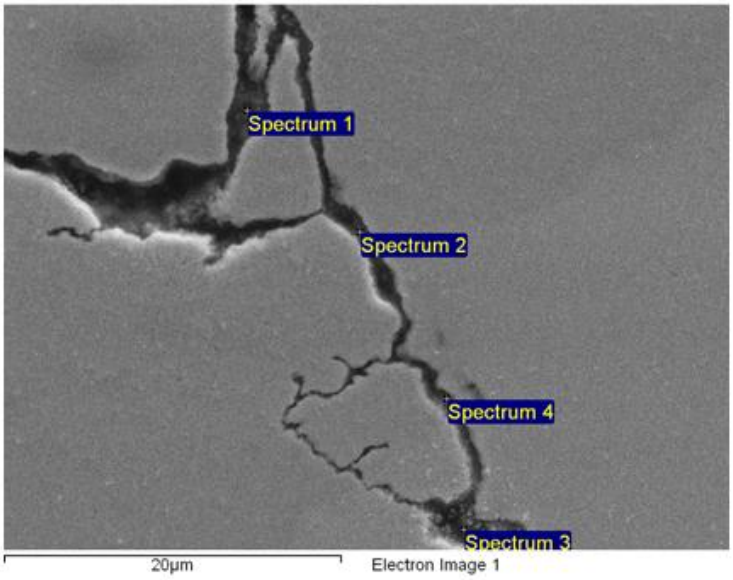

Spectrum	Dross
1	MgO
2	MgO
3	MgO
4	MgO

Sample X1-3

b)

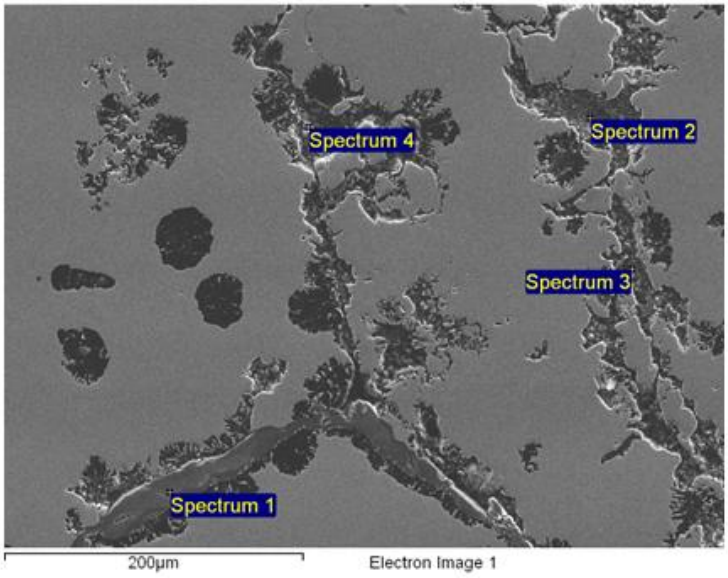

Spectrum	Dross
1	Al_2O_3, CaO
2	MgO, CaO, CaS
3	CaS, MgO, CaO
4	MgO, SiO_2

Sample X2-1

c)

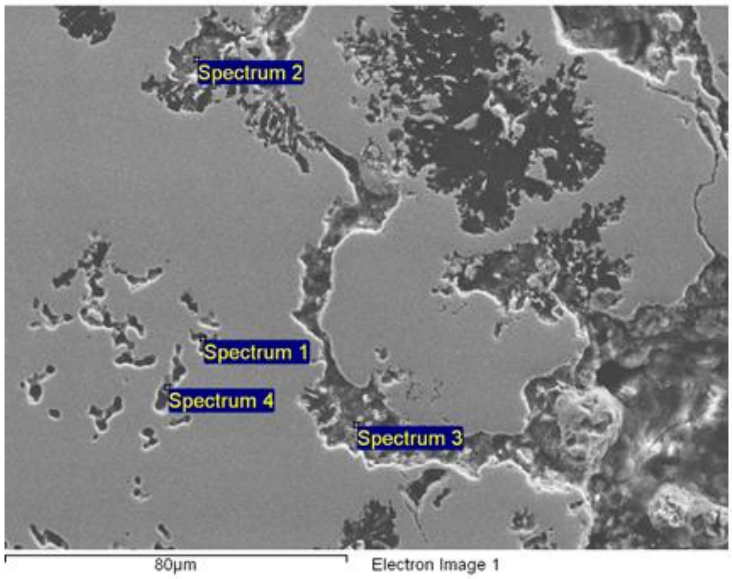

Spectrum	Dross
1	FeS
2	CaS
3	CaS, MgO
4	MgO

Sample X2-3

Figure 30. Result from EDS analyzes of dross formations in sample X1 and X2. a) EDS X1 zoom in on area 1 b) EDS X2 area 1 c) EDS X2 area 2.

4.2.2 Cooling Rates

In Figure 31 the result from the temperature measurements (method, page 33) of six separate melts can be seen. The cooling rate between 0 and 5 minutes (from start of pouring melt into the ladle and 5 minutes forward) is considerably higher than the cooling rate during the transport of the ladle to the mould (5 minutes and forward). Separate diagrams for each melt can be seen in *Appendix C,* where information regarding the ladle, melt weight and pouring times are included.

The cooling rate of the melts showed to be dependent mainly on how many times in a row the ladle had been used without maintenance. Factors such as melt weight, temperature of the ladle before melt were poured in or the start temperature of the melt did not influence the cooling rate noticeably. The melts for main shaft 9D and 10D were prepared in a ladle that had been in use for 12, 13 main shafts in a row. Main shaft 11D to 14D were prepared in ladles used for 3 to 5 main shafts in a row. The cooling rate during the first 0 to 5 minutes varied for each melt, from 11 to 19 °C/min. During the remaining 5 to 25 minutes main shaft 11D, 12D and 14D had a constant cooling rate of 3.8 °C/min whilst main shaft 9D and 10D kept a cooling rate of 4.4 to 5.5 °C/min (no calculation was done for main shaft 11D as there was no consistency during measurements). It should be noted that not all main shaft melts was transported for up to 25 minutes, it was however assumed that the cooling rate during this span would be constant (as the cooling rate 5 minutes until pouring was constant for five out of six melts).

Due to the faster cooling rate for main shaft 9D and 10D the melt temperature had passed 1,350 °C before the melt was poured into the mould. No dross indications were found in these main shafts during ultrasonic tests.

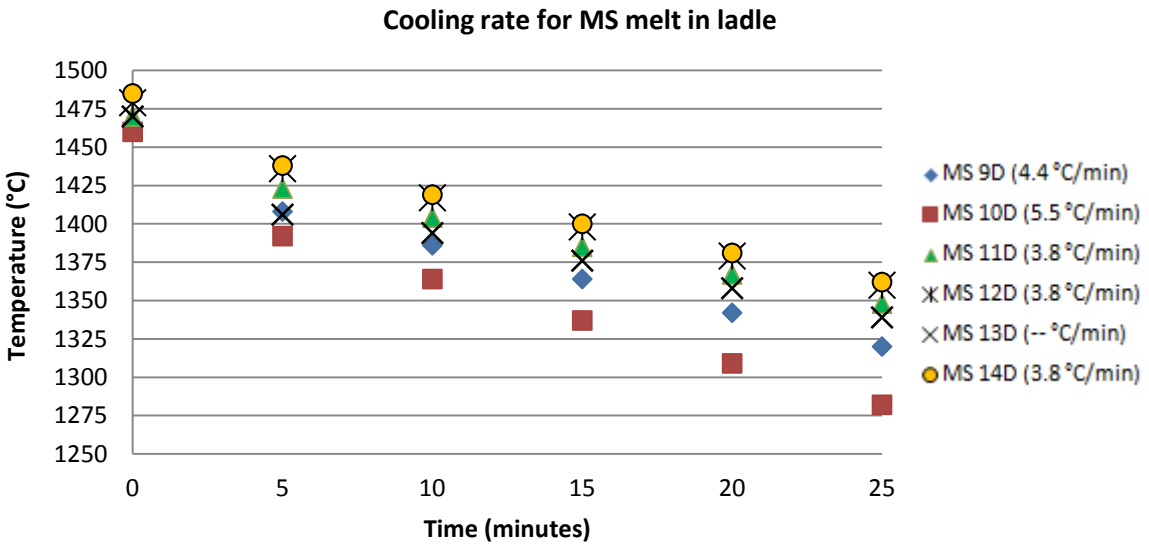

Figure 31. Cooling rates of main shaft melts. To the right: the cooling rates during transport are seen.

4.2.3 Ca and O Analyzed in Coin Samples

In Table 8 the result from analyzes (method, page 34) regarding the wt.% Ca and O can be seen. Variations detected between the two spectrometers used to analyze coin samples from the same melt are included in Table 8. The complete result from the arc and infrared spectroscopy analyzes can be seen in *Appendix D.*

In Table 8 it can be seen that the remaining Ca in 3 (S) coin samples was between 0.0012 and 0.0018 wt.%. Calculations of the Ca added to the melt (through Mg treatment and inoculation) showed a Ca addition of approximately 0.012 wt.% before the start of desulphurization and evaporation. The O level

reduces between 2 (P) and 3 (S) coin samples as a result of deoxidation that takes place when Mg and Ca reacts with O as melt is poured into the ladle [7].

Table 8. Results of coin samples from spectroscopy and combustion analyzes

MS Sample	[6]Type : [7]Location	% P	% S	% N	% Ca	% O
11D	2 (P) : DF	0.027	0.012	0.007	<0.0002	0.0009
11D	2 (P) : GSH	0.022	0.013	N/A	N/A	N/A
11D	3 (S) : DF	0.025	0.010	0.007	0.0013	0.0004
11D	3 (S) : GSH	0.023	0.011	N/A	N/A	N/A
12D	2 (P) : DF	0.025	0.011	0.007	<0.0002	0.0009
12D	2 (P) : GSH	0.022	0.012	N/A	N/A	N/A
12D	3 (S) : DF	0.026	0.009	0.009	0.0018	0.0006
12D	3 (S) : GSH	0.022	0.010	N/A	N/A	N/A
13D	2 (P) : DF	0.026	0.011	0.007	<0.0002	0.0009
13D	2 (P) : GSH	0.023	0.012	N/A	N/A	N/A
13D	3 (S) : DF	0.025	0.01	0.006	0.0012	0.0006
13D	3 (S) : GSH	0.022	0.009	N/A	N/A	N/A

4.3.4 Accuracy in the wt.% Mg Presented in QDA

When the 3 (S) coin samples are taken in the ladle, time is not a factor. In Table 9 the results of the wt.% Mg from three different melts are seen where two 3 (S) coin samples were taken from each melt (method, page 34). It was clearly showed that the wt.% Mg increased with time.

Table 9. Variations in wt.% Mg depending on how long the melt has been in the ladle

Samples	Time (s)	% Mg	% Al	% Si	% S
11D, COIN 1	215	0.038	0.008	1.95	0.011
11D, COIN 2	435	0.041	0.008	1.99	0.01
13D, COIN 1	290	0.035	0.009	2.00	0.009
13D, COIN 2	450	0.038	0.009	2.14	0.01
14D, COIN 1	180	0.036	0.007	1.87	0.01
14D, COIN 2	303	0.043	0.008	1.95	0.011

[6] Type of coin sample: 2 (P), before Mg treatment, or 3 (S), during Mg treatment.
[7] The location at where the sample was analysis d. DF; Degerfors. GSH; Guldsmedshyttan.

4.3.5 The Rate of Mg Fading

The results from analysis of coin samples (method, page 34), showing the wt.% Mg remaining in a melt before it was poured into the mould, are seen in Table 10.

During the time that the Mg treatment is distributed throughout the melt the wt.% Mg increases, as could be seen in Table 9. When the treatment has been evenly distributed the wt.% Mg normally is in the range of 0.05 wt.% [7], thereafter the fading starts where Mg evaporates or forms into dross. The coin 1 sample (standard 3 (S) sample) is not included in Table 10 since the wt.% Mg is still increasing that early into the treatment. The wt.% Mg in coin sample 2 to 4 does however show how the Mg fades and which region the remaining wt.% Mg will be in as the melt is poured into the mould.

The recommended wt.% Mg for a 95 – 100 % nodularity is 0.030 to 0.040, as was shown in Figure 17 [7]. The result from the main shaft melts indicates that the wt.% Mg follow recommendations for spheroidal DCI. The fading rate of melt 1 between coin 2 and 3 was 0.0013 wt.% per minute whilst the rate of melt 2 between coin 2 and 4 was 0.0005 wt.% per minute.

At a closer study of the differences between melts, it was noticed that for melt 1 the ladle had been in use for 6 days while the ladle for melt 2 had been in use for 3 days. The main shaft, casted out of melt 1, contained dross in the flange but it could be removed with machining.

Table 10. Fading of Mg in two main shaft melts

	Melt 1			Melt 2		
	Time (s)	Temp. (°C)	Mg (wt.%)	Time (s)	Temp. (°C)	Mg (wt.%)
START	0	1480		0	1470	
Coin 2	868	1384	0.036	745	1391	0.033
Coin 3	1059	1376	0.032	945	1382	0.032
Coin 4				1080	1377	0.030
STOP	1208			1266		

4.3.6 Notes from Observations During the Experimental Procedures

During the experimental part of the study there were opportunities to observe how operators from different shifts approached the steps included in the manufacturing process. In the following text, observations which could be of importance when it comes to dross formations are presented. The amount of FeSiMg (Mg treatment) that is added to a melt was usually not calculated; instead the operators looked at the amount used during previous melt and used that as a guideline.

The melt temperature, from furnace to ladle, was set differently depending on the operator and situation (which also could be seen in Table 6). Some operators went above the recommended melt temperature, due to a longer transport time, while other operators used a lower temperature for the same transport distance. Some operators used a lower melt temperature if the ladles were newly maintained or a higher temperature if the ladled began to be worn out (others kept a constant melt temperature regardless of the ladles condition).

Melt temperatures and coin samples were taken in the ladles by operators at different times, depths and after different amounts of slag removal. The accuracy during slag removal also differed among the shifts as well as the consistency while melt was poured into the mould.

CHAPTER 5

Discussion

5.1 A Controlled Process

Not many material samples were studied regarding the types of dross that could be found in the main shafts. However, during the analysis of QDA material and experimental results I discovered that it not is possible to find the exact reasons to why dross has formed in some of the manufactured main shafts (hence the dross categories which includes more than one dross promoting factor). It was useful to see that dross particles forms from material added during the whole melt preparation, as seen in Figure 29 and Figure 30 (page 39-40). The best information of which types of dross that can form were derived during the literature studies.

Due to inadequate data regarding O levels, data missing for a number of melts regarding the amount of added FeSiMg, melt weights, temperatures and more it was not possible to establish as to why dross has formed in some of the main shafts.

To obtaining a more controlled process and a better knowledge of the melt and what a specific melt composition can result in a suggestion would be that the operators implement the following ideas into their routines (an explanation to why these parameters/procedures are of interest will be explained further in section 5.2). The final coin sample should always be taken at (for example) 4 minutes into the Mg treatment after slag has been removed from the melt surface. The wt.% Ca could be added to the spectroscopy analysis and variations in the O levels surrounding the melt could be measured. The transport time and the total time for a melt, from the start of the Mg treatment, could be of use when it comes to dross. Overall, all parameters regarding melt weights and temperatures must be more accurately reported by the operators.

One important observation was, however, that the operators in most cases followed the guidelines regarding the casting process at GCGAB but more routines might be necessary now as the focus on product quality constantly increases.

5.2 The Categories of Dross Promoting Factors

The three categories for which main shafts containing dross have been divided into are discussed in the following text. Each category will be discussed separately and experimental results relevant to the category will be included.

In Table 7 (page 38), main shafts containing dross were presented along with main shafts where no indications of dross had been observed during ultrasonic tests. Those main shafts were placed in the table as they had similar manufacturing parameters as those with dross. As was seen during this study, several factors influence dross formation and a melt with (for example) a good chemical composition that had been exposed to just turbulence or just a low melt temperature did often not result in any severe defects.

5.2.1 Theories Regarding Worn Out Ladles and Low Melt Temperatures

5.2.1.1 Ladles and Temperatures

An initial theory regarding the condition of the ladles was that a ladle started to become worn out after a specific number of usages, this was not the case. It seems as if the accuracy during maintenance differ or that the material used during reparations of the ladles do not always keep the same standard since some

ladles can be used during a whole week without problems and others starts degrading after only a few melts.

From the varying results for the cooling rates, depending on the ladles condition (results, page 41), I would say that it is possible to determine if a ladle should be considered worn out. If the cooling rate of a melt approaches 4.5 °C/minute, it would be recommended that the ladle were taken out of production. In the coin sample tests of remaining Mg (results, page 43) it also appeared that the fading of Mg increased in a well-used ladle even though the cooling rate were normal but further studies would be necessary to establish more exactly how the condition of the ladle effects the fading.

The melt temperature has during the study shown to be rather important, more so than first indicated. When the material in QDA was analysed it was seen that a melt temperature, from ladle to furnace, below 1,460 °C was relatively common. No parallel could be found between temperature and dross at first, as a number of main shafts (where a temperature of around 1,450 °C had been used for the melt) did not contain dross formations. When I started to compare melt temperatures to how many times the ladles had been used a pattern could however be seen. For a ladle in good condition (often newly maintained) a melt temperature of 1,450 °C could be used without resulting in noticeable defects in the cast. Low temperatures used for melts in worn ladles did considerably more often result in main shafts with dross defects.

5.2.1.3 How to Avoid Dross due to Temperature and Ladles

Larger dross defects formed due to worn out ladles and incorrect melt temperatures should not be hard to avoid. Operators often know, by experience, when a ladle starts to become worn out. It can both be seen visually and during temperature measurements as the melt cools more rapidly in a worn ladle than in a ladle in good condition. If a ladle is taken out of production as soon as the operators consider it worn the standard of the ladles could be kept more consistent. Of course, extra maintenance probably requires more staff and material which increases the variable costs.

Regarding the melt temperatures, if worn ladles still are used the results from the temperature measurement and QDA shows that it is of extra importance to stay within the specified temperature range. For worn ladles both melt temperature and transport time should be more thoroughly monitored by the operators. This to avoid that the melt temperature does not reach below 1,360 °C before it is poured into the mould, thereby avoiding that dross clusters on the melt surface and ends up in the mould [6]. Perhaps the specification for melt temperatures and transport times could be more customized so that there are specific guidelines available for melts prepared in worn ladles.

If the ladles are kept in a good condition and the operators stay within the specified melt temperature range there should not be any major problems regarding dross formations due to this category. However, even if the recommendations for ladles and temperatures are followed, a slag/dross film still starts to form on the melt surface in the ladle. To avoid unnecessary risks of dross ending up in the mould a strong suggestion would be to remove slag from the melt surface right before the melt is poured in, regardless of melt temperatures or ladle conditions.

A further suggestion to avoid dross/bifilm in the cast would be to use filter systems, as seen at page 24. Filters would probably reduce the turbulence in the melt as well as capture some of the dross but at this stage a filter solution would be a relatively expensive solution as the moulds and ingate systems for the main shafts would have to be redesigned. Since most of the manufactured main shafts do not contain dross defects, the best solution would be to adjust the already existing procedures instead of adding more steps. If dross had been a problem in all casted main shafts a filter system would probably be of a higher interest.

5.2.2 Theories Regarding a High Amount of Mg Treatment

5.2.2.1 Variations in the wt.% Mg in FeSiMg

In the certificates for each batch of FeSiMg delivered to GCGAB the average wt.% Mg in the alloy can be seen. As it is today, the wt.% Mg in the Mg treatment is not taken into consideration as the operators estimate how much FeSiMg that should be added to the melt. If the amount of FeSiMg used for the

previous main shaft melt showed a good result, the operator responsible for the next coming melt often assumes that the same kg FeSiMg per tonne melt will give a similar result. For many casted main shafts these types of proceedings have not led to any defects. However, since the wt.% Mg shown in QDA is time dependent (as shown in Table 9, page 42) it is here not seen as a reliable value and I would not recommend the operators to use this value when comparing melt compositions. The wt.% Mg in QDA works more as an indicator showing that there not has been a violent Mg evaporation (in that case the wt.% Mg is assumed to be considerably lower than normal).

Another problem when it comes to looking at previously results is that when a new batch FeSiMg is used this might not contain the same wt.% Mg as the batch used for the previous melt. For a 17,600 kg melt where 210 kg FeSiMg (11.9 kg per tonne melt) has been placed in the ladle it would mean that FeSiMg containing 4.5 wt.% Mg is equal to 0.054 wt.% Mg added into the melt while a 4.75 wt.% FeSiMg would result in 0.057 wt.% Mg.

Based on the knowledge of the Mg variations it seems reasonable to assume that dross formed in the main shafts placed in category 2, containing up to 12.6 kg FeSiMg per tonne melt, is a result of excess Mg which has reacted with O.

5.2.2.2 The Effect of Ca

Since the wt.% Ca is not analyzed during spectroscopy at GCGAB it is hard to say if Ca has influenced dross formations in previously casted main shafts. From the experimental results regarding Ca in this study (Table 8, page 42) it could be seen that only a tenth of the added Ca remained in the melt after desulphurization. It is possible that the Ca, at the time when the coin samples were taken, had not been evenly distributed throughout the melt resulting in a lower, incorrect spectroscopy result.

To establish the effect of Ca on desulphurization, nodule growth and excess Mg it would be of interest to implement Ca as an element in the foundries spectroscopy analysis. As to the fact that Ca was located in dross formations in the main shaft material (Figure 30, page 40) it seems likely that there are a higher amount of Ca present in the melt than indicated during the spectroscopy (Table 8, page 42). Due to this information I would say that operators should be observant to the amount of Ca and Mg in a FeSiMg treatment before it is added into the ladle. If both the wt.% Ca and Mg are at the highest levels in the Mg treatment, and as these elements work in a similar way [7], the risk of dross formation most likely would increase as not all Ca and Mg will react with S resulting in more CaO and MgO dross formations. It should be noted that some of the MgO and CaO also bonds to Si in larger dross formations; for example $MgSiO_3$ or $MgSiO_4$ molecules [1].

The difference in results from analyzes performed in the two Thermo Scientific™ ARL™ 4460 spectrometers and presented in Table 8 (page 42) does not have a greater impact on this study. Since the results from the analyze of samples (from the same melt) was similar regarding elements that effects dross formation it is assumed that these weight percentages can be seen as correct. It was however a difference in the wt.% P between samples made in Guldsmedshyttan and Degerfors which might be of interest for the foundry as just a small amount of P strongly can influence pearlite formation [2].

5.2.2.4 How to Avoid Dross due to the Mg Treatment

If there were more knowledge among operators regarding the Mg treatment, then the amount of FeSiMg added for each melt could be better adapted reducing material costs as well as the risk of dross. Many parameters should have to be taken into account in order to better adjust the kg FeSiMg per tonne melt used for a specific melt and the current circumstances surrounding the melt.

Equation (7), page 25, could be of use as an estimation of the amount of FeSiMg that the operator should add in the ladle. If the desired value is set for R (60 %), Mg_{final} (0.035 wt.%) and S_F (0.010 wt.%) the required Mg_{added} for a specific melt temperature, S_I and transport time could be calculated. The parameter c could perhaps not be set as a constant as it, due to the fading rate for Mg seen in Table 10 (page 43), vary depending on the condition of the ladle. But since c is a relatively small value and also is regulated by O levels [23], which are not measured at GCGAB, it could probably be set to a constant value of 0.001 wt.% per minute.

The calculations could be conducted by the operator in an excel spreadsheet where only the variables for the specific melt needs to be inserted. When the required Mg_{added} has been calculated the weight of the melt along with the wt.% Mg in the FeSiMg can be used to calculate the total amount of FeSiMg that should be added in the ladle (W_{FeSiMg} in Equation (8), page 26).

Before any calculations regarding the Mg treatment are conducted the first thing would be to get a better control of the wt.% Mg analyzed during the final spectroscope analysis, 3 (S). If changes and tests were to be done for the Mg treatment it is of importance that the result can be accurately measured so that variations in wt.% Mg between melts could be compared. By implementing that the operators should take the final coin sample in the ladle four minutes into the Mg treatment, the wt.% Mg could be used to analyze trends and dross defects within the casts.

5.2.3 Theories Regarding Turbulence and Chemical Composition

5.2.3.1 How to Avoid Dross due to Turbulence

To avoid dross as a result of a slow or rapid box filling and/or turbulence during further pouring of melt into mould, the operators would need to have a more precise and standardized way of pouring. The QDA analysis (page 36) showed that a filling time of 20 to 25 seconds lowered the risk of slag/dross and it would be a recommendation to stay within this time limit if dross should not end up in the mould. The first step should, as mentioned regarding worn out ladles, be to remove slag from the ladle just before it is poured into the box. Since there are turbulent areas in the mould where slag/dross can get stuck (Figure 5, page 6) it seems unnecessary to knowingly pour slag into the box.

To lower dross in the form of bifilms the turbulence during pouring should be minimized by keeping the pouring height (h1 + h2) constant as in Figure 32. The pouring height should probably be minimized in order to get a lower pouring velocity, closer to the critical velocity (as described in page 11). If also the melt flow is kept relatively even it seems as if the amount of bifilm that ends up in the cast not causes noticeable defects. The total pouring time for a main shaft melt was around 280 s which is quite far from the recommended pouring time of 110 s for a 18 tonne melt [7]. The long pouring time did however not seem to noticeable lead to larger dross formations but in theory, a shorter pouring time keeps the melt temperature more consistent and reduces the time the melt is exposed to O [7].

The statements regarding turbulence and pouring heights for the main shafts are derived from video recordings without any scales, filmed at different angles and distances. Video recordings from more than one third of the main shafts were not available due to defect cameras and poor camera settings.

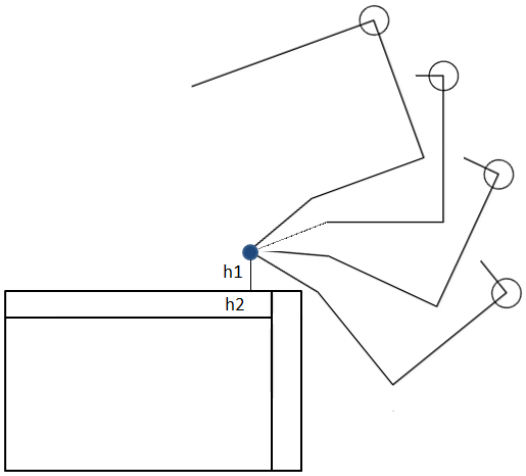

Figure 32. To keep the surface turbulence to a minimum the pouring should be kept constant and at a low pouring height (h1+h2).

The turbulent areas in the mould, seen in Figure 5, probably also is one of the reasons to that dross is captured in the flange. But since most of the main shafts do not contain dross the mould probably becomes

a problem first when dross formations, bifilm or larger dross particles formed in the ladle or pouring box flows down into the mould. If larger dross formations and bifilm could be avoided by having a, for example, extra slag station the mould should not be a major problem (even though it of course would be preferable to avoid all turbulence in the mould).

That the turbulence in the flange captures dross formations gives a lead as to why no dross was found in the samples studied in SEM and EDS, taken from side casted material of three main shafts (method, page 33). It is most likely not as turbulent in the side cast sand moulds as it is in the flange which could explain why the effect dross has on fatigue strength and ductility not is noticed during tensile and impact tests of the side casted material.

5.2.3.3 How to Avoid Dross due to Si

In QDA it was seen that a high wt.% Si and Mn more often led to dross formations. It was noticed that the wt.% Si and Mn often were increased at the same time which makes it hard to determine if both the elements or only one led to the dross. Since Si according to the literature, [1], results in more dross at levels over 2.00 wt.% it seems likely that the Si is a larger problem than the Mn (which still should be kept at lower levels to avoid carbides and pearlite [2]). It should be mentioned that GCGAB has changed the melt formula so that the maximum wt.% Si were lowered from 2.15 wt.% to 2.05 wt.% which resulted in fewer main shafts containing dross due to the Si content.

Probably the operators needs to observe the levels of for example Si, Mg, Ca, Mn, Al and rare earth metals more closely in order to avoid an increased amount of dross particles that can cluster. Even though each element lies within specification, problems can likely occur if all or many of the elements are at the highest specified level.

CHAPTER 6

Conclusion

In the main shafts at GCGAB containing dross formations, dross particles such as MgO, CaO, MgS, CaS, Al_2O_3 and MnO can be found. The amount of dross is mainly controlled by the levels of O that the melt is exposed to during Mg treatment, transport and due to turbulence. Which step in the manufacturing process that is the most critical for dross formations could not be determined, it depends on were in the process the specific melt is exposed to the highest amount of O. An increased amount of elements that are highly reactive to O results in a more rapid formation of dross particles. The following conclusions have been done regarding what has caused the dross formations in the main shafts and how dross defects could be avoided:

i. Worn out ladles where the cooling rate of the melt increases can result in dross defects. In combination with a melt temperature below 1,460 °C the dross formations becomes more severe. To avoid dross defects the ladles should be kept in a good condition and the melt temperature as the melt is poured into the ladle should be set above 1,460 °C.
ii. Excess FeSiMg (Mg treatment) results in that more Mg reacts with O forming dross particles which can lead to larger dross defects. The amount of FeSiMg must be better adapted to each specific melt by taking melt temperature, melt weight, transport time and the wt.% Mg in the FeSiMg treatment into consideration.
iii. A too rapid or slow filling of the pouring box can lead to that dross formed in the ladle flows down into the mould due to turbulence. For the best result, the main part of the box should be filled within 20 to 25 seconds. To ensure that dross/slag does not follow the melt into the mould the slag should be removed from the ladle just before the melt is poured in.
iv. Turbulence at the melt surface in the pouring box can result in that bifilm (dross) detaches from the surface and ends up in the mould leading to dross defects. To avoid that larger bifilms detaches, the turbulence should be kept to a minimum by pouring the melt from a constant, low, height and with a constant melt flow.

CHAPTER 7

Bibliography

[1] Gagné, M., Paquin, M. & Cabanne, P. (2008). Dross in ductile iron: source, formation and explanation. In *The 68th World Foundry Congress, India, Chennai, 7-11 February 2008*, pp. 101–106.

[2] *The sorelmetal book of ductile iron*. (2004). Qubéc, Canada: Rio Tinto Iron & Titanium Inc.

[3] Shirani, M. & Härkegård, G. (2011). Fatigue life distribution and size effect in ductile cast iron for wind turbine components. *Engineering Failure Analysis*, vol. 18 (1), pp. 12-24.

[4] EN-GJS-400-18-LT (5.3103). (2015). *European Steel and Alloy Grades / Numbers*. [Online]. Available: http://www.steelnumber.com/en/steel_composition_eu.php?name_id=1517. [2015-05-13].

[5] Roedter, H. (2006). *Dross in ductile iron*. Qubéc, Canada: Rio Tinto Iron & Titanium Inc. [Online]. Available: http://www.sorelmetal.com/en/publi/PDF/098_(2006).pdf. [2015-05-13].

[6] Campbell, J. (2003). *Castings* (2nd ed.). Oxford, UK: Butterworth-Heinemann.

[7] Davis, J.R. (edt.) (1996). *ASM Speciality Handbook: Cast Irons*. Geauga County. Ohio, USA: ASM International.

[8] Bower, T. F., Brody, H. D. & Flemings, M. C. (1996). Measurements of solute redistribution in dendritic solidification. *Transaction of the Metallurgical Society of AIME*, vol. 236, pp. 624-633.

[9] *Nondestructive evaluation and quality control. Metals handbook: Volume 17* (9th ed.). (1989). Ohio, USA: ASM International.

[10] Askeland, D. R. & Phulé, P. P. (2008). *The science and engineering of materials*. Mason, USA: Cengage Learning.

[11] Computational Thermodynamics Inc. (2006). *Calculation of phase diagrams using the CALPHAD method*. [Online]. Available: http://www.calphad.com/iron-carbon.html. [2015-05-13].

[12] Onsöien, M. I. (1997). *Microstructure evolution in ductile cast iron containing rare earth metals*. Disp. Trondheim, Norway: The metallurgical institution, The Norwegian University of Science and Technology (NTNU).

[13] *Internal metallurgy and process documents*. (2015). Guldsmedshyttan, Sweden: Global Castings Guldsmedshyttan AB.

[14] Skaland, T. Nucleation mechanisms in ductile iron. In *Proceedings of the AFS Cast Iron Inoculation Conference, USA, Schaumburg, 29-30 September 2005,* pp. 13–30.

[15] Çetinarslan, C. S. & Genç, S. K. (2014). Study in the variation of mechanical properties of nodular cast iron depending upon section thickness. *Materialwissenschaft und Werkstofftechnik*, vol. 45 (2), pp. 106–113.

[16] Wessén, M. & Svensson, I. L. (1996). Modeling of ferrite growth in nodular cast iron. *Metallurgical and Materials Transactions A*, vol. 27 (8), pp. 2209–2220.

[17] Nakae, H., Fukami, M., Kitazawa, T. & Zou, Y. (2010). Influence of Si, Ce, Sb and Sn on chunky graphite formation. In *The 69th World Foundry Congress, China, Hangzhou, 16-20 October 2010*, pp. 393-397.

[18] Sertucha, J., Lacaze, J., Armendariz, S. & Larrañaga, P. (2013). Statistical analysis of the influence of some trace elements on chunky graphite formation in heavy section nodular iron castings. *Metallurgical and Materials Transactions A*, vol. 44 (3), pp. 1159–1162.

[19] Goodrich, G. M. (1997). Cast iron microstructure anomalies and their causes. *American Foundry Society transactions*, vol. 105, pp. 669–683.

[20] Kalpakjian, S. & Schmid, S. (2007). *Manufacturing processes for engineering materials* (5th ed.). New Jersey, USA: Prentice Hall.

[21] Nilsson, K. F. & Vokál, V. (2009). Analysis of ductile cast iron tensile tests to relate ductility variation to casting defects and material microstructure. *Materials Science and Engineering: A*, vol. 502 (1-2), pp. 54–63.

[22] Foseco. (2015). STELEX ZR zirconium oxide filters. [Online]. Available: http://www.foseco.com/en-gb/end-markets/foundry/products-services/steel-foundry/steel-foundry-details/productsinfo/filtration-and-gating-systems/stelex-zr-zirconium-oxide-filters/. [2015-05-13].

[23] Cabanne, P. M. (2008). The efficiency of your magnesium treatment varies: check the following points! Qubéc, Canada: Rio Tinto Iron & Titanium Inc. [Online]. Available: http://www.sorelmetal.com/en/publi/PDF/114_EN.pdf. [2015-05-13].

[24] Thomsen, V. B. E. (1996). *Modern spectrochemical analysis of metals: an introduction for users of arc spark instrumentation*. Ohio, USA: ASM International.

[25] Hollas, J. M. (2004). *Modern spectroscopy* (4th ed.). Chichester, UK: John Wiley & Sons Ltd.

[26] Brandon, D. & Kaplan, W. D. (2008). *Microstructural characterization of materials (2nd ed.)*. Chichester, UK: John Wiley & Sons Ltd.

[27] University of Bristol. (2000). *Film characterisation techniques*. [Online]. Available: http://www.chm.bris.ac.uk/pt/diamond/stuthesis/chapter2.htm. [2015-05-13].

[28] Nothern Arizona University. (2008). *Microprobe-SEM signals*. [Online]. Available: http://www4.nau.edu/microanalysis/microprobe-sem/signals.html. [2015-05-13].

[29] Amptek Inc. (2015). *What is XRF?* [Online]. Available: http://www.amptek.com/xrf/. [2015-05-13].

APPENDIX

MS number in Group		Ladle		Melt temp. (°C)		[1]FeSiMg Kg/tonne	Chemical comp. (wt.%)				Pouring of melt into box/mould		
		NR	[2]Used in row	Into ladle	Into mould		Si	Mn	S	Mg	[3]Cast lid melt (s)	[4]Height in box (cm)	[5]Turbu-lence
CATEGORY 1 (Ladles & Temperature)													
1	B	6		1455	1365	11.9	2,01	0,18	0,011	0,038	N/A	N/A	N/A
2	B	6	4	1450	1365	11.4	2,02	0,18	0,011	0,041	26	15	
3	B	6	5	1440	1365	11.1	2	0,21	0,009	0,039	N/A	N/A	N/A
4	B	6	5	1464	1355	11.1	2,06	0,21	0,012	0,04	50	7	
1	A	6	8	1462	1355	11.1	2,11	0,17	0,01	0,042	30	0	
1	C	6	10	1458	1370	11.1	2,08	0,16	0,01	0,04	25	20	
2	C	6	6	1450	1365	11.3	2,06	0,16	0,01	0,042	35	10	
2	A	2	10	1425	1365	11.0	2,11	0,21	0,01	0,039	24	3	
3	A	2	12	1440	1365	10.9	2,13	0,21	0,01	0,04	N/A	N/A	N/A
3	C	2	7	1440	1365	11.7	2,09	0,24	0,01	0,035	31	15	
4	A	2	8	1470	1365	12.0	2,14	0,17	0,011	0,04	23	10	X
5	A	2	9	1440	1365	12.1	2,07	0,18	0,011	0,038	N/A	N/A	N/A
4	C	2	10	1470	1365	10.3	2,16	0,21	0,01	0,036	25	10	
5	C	2	11	1465	1365	12.0	2,15	0,19	0,01	0,036	25	7	
6	C	2	12	1465	1365	12.0	2,14	0,18	0,01	0,037	N/A	N/A	N/A
5	B	1	2	1470	1365	12.5	2,13	0,17	0,011	0,037	N/A	N/A	N/A
6	A	1	3	1460	1360	10.6	2,08	0,22	0,009	0,039	N/A	N/A	N/A
7	C	1	4	1465	1355	10.8	2,14	0,17	0,011	0,042	N/A	N/A	N/A
8	C	1	5	1470	1365	11.7	2,07	0,22	0,009	0,036	N/A	N/A	N/A
9	C	1	6	1465	1365	11.9	2,19	0,17	0,01	0,035	23	7	
10	C	1	7	1460	1365	12.0	2,09	0,16	0,011	0,034	N/A	N/A	N/A
11	C	1	8	1470	1365	12.0	2,08	0,16	0,011	0,035	N/A	N/A	N/A
12	C	6	5	1475	1365	N/A	1,99	0,19	0,012	0,041	N/A	N/A	N/A
13	C	6	6	1468	1365	11.4	2,02	0,18	0,011	0,037	22	0	X
7	A	6	8	1460	1365	11.4	1,99	0,16	0,011	0,037	N/A	N/A	N/A
8	A	1	8	1475	1359	N/A	2,02	0,21	0,011	0,043	N/A	N/A	N/A
14	C	6	4	1475	1360	11.5	1,99	0,19	0,012	0,042	24	10	
15	C	6	5	1475	1355	11.0	2,04	0,21	0,01	0,038	26	7	X
16	C	6	6	1470	1360	N/A	1,97	0,2	0,012	0,038	23	25	
9	A	6	7	1480	1349	N/A	1,85	0,2	0,012	0,045	22	3	
6	B	6	11	1475	1365	12.1	2,02	0,21	0,011	0,038	28	10	X
17	C	2	7	1470	1360	12.3	1,94	0,17	0,01	0,044	N/A	N/A	N/A
18	C	2	8	1475	1360	12.0	1,93	0,19	0,011	0,04	32	0	
19	C	2	9	1475	1360	12.0	1,93	0,19	0,01	0,04	27	0	
20	C	1	9	1480	1364	N/A	1,9	0,16	0,009	0,041	N/A	N/A	N/A

MS number in Group		Ladle		Melt temp. (°C)		[1]FeSiMg Kg/tonne	Chemical comp. (wt.%)				Pouring of melt into box/mould		
		NR	[2]Used in row	Into ladle	Into mould		Si	Mn	S	Mg	[3]Cast lid melt (s)	[4]Height in box (cm)	[5]Turbu-lence
CATEGORY 2 (Mg treatment)													
7	B	1	1	1460	1368	N/A	2,02	0,17	0,011	0,042	15	P.O	X
10	A	1	3	1460	1370	N/A	2,02	0,16	0,011	0,04	23	10	X
11	A	7		1470	1368	11.2	2,13	0,18	0,011	0,043	27	25	
8	B	6	1	1470	N/A	N/A	2,11	0,17	0,01	0,04	N/A	N/A	N/A
9	B	2	1	1475	1370	N/A	2,12	0,16	0,01	0,042	28	7	
21	C	6	3	1473	1360	11.3	2,07	0,2	0,011	0,044	27	25	
22	C	6	1	1470	1365	12.5	2,16	0,2	0,01	0,038	27	0	X
23	C	6	3	1470	1365	12.5	2,1	0,16	0,01	0,036	22	3	
10	B	6	8	1470	1365	12.5	2,11	0,17	0,011	0,038	25	5	
24	C	1	1	1475	1365	12.5	2,11	0,17	0,011	0,035	30	10	
12	A	1	3	1465	1365	12.6	2,17	0,17	0,012	0,042	18	25	X
13	A	1	4	1475	1365	12.6	2,15	0,21	0,01	0,037	20	7	
25	C	6	4	1465	1365	11.8	1,95	0,16	0,01	0,043	N/A	N/A	N/A
26	C	2	3	N/A	N/A	N/A	1,85	0,18	0,011	0,042	N/A	N/A	N/A
14	A	6	1	1470	1365	N/A	2,06	0,26	0,01	0,046	N/A	N/A	N/A
27	C	6	2	1475	1360	12.6	1,91	0,18	0,01	0,038	36	7	
28	C	6	3	1471	1363	12.6	2,01	0,17	0,01	0,04	N/A	N/A	N/A
29	C	1	4	1465	1360	10.9	1,97	0,15	0,008	0,038	N/A	N/A	N/A
30	C	1	5	1465	1365	12.3	1,99	0,17	0,009	0,041	17	10	X
CATEGORY 3 (Chemical composition & Turbulence)													
11	B	1		1463	1370	12.1	2,07	0,19	0,009	0,037	15	0	
31	C	6		1456	1370	12.3	2,14	0,17	0,009	0,038	26	10	
12	B	1	1	1450	1375	10.6	2,07	0,23	0,01	0,037	17	P.O	X
32	C	7		1450	1370	10.6	2,12	0,19	0,01	0,041	N/A	N/A	N/A
15	A	1		1475	1365	N/A	2	0,16	0,01	0,04	23	5	
33	C	1		1475	1365	N/A	2,08	0,2	0,01	0,037	15	10	
16	A	2	9	1465	1365	11.3	2,08	0,19	0,009	0,039	20	20	X
34	C	1	3	1470	1365	11.5	2,09	0,27	0,011	0,034	18	10	X
35	C	1	4	1460	1365	11.9	2,15	0,26	0,01	0,038	N/A	N/A	N/A
13	B	2	5	1477	1365	N/A	1,97	0,18	0,01	0,04	21	5	X
36	C	2	10	1475	1365	N/A	1,97	0,24	0,01	0,038	N/A	N/A	N/A
14	B	6	5	1473	1365	12.2	1,95	0,24	0,01	0,037	20	10	X

MS number in Group		Ladle		Melt temp. (°C)			Chemical comp. (wt.%)				Pouring of melt into box/mould		
		NR	[2]Used in row	Into ladle	Into mould	[1]FeSiMg Kg/tonne	Si	Mn	S	Mg	[3]Cast lid melt (s)	[4]Height in box (cm)	[5]Turbu-lence
No apparent reason to dross formation. Lack of info regarding O/turbulens in mould													
15	B	2		1460	1368	11.8	2,01	0,17	0,01	0,041	25	10	
37	C	1	7	1465	1365	11.8	2,09	0,17	0,011	0,04	21	10	
17	A	6	3	1465	1365	11.0	1,92	0,22	0,01	0,038	26	5	
38	C	1	1	1470	1365	11.5	1,96	0,23	0,01	0,04	20	10	
39	C	2	4	1480	1365	11.4	1,91	0,21	0,01	0,038	21	7	
40	C	2	6	1480	1360	11.4	1,91	0,21	0,01	0,039	25	10	
16	B	2	1	1468	1365	11.6	1,97	0,21	0,01	0,037	27	0	
41	C	2	6	1475	1360	12.1	1,97	0,22	0,011	0,039	34	3	
42	C	6	1	1470	1360	12.1	2,03	0,16	0,009	0,039	34	3	
Lack of info													
17	B	1	2	1465	1370	11.3	2,08	0,22	0,01	0,036	N/A	N/A	N/A
43	C	2	4	1480	1370	N/A	2,07	0,18	0,013	0,041	32	10	
44	C	1	5	1460	1365	11.9	2,06	0,2	0,01	0,037	N/A	N/A	N/A
18	A	6	5	1485	1365	N/A	2,13	0,16	0,011	0,038	N/A	N/A	N/A
45	C	6	2	1465	1360	12.0	1,86	0,16	0,011	0,041	N/A	N/A	N/A
18	B	1	5	1475	1365	11.1	1,86	0,17	0,011	0,041	N/A	N/A	N/A
46	C	6	10	1485	1372	N/A	1,89	0,21	0,011	0,037	36	10	
47	C	2	6	1475	1360	11.3	1,89	0,17	0,01	0,035	N/A	N/A	N/A
48	C	2	9	1470	1365	11.9	1,93	0,17	0,011	0,04	N/A	N/A	N/A
19	B	6	4	1470	1365	N/A	2	0,21	0,009	0,039	N/A	N/A	N/A
49	C	2	1	1472	N/A	11.9	1,92	0,19	0,011	0,04	N/A	N/A	N/A
50	C	6	7	1470	1365	10.9	2,03	0,17	0,009	0,038	N/A	N/A	N/A

[1]Kg FeSiMg (Mg treatment) added per tonne melt.
[2] The number of times a ladle has been used for main shafts without maintenance.
[3] How long it takes for the cast lid to completely melt during filling of the pouring box.
[4] How much of the pouring box that remains unfilled as the cast lid completely has melted.
[5] Turbulence in the pouring box due to a varied pouring height or flow.

Sample X1-1 (seen in figure 31 a)

Spectrum 1

Element	Weight%
C K	9.87
O K	16.06
Mg K	20.73
Al K	0.35
Si K	1.59
S K	0.91
Ca K	0.65
Ti K	0.49
Fe K	66.49
Totals	117.15
Dross:	MgO

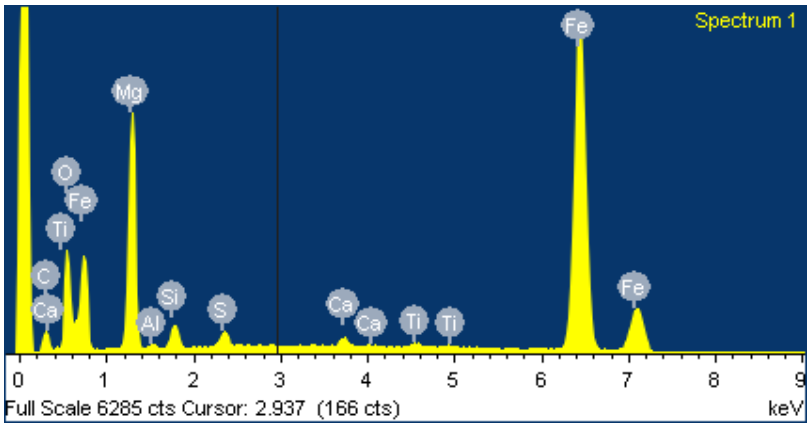

Spectrum 2

Element	Weight%
C K	11.13
O K	12.14
Mg K	18.47
S K	31.06
Ca K	7.00
Fe K	4.98
Te L	1.04
Totals	85.83
Dross:	MgO, MgS

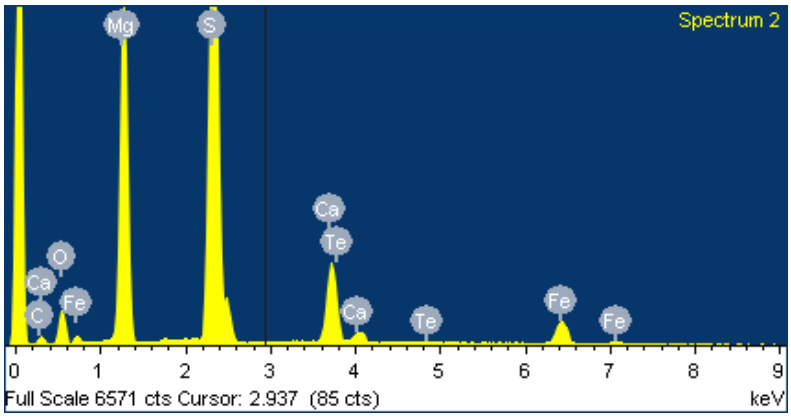

Spectrum 3

Element	Weight%
C K	8.19
O K	18.45
Mg K	29.31
Al K	0.40
Si K	2.09
S K	0.53
Ca K	0.27
Mn K	0.42
Fe K	78.70
Totals	138.36
Dross:	MgO

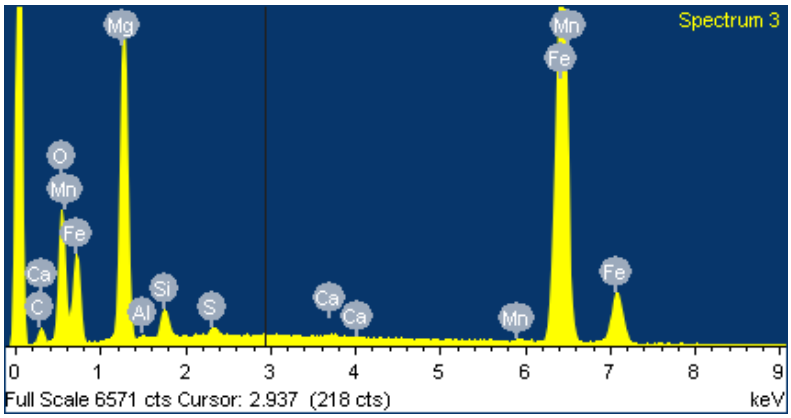

Spectrum 4

Element	Weight%
C K	111.61
O K	4.75
Mg K	4.58
Si K	0.39
S K	4.64
Ca K	2.02
Fe K	26.46
Totals	154.44
Dross:	MgO

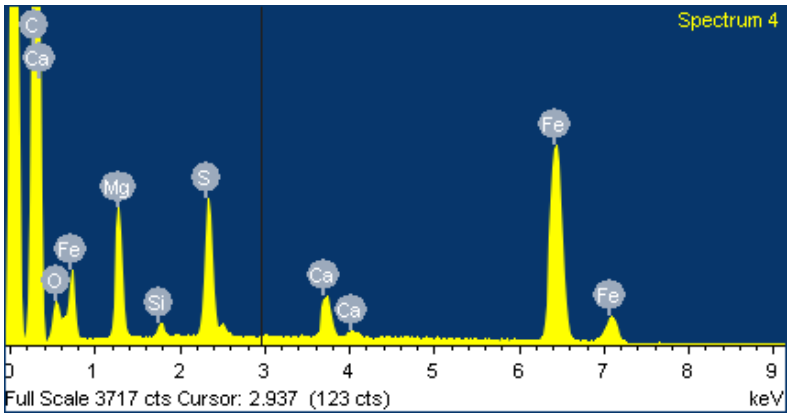

Sample X1-2 (seen in figure 31 b)

Spectrum 1

Element	Weight%
C K	3.25
O K	31.38
Mg K	49.88
Al K	0.44
Si K	3.56
S K	0.68
Ti K	0.27
Fe K	28.08
Totals	117.53
Dross:	MgO

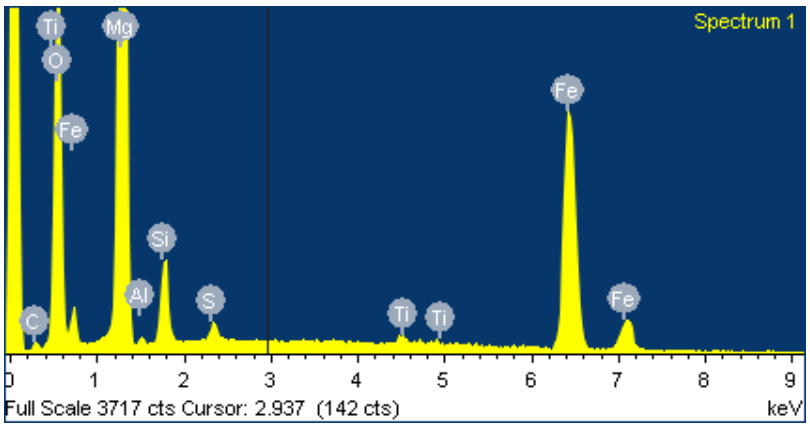

Spectrum 2

Element	Weight%
C K	47.50
O K	8.46
Mg K	4.84
Si K	2.53
S K	1.54
Ca K	1.35
Fe K	76.97
Totals	143.18
Dross:	MgO

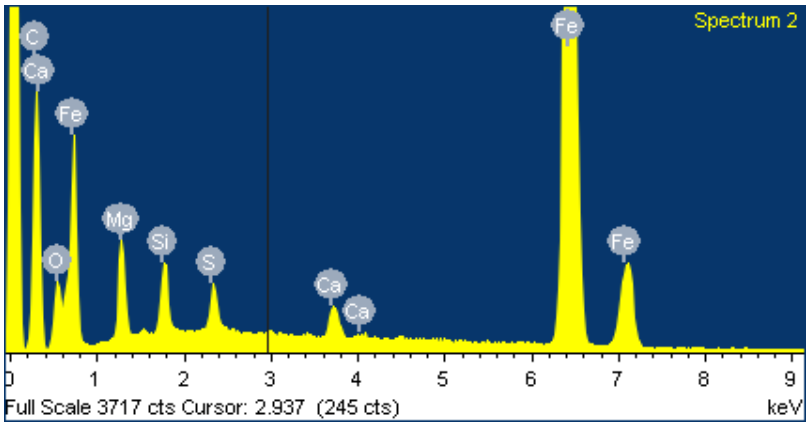

Spectrum 3

Element	Weight%
C K	5.12
O K	4.30
Mg K	3.98
Si K	0.09
S K	8.99
Ca K	6.73
Fe K	4.05
Te L	1.29
Totals	34.55
Dross:	---

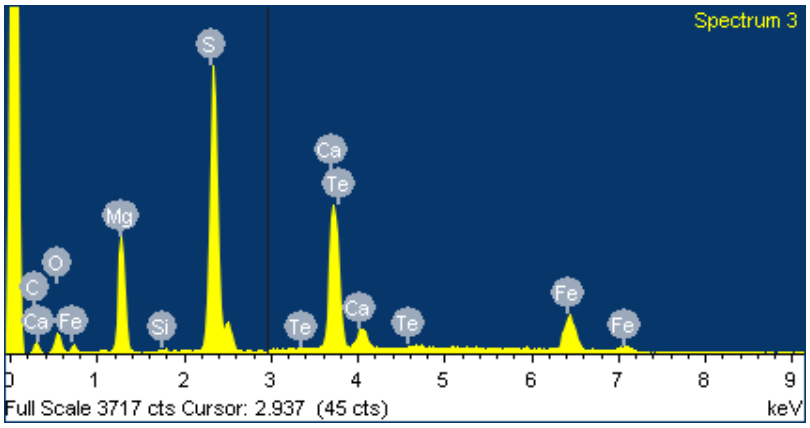

Sample X1-3 (seen in figure 32 a)

Spectrum 1

Element	Weight%
C K	7.50
O K	27.26
Mg K	36.59
Al K	0.94
Si K	4.31
S K	2.16
Ca K	1.54
Ti K	0.34
Fe K	16.03
Ce L	0.68
Totals	97.34
Dross:	MgO

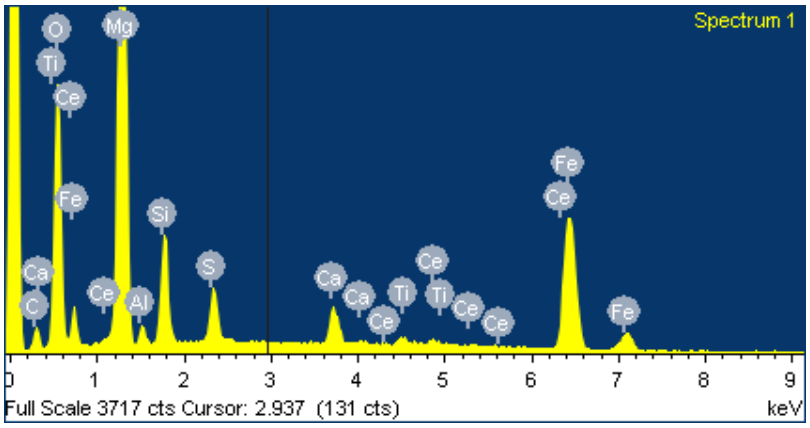

Spectrum 2

Element	Weight%
C K	7.24
O K	14.06
Mg K	22.41
Al K	0.54
Si K	5.11
S K	2.33
Ca K	2.35
Ti K	0.41
Fe K	44.68
Te L	0.73
Totals	99.85
Dross:	MgO

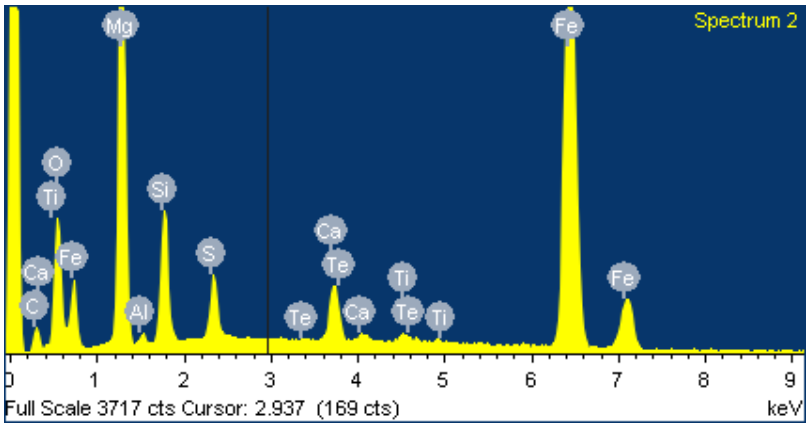

Spectrum 3

Element	Weight%
C K	5.09
O K	13.91
Mg K	25.59
Si K	1.04
S K	1.96
Ca K	0.53
Fe K	28.20
Te L	0.44
Totals	76.77
Dross:	MgO

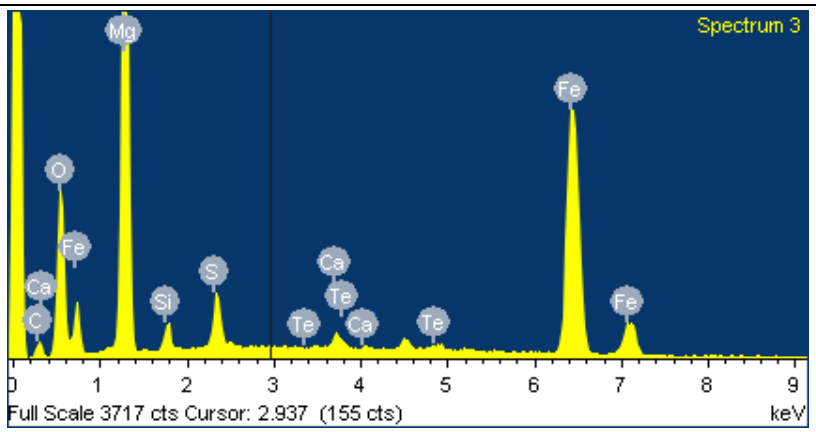

Spectrum 4

Element	Weight%
C K	7.36
O K	17.16
Mg K	16.69
Al K	0.21
Si K	1.39
S K	1.65
Ca K	0.99
Ti K	0.34
Fe K	48.24
Totals	94.04
Dross:	MgO

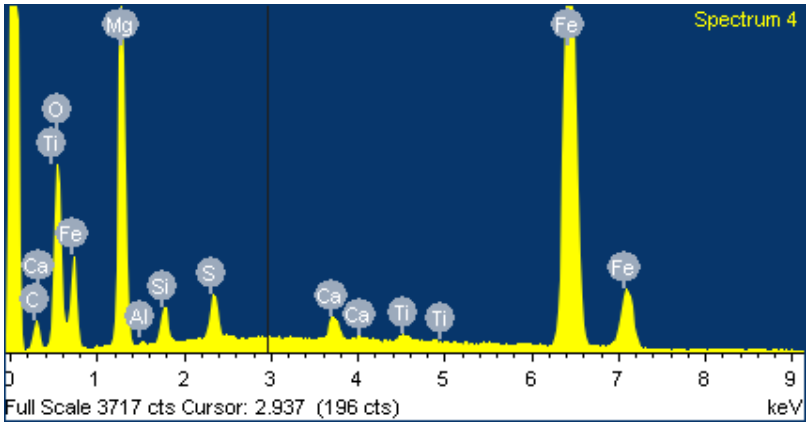

Sample X2-1 (seen in figure 32 b)

Spectrum 1

Element	Weight.%
C K	5.81
O K	40.56
Mg K	2.08
Al K	24.17
Si K	2.45
Ca K	26.34
Fe K	0.64
Te L	1.30
Totals	103.35
Dross:	Al_2O_3, CaO

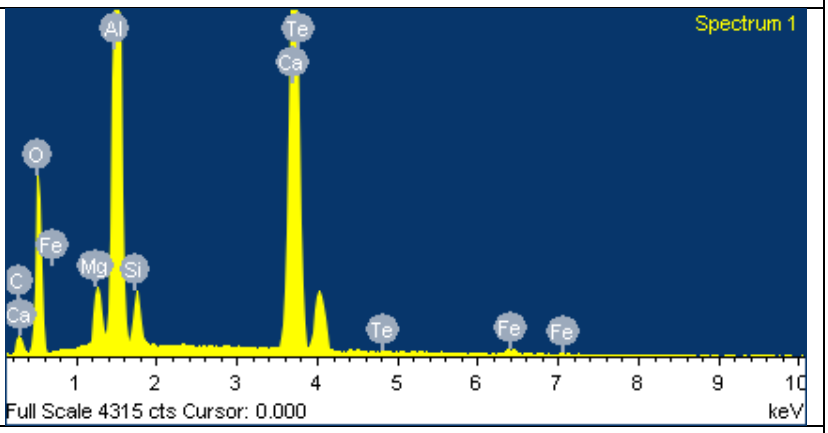

Spectrum 2

Element	Weight%
C K	35.43
O K	42.87
Mg K	14.57
Si K	0.40
S K	14.40
Ca K	11.68
Fe K	3.01
Te L	0.92
Totals	123.27
Dross:	MgO, CaO, CaS

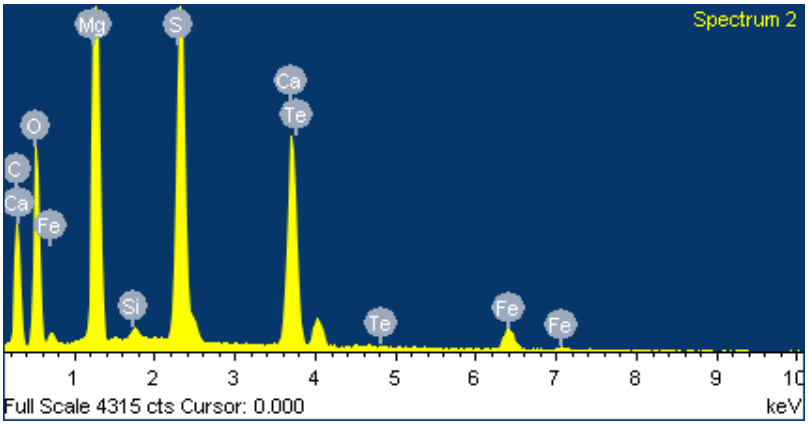

Spectrum 3

Element	Weight%
C K	24.60
O K	32.80
Mg K	6.39
Si K	0.62
S K	18.10
Ca K	11.35
Fe K	8.10
Te L	0.87
Ba L	0.79
Eu L	0.71
Totals	104.33
Dross:	CaS, MgO, CaO

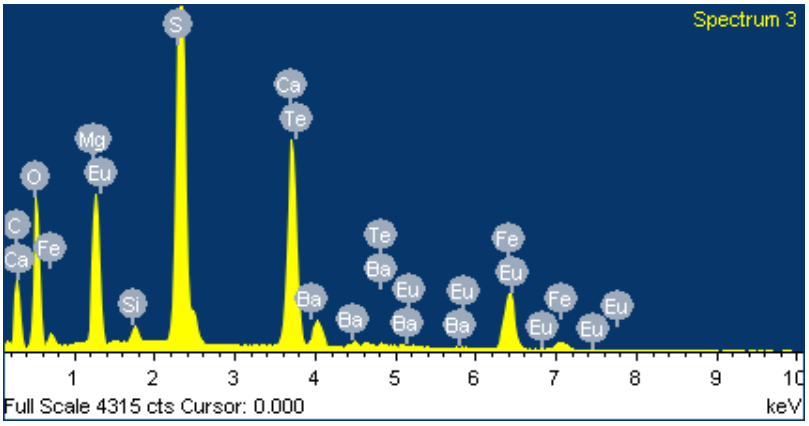

Spectrum 4

Element	Weight%
C K	7.54
O K	8.64
Mg K	17.56
Al K	1.41
Si K	11.23
S K	0.78
Ca K	0.67
Fe K	73.17
Totals	121.01
Dross:	MgO, SiO_2

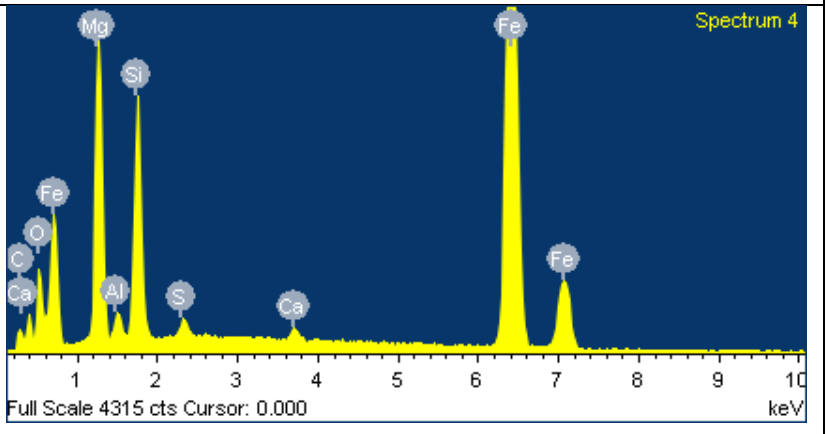

Sample X2-3 (seen in figure 32 c)

Spectrum 1

Element	Weight%
C K	4.09
O K	2.02
Mg K	3.93
Si K	0.42
S K	8.07
Ca K	1.57
Mn K	0.34
Fe K	62.03
Te L	0.55
Totals	83.01
Dross:	FeS

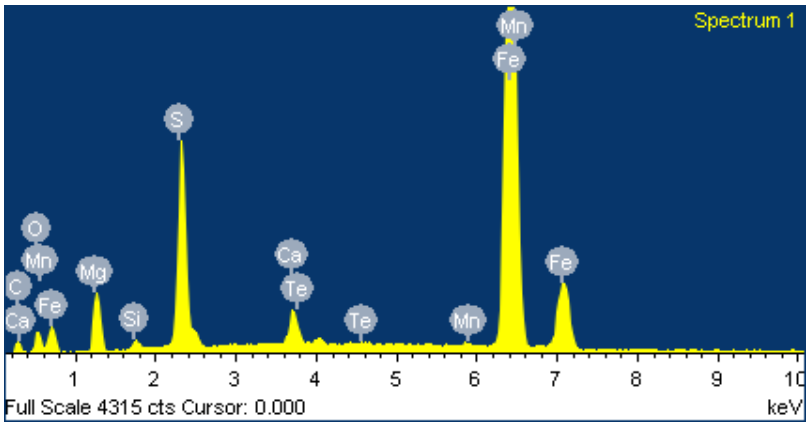

Spectrum 2

Element	Weight%
C K	15.56
O K	12.46
Mg K	6.38
S K	39.74
Ca K	34.89
Sc K	0.78
Fe K	5.12
Sn L	0.66
Te L	5.91
Totals	121.50
Dross:	CaS

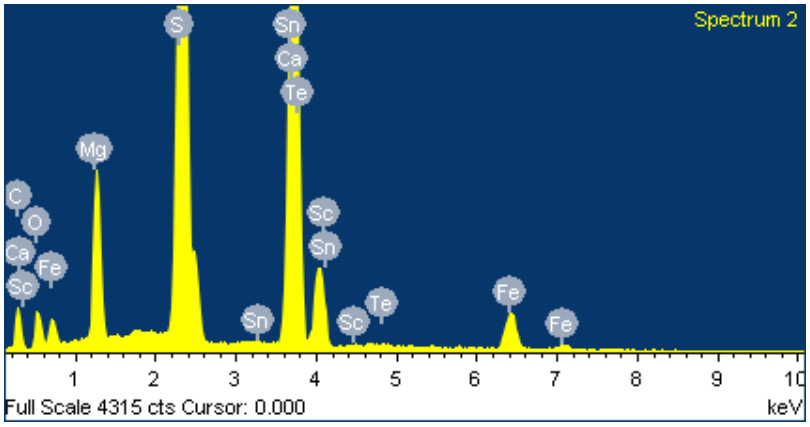

Spectrum 3

Element	Weight%
C K	5.74
O K	18.63
Mg K	7.64
Si K	0.91
S K	20.41
Ca K	20.66
Sc K	0.13
Fe K	5.26
Te L	4.89
Ba L	5.68
Totals	89.96
Dross:	CaS, MgO

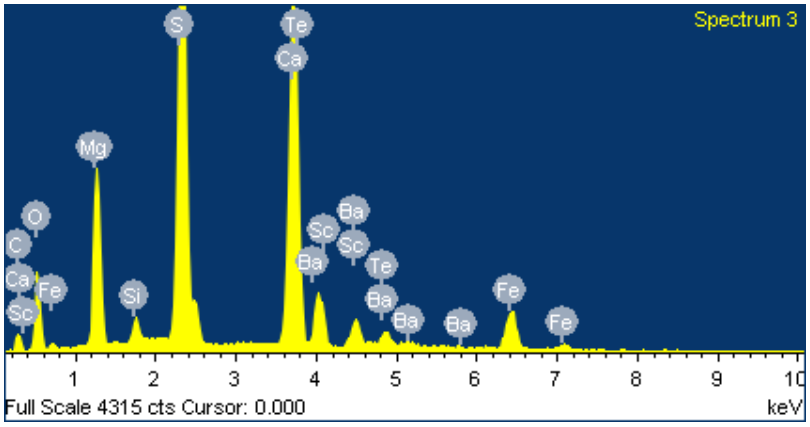

Spectrum 4

Element	Weight%
C K	124.05
O K	21.59
Mg K	12.42
Si K	0.14
S K	4.19
Ca K	0.84
Fe K	23.31
La L	1.13
Eu L	0.99
Totals	188.67
Dross:	MgO

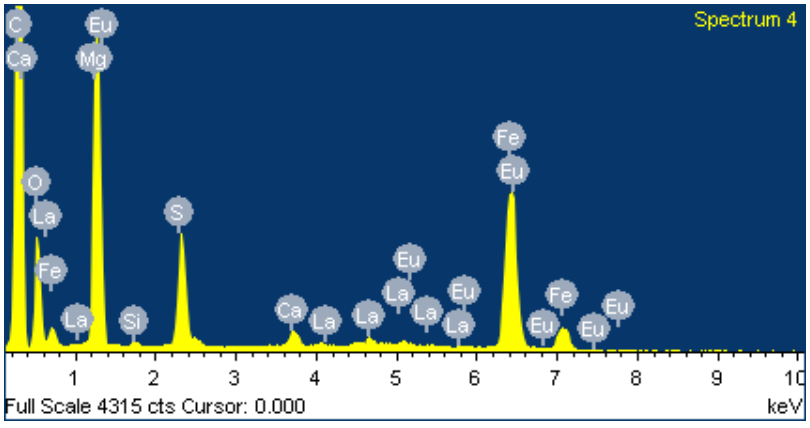

MS Nr/Group	9D
Temperature ladle	120 °C
Nr. of times the ladle has been used in a row before maintenance	12
Weight of melt poured into ladle	17,500 kg
Time. Start of pouring melt into ladle to right before melt is poured into mould.	1,061 s (17 min, 41 s)
Total time. Start of pouring melt into ladle to when melt has been poured into mould.	1,311 s (21 min, 51 s)
Cooling rate; pouring into ladle	**17.6 °C/min**
Cooling rate; transport	**4.4 °C/min**

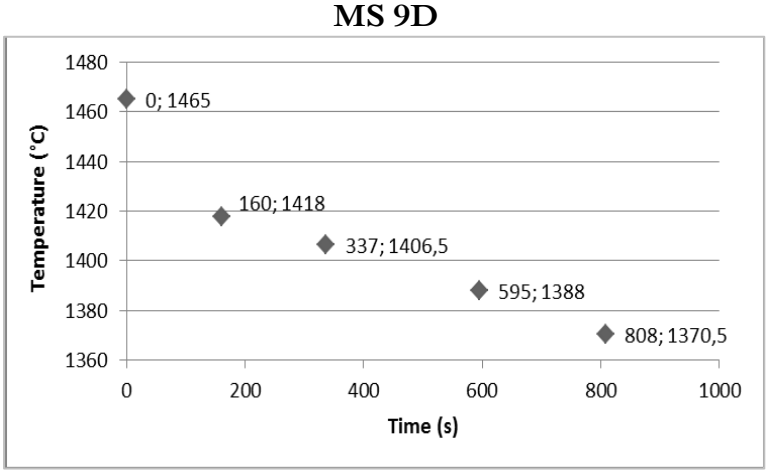

MS Nr/Group	10D
Temperature ladle	90 °C
Nr. of times the ladle has been used in a row before maintenance	13
Weight of melt poured into ladle	17,800 kg
Time. Start of pouring melt into ladle to right before melt is poured into mould.	863 s (16 min, 23 s)
Total time. Start of pouring melt into ladle to when melt has been poured into mould.	1,089 s (18 min, 9 s)
Cooling rate; pouring into ladle	**14.4 °C/min**
Cooling rate; transport	**5.5 °C/min**

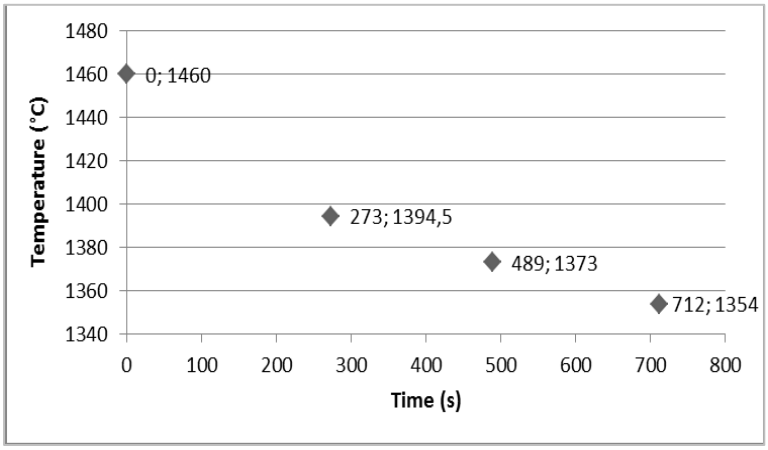

MS Nr/Group	11D
Temperature ladle	65 °C
Nr. of times the ladle has been used in a row before maintenance	3
Weight of melt poured into ladle	17,400 kg
Time. Start of pouring melt into ladle to right before melt is poured into mould.	1,263 s (21 min, 3 s)
Total time. Start of pouring melt into ladle to when melt has been poured into mould.	1,512 s (25 min, 12 s)
Cooling rate; pouring into ladle	**16.6 °C/min**
Cooling rate; transport	**3.8 °C/min**

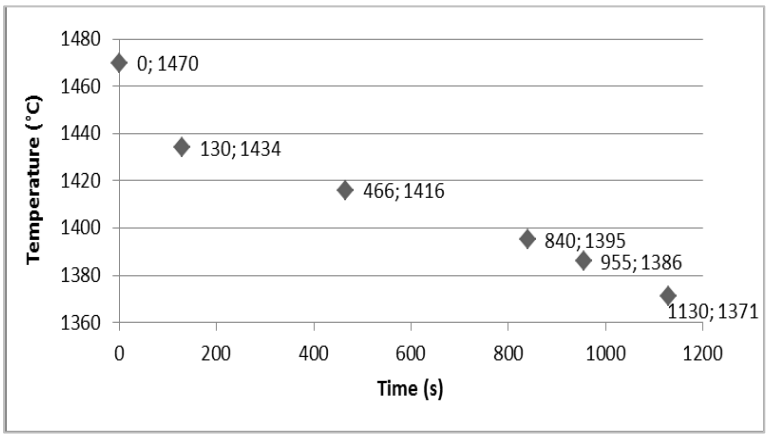

MS Nr/Group	12D
Temperature ladle	78 °C
Nr. of times the ladle has been used in a row before maintenance	4
Weight of melt poured into ladle	17,900 kg
Time. Start of pouring melt into ladle to right before melt is poured into mould.	1,597 s (26 min, 37 s)
Total time. Start of pouring melt into ladle to when melt has been poured into mould.	1,891 s (31 min, 31 s)
Cooling rate; pouring into ladle	**11.1 °C/min**
Cooling rate; transport	**3.8 °C/min**

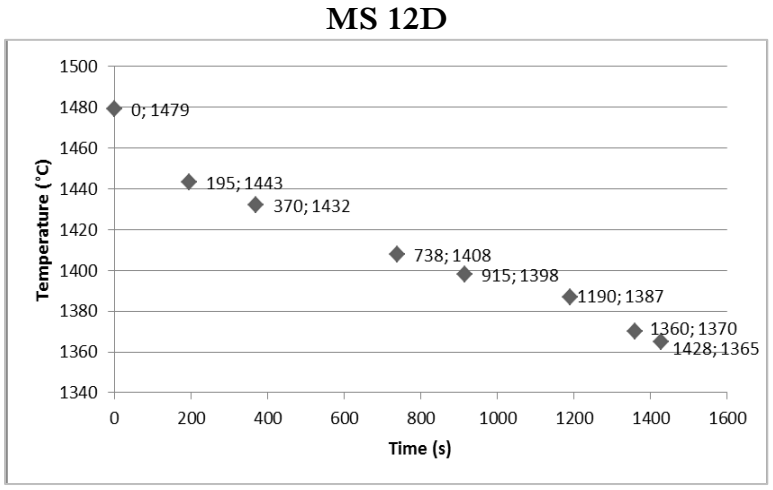

MS Nr/Group	13D
Temperature ladle	85 °C
Nr. of times the ladle has been used in a row before maintenance	5
Weight of melt poured into ladle	17,600 kg
Time. Start of pouring melt into ladle to right before melt is poured into mould.	1,020 s (17 min)
Total time. Start of pouring melt into ladle to when melt has been poured into mould.	1,294 s (21 min, 34 s)
Cooling rate; pouring into ladle	**18.4 °C/min**
Cooling rate; transport	**--- °C/min**

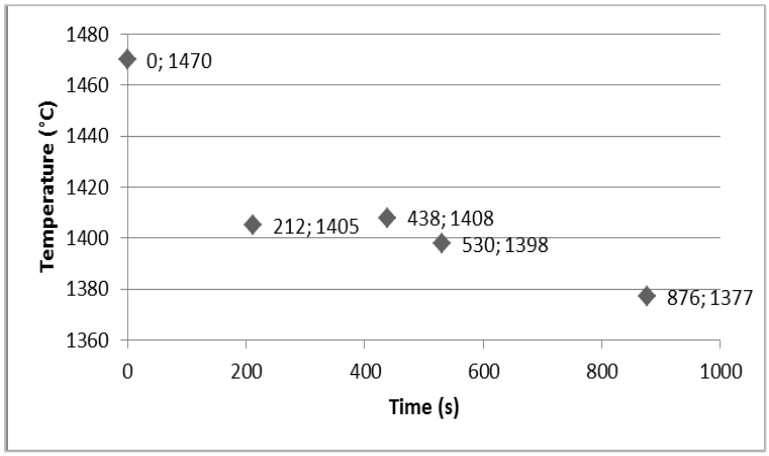

MS Nr/Group	14D
Temperature ladle	95 °C
Nr. of times the ladle has been used in a row before maintenance	3
Weight of melt poured into ladle	17,600 kg
Time. Start of pouring melt into ladle to right before melt is poured into mould.	1,422 s (23 min, 42 s)
Total time. Start of pouring melt into ladle to when melt has been poured into mould.	1,695 s (28 min, 15 s)
Cooling rate; pouring into ladle	**11.2 °C/min**
Cooling rate; transport	**3.8 °C/min**

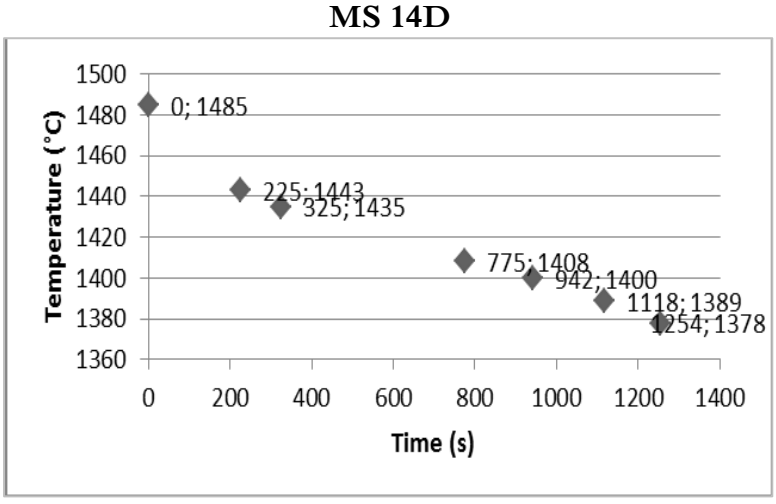

MS Sample	Type : Location	%C	%Si	%Mn	%P	%S	%Cr	%Ni	%Mo	%Ti	%Cu	%Co
11D	2 (P) : DF	3.85	1.23	0.16	0.027	0.012	0.03	0.05	<0.02	<0.01	0.01	0.02
11D	2 (P) : GSH	3.79	1.20	0.16	0.022	0.013	0.03	0.04	0.00	0.008	0.02	0.023
11D	3 (S) : DF	3.81	2.00	0.17	0.025	0.010	0.03	0.05	<0.02	<0.01	0.01	0.02
11D	3 (S) : GSH	3.83	1.95	0.17	0.023	0.011	0.03	0.04	0.00	0.009	0.02	0.023
12D	2 (P) : DF	3.87	1.23	0.20	0.025	0.011	0.06	0.06	<0.02	<0.01	0.007	0.02
12D	2 (P) : GSH	3.80	1.20	0.20	0.022	0.012	0.06	0.05	0.00	0.01	0.01	0.024
12D	3 (S) : DF	3.77	2.00	0.20	0.026	0.009	0.06	0.05	<0.02	0.011	0.008	0.02
12D	3 (S) : GSH	3.81	1.89	0.20	0.022	0.010	0.06	0.04	0.00	0.011	0.02	0.024
13D	2 (P) : DF	3.90	1.25	0.18	0.026	0.011	0.04	0.05	<0.02	<0.01	0.009	0.02
13D	2 (P) : GSH	3.80	1.20	0.18	0.023	0.012	0.05	0.04	0.00	0.01	0.02	0.024
13D	3 (S) : DF	3.83	2.01	0.18	0.025	0.01	0.04	0.05	<0.02	0.010	0.008	0.02
13D	3 (S) : GSH	3.84	2.00	0.19	0.022	0.009	0.05	0.04	0.00	0.011	0.02	0.024

MS Sample	Type : Location	%N	%Sn	%W	%V	%Al	%Ca	%B	%As	%Fe	%O	%Mg
11D	2 (P) : DF	0.007	<0.005	<0.01	0.013	<0.002	<0.0002	<0.001	0.001	94.54	0.0009	0.002
11D	2 (P) : GSH	N/A	0.00	0.000	0.01	0.001	N/A	0.0000	0.001	94.90	N/A	0.000
11D	3 (S) : DF	0.007	<0.005	<0.01	0.013	0.007	0.0013	<0.001	0.001	93.76	0.0004	0.035
11D	3 (S) : GSH	N/A	0.00	0.001	0.01	0.008	N/A	0.0000	0.001	94.26	N/A	0.038
12D	2 (P) : DF	0.007	<0.005	<0.01	0.015	<0.002	<0.0002	<0.001	0.001	94.44	0.0009	0.002
12D	2 (P) : GSH	N/A	0.00	0.000	0.02	0.001	N/A	0.0000	0.001	94.99	N/A	0.000
12D	3 (S) : DF	0.009	<0.005	<0.01	0.015	0.007	0.0018	<0.001	0.001	93.74	0.0006	0.036
12D	3 (S) : GSH	N/A	0.00	0.001	0.02	0.009	N/A	0.0001	0.001	94.29	N/A	0.038
13D	2 (P) : DF	0.007	<0.005	<0.01	0.015	<0.002	<0.0002	<0.001	0.001	94.44	0.0009	0.002
13D	2 (P) : GSH	N/A	0.00	0.000	0.02	0.002	N/A	0.0000	0.001	95.12	N/A	0.000
13D	3 (S) : DF	0.006	<0.005	<0.01	0.015	0.006	0.0012	<0.001	0.001	93.72	0.0006	0.034
13D	3 (S) : GSH	N/A	0.00	0.000	0.02	0.009	N/A	0.0001	0.001	94.36	N/A	0.035